# GENE THERAPY IN SPINAL MUSCULAR ATROPHY: RNA-BASED STRATEGIES TO MODULATE THE PRE-mRNA SPLICING of SURVIVAL MOTOR NEURON

A Dissertation

Presented to

the Faculty of the Graduate School

at the University of Missouri-Columbia

---

In Partial Fulfillment

Of the Requirements for the Degree

Doctor of Philosophy

---

by

TRAVIS BAUGHAN

Dr. Christian L. Lorson, Dissertation Supervisor

December 2008

The undersigned, appointed by the dean of the Graduate School, have examined the dissertation entitled

**GENE THERAPY IN SPINAL MUSCULAR ATROPHY: RNA-BASED STRATEGIES TO MODULATE THE PRE-mRNA SPLICING of SURVIVAL MOTOR NEURON**

presented by Travis Baughan,

a candidate for the degree of doctor of philosophy,

and hereby certify that, in their opinion, it is worthy of acceptance.

Professor Christian Lorson

Professor David Pintel

Professor Dongsheng Duan

Professor Donald Burke

Professor Marc Johnson

## ACKNOWLEDGMENTS

I would like to thank my advisor, Dr. Chris Lorson, for his support and instruction and for assisting me in becoming a more developed scientist. Under his tutelage I was able to make strides in this exciting gene therapy field. Through the opportunities that he was instrumental in finding I had multiple chances, and encouraged to present this work at international meetings which had been a dream of mine since I can remember. Thanks also to my committee: Dr. David Pintel, Dr. Dongsheng Duan, Dr. Don Burke, and Dr. Marc Johnson for advising on additional experiments, and challenging me to place effort into understanding every variable. I would also like to thank the Lorson laboratory for their steadfast support. Monique Lorson taught me that one always has to remember to logically analyze the data irrespective of source. Monir Shababi has been instrumental in the first published work of this project, without her, and all the cooking recipes I would not have had as successful graduate career. Hans Rindt has been extremely helpful in troubleshooting through experiments and theorizing about potential pathways. John Marston for his expertise in the mouse models through his work this project was able to advance quickly, and always a great conversation. Tristan Coady; the written word can not describe how much scientific, and non-scientific knowledge has been learned through our interactions. I would like to acknowledge Virginia Mattis for the friendship, collaborations, and the theory of combustible radioactive gel apparatuses. To Alexa Dickson for the friendship and continuing support throughout the entire graduate school process. To Erkan Osman for his hard work in the continuation of these projects and for allowing me a room to live in while trying to finish this process. Thank you very much.

To Frankie Rose, Melissa Terryberry, Philip Mehan, Desiré Buckley, and Sarah Rhoades: thanks for the support, scientific and otherwise, including the laughs.

Thanks to many friends from the Universities I have attended: Adam Perkins, Elliot Drury, J.C. Hardaway, and Kimberly Perkins, Justin Schwartz, Jason Clapper, Nate Sayre. Without the 'degenerate' environment that you provided I doubt that graduate school would have been half as fun. Special thanks to Jana Clark for all her hard work, dealing with all of my paper work and helping to make this experience fun.

I especially thank my family. I dedicate this to my wife Keli, I could not have gotten through the late nights, early mornings, and weekends in the laboratory without her continued support and understanding. My mother and my father, Maureen and Mark, constantly supported me and always had an ear or a shoulder if it was needed. My brother and sister-in-law, Derick and Jordan were always there for a phone call or laugh to help me realize what is really important in life. To my mother-in-law and father-in-law, Kathy and Don, thank you for the unabashed support and continuous availability of a home in the mid-west, both literally and figuratively. Thank you to my entire extended family for their encouragement and understanding for the past several years. To the mantra of the undergraduate 'gang' of delayed gratification, this is truer than I would care to admit and helped me everyday.

**GENE THERAPY IN SPINAL MUSCULAR ATROPHY: RNA-BASED STRATEGIES TO MODULATE THE PRE-mRNA SPLICING of SURVIVAL MOTOR NEURON**

Travis Baughan

Christian L. Lorson, Dissertation Supervisor

ABSTRACT

Gene expression is the required process in eukaryotes in which DNA is transcribed into pre-mRNA, spliced to produce "mature" mRNA and translated into proteins. This process is highly regulated and requires high fidelity. Inaccuracies in splicing events are receiving more attention as there is the finding that nearly 59% of all genes express alternative forms of mRNA. Spinal Muscular Atrophy (SMA) the disease that this project studies is not caused by alternative RNA splicing, but rather a duplicate gene product is skewed due to an inherent alternative splicing event. To expand on the knowledge of how a mirror copy of the causative gene (SMN2) can be regulated, we developed multiple types of small RNA molecules to manipulate the alternative splicing process. This manipulation had an ultimate goal of increasing the inclusion of a required exon, exon 7. It is known in SMA if there is an increase in full length expression there is a correlative decrease in disease severity. To better understand how aberrant RNA processing events occur and how we could manipulate these signals, we identified two *trans* elements associated with survival motor neuron (SMN) pre-mRNA splicing, and targeted

therapeutic RNA to this region. In addition, we used a translational approach to restore proper SMN pre-mRNA splicing by the development of bifunctional RNAs, antisense RNAs, and a multiple-antisense therapy targeting various regulator regions in and around the required exon. Ultimately this work has shown the feasibility of multiple types of therapeutic RNA modalities in several assays both *in vitro* and in a disease-relevant context, the SMA mouse models.

**TABLE OF CONTENTS**

## LIST OF FIGURES

## Introduction

### Spinal Muscular Atrophy: Phenotypic Account and Underlying Molecular Mechanisms

Spinal Muscular Atrophy (SMA) is a progressive proximal muscle atrophy due to a loss of ventral horn motor neurons (1, 2). SMA was first described in 1891 and was labeled clinically as Werdnig-Hoffmann disease after the clinicians who found the loss of motor neurons in severe muscle atrophic patients. Further research in describing the patients led to two more types of SMA called type II and type III or Kugelberg-Welander disease for the latter (3). The delineations in types are determined by age of onset of symptoms and degree of severity of those symptoms. In SMA type I (Werdnig-Hoffmann disease) children there is an extensive weakness, wasting, and areflexia or lack of simple muscle reflexes (4). This observation manifests between the ages of zero to 6 months and patients never gain the ability to sit upright, and usually die from respiratory failure before the age of 2 years. This is the reasoning why SMA type I is sometimes referred to as "floppy baby syndrome." Type II patients may sit up right, but never develop the ability to stand unassisted and death is a bit more variable depending on the degree of atrophy seen in the respiratory muscles. Type II SMA patients usually do not survive past 4 years of age. The third type of SMA (type III) is sometimes referred to as adult onset form of the disease, however this most likely refers to the fact that type III patients can live to adulthood. Symptoms are exhibited after the age of 2, however type III patients will lose the ability to walk at some stage of life with variability of ambulation but

usually require assistance later in life, though the age at which assistance is needed can be variable as well. Type III patients have a normal life span, which makes it unique among SMA types. The previously described types are the classical descriptions of SMA, however as the technology of diagnosis is changing there has been an increase in the number of recognized types of SMA. The type III group has been further subdivided into two groups a more severe type IIIa, with disease onset before three years and a milder form, IIIb, that have an onset of symptoms after three years of age (5). Furthermore an SMA type IV categorizes patients who become symptomatic after 30 years (5) the patients classically placed under the umbrella of adult onset SMA.

SMA, irrespective of type, is caused by the loss of the SMN1 gene found on chromosome 5q13 (6-10). The SMN1 gene is a 20 kb gene encoding a 294 amino acid protein from 9 exons only 8 of which are ever expressed (11). SMN1 encodes a protein that is 38 kDa in size and is expressed in all tissues (12, 13). There is a direct correlation between SMN protein level and severity of SMA (14). The 5q13 chromosomal region is highly unstable and is prone to large deletions and multiplications (6). This inherent instability created the SMA state, because in the 5q13 region is a 500 kb domain that has been duplicated and inverted. This region is present in all humans. One of the genes that is duplicated is a copy of the SMN1 gene called SMN2 (15). The SMN2 gene has been implicated in alleviation of disease severity (16), resulting in the various types of SMA. Interestingly SMN2 rescues SMN knockout mice from pre-implantation lethality (17), suggesting in humans without the duplication event resulting in the SMN2 gene SMA would not be present. It was shown that SMN2 had five nonpolymorphic nucleotide differences, but these are silent changes that do not affect the protein coding sequences

(11, 18, 19). However, research showed that SMN2 exon 7 was undetectable in ~95% of SMA patients (20, 21). Initially it was thought to be due to a truncation of the protein (3) or deletions in the region. However it was later shown that a silent C-T transition found six nucleotides within exon 7 causes an alternative splicing event (22). This alternate splice decision causes the majority of RNA transcripts produced from the SMN2 gene to loose exon 7 (23). Exon 7 is essential for protein stability, and therefore function (24). The alternate RNA process found in SMN2 is due to an overall splicing signal change in the 3' region of SMN2 exon 7. To fully understand how/why SMN2 transcripts functions in this way one has to consider the basic mechanisms of RNA splicing.

**RNA processing**

The vast majority of transcribed RNA consists of non-coding sequences that are not used as a template to construct a protein. *In silico* analysis of the human genome suggests the average length of a human exon is 170 base pairs with about 80-85% of exons found on all chromosomes being less than 200 base pairs (25). For introns however, the average size is about 5400 base pairs in length (25, 26). To ensure correct expression of the coding sequences higher eukaryotes must have a process that is efficient and accurate to join the relatively short exons in a coordinated effort for proper protein expression. The basic machinery used in pre-mRNA splicing consists of five small nuclear ribonucleoproteins (snRNPs) and ~100 additional proteins (27). The five snRNAs are as follows: U1, U2, U4, U5 and U6 and once combined with scaffolding proteins are called the spliceosome. Each snRNP is composed of a uridine-rich small

nuclear RNA (snRNA) that is blanketed with multiple proteins. The splicesome is a dynamic complex with many protein constituents changing throughout the entire process of splicing. The UsnRNPs use consensus sequences found flanking exons to bind to immature RNA molecules and identify exons that are needed for proper protein expression. These required sequences are the branchpoint adenosine, the polypyrimidine track, and the conserved dinucleotide sequences that define the exon/intron boundary (28). These *cis* components are highly conserved: roughly 99.24% of introns have a GT-AG dinucleotide boundary (29). The splicesome complex catalyzes exon splicing in a step by step process mediated by specific UsnRNPs at each step culminating in the mature complex ligating upstream and downstream exons together. Briefly the first step in recognition by the splicesome is the 5' splice site dinucleotide by the U1 snRNP, and the U2 auxiliary factor U2AF to the branchpoint, polypyrimidine tract and the AG of the 3' splice sight (28). U2 snRNP then binds to the branchpoint and the tri-snRNP of U4-U5-U6 join to make the mature splicesome and catalyze the double cleavage that result in the remove of the lariat intron and ligation of the now juxtaposed exons. The sequences that the splicesome uses to identify intron/exon boundaries are required but are not sufficient for complete definition at such a high fidelity that is required in this process. There are additional sequences required for a splice competent transcript and these additional sequences help aid in the process of alternative splicing.

**Alternative Splicing**

There is a higher order of complication in the language of splicing called alternative splicing. Its importance in the reliability of the basal splicing machinery and in expanding the proteome is just recently being appreciated. Upon sequencing the human genome it was found that there were only 31,000-39,000 genes (30), and after further analysis it was realized that nearly 59% of human genes generate multiple mRNAs by alternative splicing (26). Auxiliary *cis*-elements known as exonic and intronic splicing enhancers (ESEs and ISEs) and exonic and intronic splicing silencers (ESSs and ISSs) help make the pre-mRNA ready to be spliced by the splicesome (31). The proteins that bind to or block these degenerative signals are at the center of a high fidelity pre-mRNA process. They help in the expansion of transcripts that lead to a very complex level of regulation and expression of multiple isoforms which allows the genome of higher eukaryotes to express many more proteins than they encode (32). ESEs are bound by a family of proteins called the serine-arginine-rich (SR proteins). They have RNA recognition motifs (RRMs) and arginine-serine-rich protein interacting domains (RS domains) (33-36). These proteins are generally considered positively acting in terms of aiding the general splicesome to clearly define exon/intron borders. A number of SR proteins have been identified thus far, to name a few; ASF/SF2, SC35, SRp55c, and 9G8. In addition there are SR-like proteins that are more diverse from the SR super family; hTra2α, hTra2β1, $U2AF^{35}$ and $U2AF^{65}$ (34). These also have been implicated in positively aiding the recognition of exon/intron borders. By site-directed mutagenesis of mini-gene splicing constructs, protocols based on SELEX (Systematic Evolution of Ligands by EXponential enrichment) techniques and analyzing disease alleles, researchers have identified many ESE sequences for specific SR proteins (31, 37-41).

The RRMs found in different SR proteins serve to give specificity to each SR protein because each SR protein has a unique (though sometimes overlapping) ESE that it binds to (31, 37, 40). There is a multitude of sequence variance seen for ESEs specific for any given SR protein suggesting an even higher level of complexity. The degeneracy of most ESE sequences is intriguing but when multiple sequences are aligned a 6-8 nucleotide sequence motif becomes apparent (42, 43). As it is understood now SR proteins recognize specific, but degenerate and partially redundant sequences that lend to a highly regulated splice signal.

On the other hand a family of proteins termed heterogeneous nuclear ribonucleoproteins (hnRNP proteins) binds to ISSs and ISEs that serves to decrease the fidelity of the splicesome in the area (32, 44).This family of proteins and splice signals are less well understood. Though less defined it was shown that roughly one third of randomly selected short human DNA sequences retained a splice inhibitory activity in a splicing cassette (45). This was interesting to consider, perhaps suggesting that most exons are in a general deregulated state, and only after the addition of ESEs or ISEs exon inclusion occurs. This finding put further emphasis on the requirement of SR proteins and their ESEs/ISEs for splicing in general. Similar to SR proteins hnRNP proteins contain RNA-binding domain(s) and a protein-protein interaction domain to disrupt the general splicing machinery. Most silencers identified so far have been intronic silencers (46-49). The most studied proteins in this family of suppressors are; hnRNPI (PTB), hnRNPA/B, and hnRNP H sub-family of proteins (50-55). Both SR and SR-like proteins along with their antagonistic counterparts work in unison to create a fully splice competent pre-mRNA transcript. The above mentioned positive and negative regulators allow the process of

alternative splicing to be cell, temporal, and developmentally specific. This alternative splicing in transcript expression seen in higher eukaryotes is required for complex organisms.

**Alternative Splicing in Disease: the SMN2 Connection**

The silent C-T transition found within exon 7 that causes an alternative splicing event (22) in the majority of SMN2 transcripts is due to a loss of alternative splice signals (23). The molecular mechanism is still debated, however, it appears likely that the C-T transition disrupts an important ASF/SF2 binding site found at the 5'- of exon 7 (56). Later it was shown that the T substitution actually created a ESS that was bound by hnRNP A1 (57). This apparent contradiction hints at the possibility that both are correct and is an example of the complexity of alternative splicing. These reports support that both a creation of an ESS, and a loss of an ESE happen due to the C-T transition found in the SMN2 gene. Recent evidence has shown there are additional regulatory elements in and around exon 7. Over expression of hTra2β1 increases the SMN2 inclusion of exon 7 seen in cultured cells (58). Furthermore hTra2β1 interacts with SRp30c to facilitate SMN2 exon 7 inclusion even though SRp30c fails to bind directly to the RNA (59). Additionally an SC35 specific ESE was functional in exon 7 inclusion, and nearly overlapping the SF2/ASF ESE (39). These findings prove that SMN2 exon 7 relies heavily on auxiliary splicing factors to instigate the basal splicing machinery. There have been additional ISSs flanking SMN2 exon 7 that have been recently identified that add to the requirement of SMN2 exon 7 on positive splice signals (46, 48). One ISS was

identified at roughly -67 base pairs upstream of exon 7, while the other ISS was found 10 base pairs downstream. It is clear that SMN2 pre-mRNA processing is highly regulated and there are multiple layers of regulation, however it also presents a perfect target for a multitude of potential SMA gene therapies.

We focus on the following therapies in this report: therapeutic RNAs that can manipulate the transcript overall splice signal to increase the inclusion of the required exon, exon 7. The first series of RNAs are called bi-functional RNAs that are modified antisense oligonucleotides (AONs) that are designed to recruit positive splice signals. We develop three different panels of bi-functional RNAs with antisense domains specific for the 3' splice site region of exon 7, or two intronic repressor regions. These RNAs have the ability to increase exon 7 inclusion by an enzymatic reporter assay, and have the ability to increase the SMN protein levels in a SMA mouse model. Further work will be presented that show the increased applicability of AONs in an effort to increase a *trans*-splicing event by de-regulating a downstream splice signal. The final AONs therapy that will be discussed in this work is the use of a multi-AON therapy in SMA mice targeting three separate splice regulators congruently. Even though SMN2 is a low functioning copy of SMN1 it still has the capacity to encode an identical protein thus these techniques of increasing full length expression from the SMN2 gene is a promising method for SMA therapy. There has been a handful of protein functions assigned to SMN though none has been linked to the reasoning for the specific loss of motor neurons seen in SMA patients.

**SMN Protein Function**

SMN1 encodes a protein of 38 kd that is 294 amino acids in length. It is the loss of this protein that causes SMA, and though humans have a partially functional paralogue in the SMN2 gene, it is unable to produce enough full length protein. It has been previously shown that both the mRNA and protein products of SMN1 are expressed ubiquitously without any overt differences (14, 60, 61). It is enriched early in development in the anterior horn cells of the spinal cord and expression decreases with post-natal development (13, 61, 62). This trait is true for all mammals examined including humans. It is a conundrum in the field that a ubiquitously expressed protein has a temporal and specific effect seen in SMA pathology. To solve this contradiction many groups have sought to assign SMN a specific role in cells, but especially motor neurons. SMN is found in both the cytoplasm and nucleus in somatic sells, where it is enriched in a nuclear structure termed gems (Gemini of coiled bodies) (63). Though there is no single function described for the discreet nuclear structure it is a well described localization pattern for the SMN protein. It was shown that the SMN protein self-associates in vitro (12). This activity is facilitated through exon 7 and is diminished when there is less full length protein present (12). This suggests that protein oligomerization is required for protein function. SMN has been shown to form and function in a complex with the Gemin family of proteins. The SMN complex has been identified to include dimers of the SMN protein and Gemins 2-7 in the cytosol and in gems (63-68). Through SMN's dimerization and association with the gemin proteins it performs a critical function in spliceosomal small nuclear ribonucleoproteins (snRNP) maturation (63, 64, 68). The SMN complex binds the Sm-core proteins and loads them onto immature snRNPs prior to nuclear localization. It has been shown that the SMN complex interaction with the Sm

proteins is required for snRNP maturation (69) where the Sm proteins $D_1$-$D_2$, E-F-G and $D_3$-B are bound to the UsnRNAs (70). This function is carried out by a conserved Tudor domain found in exon 3 in the SMN protein (71, 72). The Tudor domain interaction with the sm proteins is essential for UsnRNP biogenesis (72, 73). In a zebra fish model of SMA it was seen that normal axon pathfinding was restored after addition of external UsnRNPs, implicating a reduction of UsnRNP biogenesis could cause motor axon degeneration (74).

In addition to UsnRNP biogenesis, and iterative to the axonal pathfinding defect, SMN has been shown to colocalize in motor axons with RNA-binding heterogeneous nuclear ribonucleoproteins R and Q (hnRNP R and hnRNP Q) (75, 76). Axons have a high requirement for RNA transport due to the incredibly large size of the cell body. The hnRNP R/Q proteins with the SMN complex have been shown to be concentrated in the distal axon of embryonic motor neurons (76), suggesting that these proteins transport RNAs to the growing axon. Recently cytoskeletal-based active transport of SMN positive granules along neuronal axons to growth cones was shown in tranfected cultured neurons further linking SMN to a transport role in neurons (77). SMN has been implicated in not just mRNA transport, but protein localization in the neuron.

The β-actin protein is highly enriched in distal parts of axons and growth cones, and its polymerization plays an important role in axon initiation, growth, guidance, branching, and retraction (78). It has been shown that β-acting distribution and localization in the neuronal growth cone is disrupted in $Smn^{-/-}$ motorneurons (76). These observations suggest that the loss of SMN could disrupt the expression, and localization of a highly required protein for neuronal fitness. Further experiments would have to link

the SMN-hnRNP complex to more than just axonal growth in tissue culture nevertheless it is still a very exciting connection. This could help explain the tissue and temporal pathophysiology seen in SMA patients. Current work is ongoing to link the SMN protein to known neuronal-specific roles, ubiquitous cellular roles that are highly enriched in neurons, or identify novel functions of SMN protein to resolve the reasoning for the physiology of the SMA disease.

**Stimulating full-length SMN2 expression by delivering bi-functional RNAs via a viral vector**


**ABSTRACT**

Spinal muscular atrophy (SMA) is caused by the loss of *survival motor neuron-1* (SMN1). A nearly identical copy gene called SMN2 is present in all SMA patients. SMN2 produces low levels of functional protein, while nearly 90% of *SMN2*-derived transcripts are alternatively spliced and encode a truncated protein that lacks the final coding exon (exon 7). While SMN is ubiquitously expressed, motor neurons are especially sensitive to the low levels of SMN and this heightened sensitivity leads to the development of SMA. Even though the majority of SMN2-derived transcripts are alternatively spliced and encode a protein that is truncated and unstable, the presence of SMN2 represents a unique therapeutic target because the SMN2 gene has the capacity to encode a fully functional protein. Here we describe an in vivo delivery system for short bi-functional RNAs that modulate SMN2 splicing. Bi-functional RNAs derive their name

due to the presence of two functional domains: an RNA sequence that is complimentary to a specific cellular RNA (e.g. SMN exon 7); and an untethered RNA segment that serves as a sequence-specific binding platform for cellular splicing factors, such as SR proteins. Plasmid-based and recombinant adeno-associated virus vectors were developed that express bi-functional RNAs that were capable of stimulating SMN2 exon 7 inclusion and total SMN protein levels. The experiments described in this chapter shed light upon the molecular regulation of a critical disease-causing gene and have implications for the development of a SMA therapy.

## INTRODUCTION

Spinal Muscular Atrophy (SMA) is a neuromuscular disorder that is the leading cause of infantile death (79). SMA is an autosomal recessive disorder that has an incidence of 1 in 6,000 live births and a carrier frequency of nearly 1 in 40 (79, 80). SMA is characterized by progressive atrophy of voluntary muscles due to the specific loss of motor neurons. There are three types of SMA based upon the age of onset and the severity of the symptoms. The gene mutated in all of these types of SMA is called *survival motor neuron-1* (SMN1) (8). SMN1 is present on the long arm of chromosome 5. A nearly identical copy gene called SMN2 is also present on chromosome 5. While SMN1 and SMN2 have the capacity to encode identical proteins, SMN1 is the sole SMA-determining gene. This apparent paradox is due to a silent non-polymorphic nucleotide difference in a critical exon (exon 7) that disrupts a splice enhancer and causes the majority of SMN2-derived transcripts to be alternatively spliced (56). This alternative splicing event results in a truncated and unstable protein that is biochemically defective and cannot provide protection from disease development in the absence of SMN1 (24).

The 38 kDa SMN protein is ubiquitously expressed and localizes to the nucleolus, diffusely within the cell cytoplasm, and to punctate nuclear structures called gems ("gemini of coiled bodies") (63, 81, 82). In cells and tissues from SMA patients, total SMN levels are dramatically reduced. The number of gems has served as a surrogate marker for SMN protein levels and disease severity since SMA type I cells can have as few as 2-3 gems/100 nuclei, while type III-derived cells can contain 40-50 gems/100 nuclei (83-85).

The SMN protein has been shown to be involved in U snRNP biogenesis and pre-mRNA splicing (64, 86, 87), transcription (88, 89), nucleocytoplasmic transportation (76), apoptosis (90-92) and ribosomal assembly (81, 93). The SMNΔ7 protein interacts less efficiently with essentially all SMN-interacting factors and is defective in most functional assays. While the SMN exon 7 peptide does not directly mediate the multitude of SMN activities, the requirement for exon 7 is likely indirect and this requirement is predicated upon its role in SMN self-association and protein stability, consistent with the premise that SMN self-association is a prerequisite for SMN activities.

At the RNA processing level, *SMN* exon 7 is highly regulated by a complex interplay between positive and negative acting factors. An AG-rich enhancer, called SE2, is required for full-length SMN expression and is bound directly by the SR-like factor hTra2β1 (24). Over-expression of hTra2β1 can stimulate high levels of exon 7 inclusion from SMN2-derived transcripts (58). Additionally, factors such as SRp30c, RBMY, and hnRNP-G have similar exon 7-stimulating activities and function through the SE2 region (59, 94) SF2/ASF, an SR protein, binds an enhancer which overlaps the critical C/T transition (56). The inability of SF2/ASF to bind this region in the SMN2 context demonstrates a direct correlation between SF2/ASF activity and disease development. Not only does the C/T disruption cause the loss of the SF2/ASF enhancer, but a novel hnRNP-A-1 dependent splicing silencer is created by the C/T transition (57). Additional regulatory elements with exon 7 and within the flanking introns have been identified that contribute to the overall regulation of this critical exon, including the EXtended INhibitory ContexT (Exinct) (48, 95-98).

Essentially all SMA patients retain at least one copy of SMN2. While SMN2 produces primarily alternatively spliced transcripts, it has the capacity to encode an identical protein compared to SMN1. Therefore, a number of strategies have recently been developed that are designed to induce exon 7 inclusion in SMN2-derived transcripts as potential novel SMA therapies (84, 85, 99 100-103). Compounds such as valproic acid, phenylbutyrate, hydroxyurea, and SAHA have been shown to modulate SMN2 expression at the transcriptional or RNA processing level or both.

A number of nucleic acid technologies have been employed to modify SMN2 splicing. For example, oligonucleotides that disable the SMN exon 8 splice site results in an increase in the usage of the exon 7 splice site (104, 105). Full length SMN expression was also elevated from SMN2 by the use of small fragment homologous replacement that changed the single nucleotide alteration from a "T" to a "C" (106). Peptide nucleic acids comprised of an SMN exon 7 anti-sense domain and minimalistic splicing activation domain peptide were shown to efficiently increase SMN2 exon 7 inclusion (31). Similarly, a novel synthetic RNA class called bi-functional RNAs were developed that contained an exon 7 targeting domain and non-compelementary tail region that acts to recruit splicing factors to the region (107). In a cell free assay and in transient transfection studies, these oligoribonucleotides can stimulate SMN2 exon 7 inclusion (107).

Here we describe an in vivo delivery system for bi-functional RNAs that modulate SMN2 splicing that are expressed from a transiently transfected plasmid or from recombinant adeno-associated virus vectors. Since rAAV has the ability to be

efficiently retrogradely transported to neurons through intramuscular injections, this strategy represents an inroad into a novel SMA therapeutic.

## RESULTS

### Modulating SMN2 splicing

The mechanistic premise of a bi-functional RNA molecule requires that the SMN exon 7 splice site can be modulated by heterologous enhancers and that the intrinsic deficiency of the splice site is not intractable. To address these critical issues, a series of SMN mini-genes were created in which a high affinity hTra2β1 splice enhancer replaced the native SE1 enhancer element at the 5' end of SMN exon 7. In the SMN1 context, high levels of full-length SMN were detected, comparable to levels produced by the normal SMN1 mini-gene, suggesting that the SE1 sequence was not specifically required for SMN exon 7 inclusion (Fig. 1A). In the *SMN2* mini-gene context, the creation of an hTra2β1 enhancer at the SE1 site supported high levels of exon 7 inclusion, in contrast to the native SMN2 mini-gene which primarily produced transcripts that lacked exon 7 (Fig. 1A). This suggests that the intrinsic weakness of the SMN2 exon 7 splice site can be overcome by the presence of strong enhancers, specifically hTra2β1 enhancer elements. In each instance, the native hTra2β1 site was unaltered.

As a confirmatory measure to demonstrate that the SMN exon 7 splice site was not irreversibly deficient, the upstream sub-optimal poly-pyrimidine tract was mutated to create a more consensus poly-pyrimidine tract. In the native sequence, there are a number of non-consensus "C" nucleotides, whereas the consensus sequence would be comprised exclusively of "T" residues. By changing any of the three individual non-consensus

nucleotides to consensus "T" residues, full-length SMN expression was dramatically elevated while the exon-skipped product was essentially undetectable (Fig. 1B). Taken together, these results demonstrate that the defect in the SMN2 exon 7 splice site can be overcome and that hTra2β1 is a potent activator of SMN exon 7 inclusion.

The following strategy was developed as a means to stimulate SMN2 exon 7 inclusion by providing potent exonic enhancers in trans to the SMN2 exon 7 splice site. Similar to previously described in vitro synthesized RNAs that contained an exon 7 anti-sense sequence and tandem repeats of exonic enhancers (107), an in vivo delivery system has now been developed that expresses short bi-functional RNAs. We have developed an *in vivo* plasmid-based system (pMU2) for the expression of short RNAs that alter SMN2 exon 7 splicing (Fig. 2A). While pMU2 functions in many respects like a typical plasmid, it has the advantage that when expressed in the appropriate packaging cell line, pMU2-derived recombinant Adeno Associated Virus (rAAV) vectors can be easily developed. The AAV2 Terminal Repeats (TRs) are present and facilitate the excision and subsequent replication of the rAAV genome. The AAV coding sequences have been removed and replaced with heterologous sequences including the polymerase III-dependent U6 promoter which transcribes the SMN bi-functional RNAs, and a polymerase II-driven reporter gene, GFP. Transfected cells can therefore be identified by GFP expression.

Bi-functional RNAs derive their name due to the presence of two functional domains: an RNA sequence that is complimentary to a specific cellular RNA (e.g. SMN exon 7); and an untethered RNA segment that serves as a sequence-specific binding platform for cellular splicing factors, such as SR and SR-like proteins: SF2/ASF, SC35, and hTra2β1 (Fig. 2B). The ESEs were derived by two mechanisms: 1) from a web-based

algorithm (ESE Finder 2.0)(108) which identifies ESE motifs based upon an *in vitro* enrichment protocol (SF2/ASF; SC35)(109); and 2) the hTra2β1 ESE was empirically determined by genetic analysis of the SMN exon 7 region. A similar series of bi-funcitonal RNAs were created in which the relative position of the anti-sense and enhancer domains was switched. The expression of the bi-functional RNAs was confirmed by RNase protection assay using probes specific for the SMN anti-sense sequence and a portion of the enhancer binding motif (Fig. 3).

To determine whether the plasmid-derived bi-functional RNAs could alter SMN2 exon 7 splicing, a previously characterized SMN2 luciferase reporter plasmid was used. In this system, luciferase is out of frame when exon 7 is excluded. However, when exon 7 is included in the final mRNA transcript, the downstream luciferase gene is in frame, allowing for the rapid and straight-forward measurement of luminescence. As expected, when the SMN2-luciferase construct was transiently expressed, low levels of expression were detected, consistent with the low levels of full-length transcript that are typically produced by SMN2 (Fig. 4). Co-transfection of any of the six bi-functional RNAs resulted in a several fold increase in luciferase activity compared to SMN2 alone. Importantly, when the SMN2-luciferase construct was co-transfected with the empty pMU2 construct, there was little change in luciferase expression (Fig. 4). The empty pMU2 construct expresses a non-SMN-derived RNA that is derived from the plasmid backbone. Taken together, these results demonstrate that the transiently expressed RNAs can stimulate the inclusion of SMN2 exon 7 and should provide a means to increase SMN protein levels in SMA-derived cells.

SMA Type I patient fibroblasts (3813 cells) are an important cellular context to assess bi-functional RNA activity because these cells: 1) have very low levels of SMN protein and SMN-positive gems, 2) lack SMN1, and 3) contain 2 copies of SMN2. While transfection levels are low in 3813 cells, transfected cells can be readily identified due to the plasmid-derived expression of GFP. Therefore, in the initial screening of the bi-functional expressing plasmids, we were interested in identifying GFP-positive cells that exhibited increased levels of SMN protein expression as detected by indirect immunofluorescence. When the bi-functional RNAs were individually expressed in 3813 cells, a qualitative increase in total SMN levels was detected (Fig. 5). Since gems are an established measure of SMN protein levels and the numbers of gems correlate with disease severity, semi-quantitative gem counts were performed to determine the relative effectiveness of the six bi-functional expressing plasmids. Consistent with the observation that the bi-functional RNAs increased *SMN2* exon 7 inclusion, SMN-positive gem numbers were also elevated by the transient expression of the plasmid-based bi-functional RNAs (Fig. 5 and data not shown). Importantly, the parental pMU2 vector, which did not induce SMN2-luciferase expression, did not induce endogenous SMN expression (Fig. 5).

The development of rAAV vectors that express the bi-functional RNAs would provide a gene therapy approach that is directly applicable to SMA since recombinant AAV serotypes can be efficiently delivered to the central nervous system through retrograde transport. To determine whether the bi-functional RNAs could be efficiently delivered by a viral vector, SMA patient fibroblasts were transduced with rAAV2 vectors expressing the six bi-functional RNAs. Transduced cells were identified by the

expression of GFP. Using a multiplicity of infection (MOI) of 100, patient fibroblasts were transduced for 4, 8 or 16 days with each vector. At the end of each time point, cells were analyzed by indirect immunofluorescence to identify SMN-staining gems. As expected, very few gems were detected in untreated cells.

In cells transduced with the rAAV vectors expressing the bi-functional RNAs, a significant increase in gem numbers were observed as early as 4 days after infection as each of the bi-functional vectors resulted in no less than 20 gems per 100 GFP-positive cells. The highest increase in gems observed was with the 3'-SF2/ASF vector that had an average of 69 gems per 100 GFP-positive cells. In contrast the negative control vector (vMU2) at an MOI of 100 did not elevate gem numbers to comparable levels (Fig. 7A). At later time points, the same low baseline level of gems was observed with the negative control vector, while the bi-functional RNAs were capable of maintaining high levels of SMN-positive gems at 8 and 16 days post-infection (Figs. 7B,C). The 5'-hTra2β1 vector consistently induced higher gem counts than the other 5'-rAAVs, ranging from 30-83 gems per 100 cells at 16 days post-infection. 5'-SF2/ASF and 5'-SC35 vectors also resulted in high levels of SMN-positive gems, although the numbers were slightly less than those achieved by the 5'- hTra2β1 vector. The highest average gem counts were attained by the 3'-hTra2β1 at 16 days after infection at which time, 72 gems per 100 GFP-positive nuclei were observed. The data are also presented as "gems per cell." This was necessary to demonstrate that there was not an unusually high distribution of gems in a small percentage of aberrant cells since this would dramatically skew the interpretations of the total gem count data. Importantly, the rAAV-delivered bi-functional RNAs

restored SMN-positive gems to levels consistent with those of unaffected control fibroblasts levels, typically 1-2 gems per cell (Figs. 7D-F).

As a confirmatory measure, SMA patient fibroblasts were transduced with the bi-functional viruses and total SMN protein was measured by western blotting with an SMN monoclonal antibody. Each of the six bi-functional RNA expressing viruses resulted in an increase in total SMN protein (Fig. 8). The uninfected baseline of the SMA fibroblasts was expectedly low, while there was a modest increase when a control virus was used ("Activation Domain" virus). The "activation domain" virus expresses an RNA that corresponds to SC35 enhancers, but lacks the anti-sense SMN targeting sequence. Taken together, these results demonstrate that the bi-functional RNAs facilitate the expression of full-length SMN by promoting *SMN2* exon 7 inclusion.

## DISCUSSION

Modulating pre-mRNA processing through the use of therapeutic RNA molecules is an expanding area of investigation (110-114). As a therapeutic agent, the delivery of *in vitro* synthesized RNAs is not currently practical for many genetic disorders given the obstacles concerning delivery and sustainability. However, the delivery of similar RNAs through the use of a viral vector represents a means to target specific cell populations and deliver a therapeutic RNA molecule that can persist for a significant period of time.

The molecular genetics of SMA make this disease especially amenable to therapeutic strategies that promote full-length expression from SMN2. First, greater than 99% of SMA cases are caused by the loss of SMN1; secondly, SMN2 encodes an identical protein, therefore, even though there are 2 non-polymorphic nucleotide differences in the coding sequences of SMN1 and SMN2, these changes do not alter the protein coding capacity of the genes; thirdly, the SMA population is remarkably homogenous with regards to SMN2. Individuals homozygous null for SMN1 and SMN2 have not been identified presumably because this condition would be lethal (consistent with the knock-out mouse model). Therefore, essentially all SMA patients carry at least 1 SMN2 gene (frequently 2 or more copies of SMN2 are present in normal and SMA individuals) – a gene that encodes normal SMN protein. Finally, transcripts generated from SMN2 are stable. In some instances, single nucleotide substitutions can dramatically alter the stability of the resultant RNA, however, the C/T in SMN2-derived transcripts does not alter full-length and SMNΔ7 RNA stability.

Since SMN2 has the capacity to encode a normal, full-length SMN protein, and all SMA patients retain at least one copy of the SMN2 gene, modulating its expression is a key area in SMA therapeutic development. Compounds including HDAC inhibitors such as valproic acid (99, 100, 115), SAHA (99), phenylbutyrate (101, 116), hydroxyurea (117), and sodium butyrate (102) have been identified that stimulate the SMN2 promoter and/or stimulate *SMN* exon 7 inclusion. These mechanisms collectively result in an increase in full-length SMN protein. Additional compounds such as indoprofen and aminoglycosides have been identified that increase SMN levels (118, 119), although their mode of action is less well characterized. Alternatives to these chemical-based approaches include traditional gene therapy as well as small oligonucleotides that increase SMN exon 7 inclusion (104-108, 120).

In this report, we describe the first example in which viral vectors have been used to deliver bifunctional RNAs that modulate SMN2 splicing. These results demonstrate that SMN2 splicing can be directed to include SMN exon 7 by supplying a binding platform in *trans* for positively-acting factors such as SF2/ASF and hTra2β1. The binding sites for the splicing factors were derived from *in vitro* binding data or from the native SMN exon 7 sequence. However, it is possible that additional binding substrates could result in even more potent bi-functional molecules. It is not completely unexpected that of the three types of sequences evaluated, the ones that regulate the native SMN exon 7 sequence, SF2/ASF and hTra2β1, were routinely more efficient at stimulating SMN exon 7 inclusion.

Adeno-Associated Virus is a single stranded DNA virus, part of the parvovirus family that is replication deficient unless another helper virus is present to allow

maturation of its infectious cycle. Though recombinant Adeno Associated viruses can integrate into chromosomal DNA at a specific spot it does so at such a low incidence it is negligible. The majority of the rAAV genomes stay as episomal concatetmers within either dividing or nondividing cells. Furthermore rAAVs serotype tissue tropism or more importantly tissue promiscuity increases their usefulness in becoming vectors for gene therapy. rAAV has been used as a potential gene therapy vector in research for the past 15 years. Interestingly, it has been shown that rAAV-2 has a high tropism for both neurons and muscle cells, and, importantly in the SMA context, can be retrogradely transported to neurons in vivo. Retrograde delivery of the full-length SMN cDNA has also recently been reported using a pseudo-typed lentiviral vector with only modest results (120).

Currently it is unclear when an SMA therapy must be administered to prevent SMA development. Potentially the developmental signal that will eventually trigger motor neuron death occurs early in prenatal development and, in turn, this SMN-deficiency effectively pre-determines the fate of motor neurons. This model could account for why recent avenues into SMA therapies show elevated SMN protein levels, but result in a less robust effect regarding overall survival and correction of the disease phenotype (120, 121).

A number of human diseases are due to aberrant splicing (122). While the experiments described in this report have immediate implications for the development of a SMA therapy, the results could be used as a model for a broad range of genetic disorders in which correcting a splicing defect would restore functionality to a disease-

causing gene by effectively being able to promote the inclusion of specific exons that are misprocessed in the disease state.

## MATERIALS AND METHODS

### Cloning

In the SMN1 and SMN2 mini-genes, the hTra2β1 splice enhancer (5'-GAAGGAA-3') was cloned into the 5' end of SMN1 and SMN2 exon 7 by overlapping PCR mutagenesis (96) . The enhancer replaced the endogenous sequences starting at SMN exon 7 +7/+13. Site directed mutagenesis of the pSMN2 mini gene introduced consensus sequences into the poly-pyrimidine tract upstream of exon 7: $SMN2^{1TPPT}$: 5'-TTTTTTTCCTT-3'; $SMN2^{2TPPT}$: 5'-TTATTTTTCTT-3'; $SMN2^{3TPPT}$: 5'-TTATTTTCTTT-3'; $SMN2^{12TPPT}$: 5'-TTTTTTTTTTT-3'. The bi-functional clones were generated with annealed complementary pairs of DNA oligonucleotides (IDT; Coralville, IA) that were cloned into the pMU2 between the *Bam*HI and *Spe*I sites. Sequences for the 5' bi-functional oligonucleotides are as follows: SF2/ASF, top, 5'-GATCCCTTCTTATTGATTTTGTCTAATCATTCACACGACACACGACACACGATTTTTTA-3';bottom,5'-TAGTAAAAAATCGTGTGTCGTGTGTCGTGTGAATGATTAGACAAAATCAATAAGAAGG-3'; SC35, top, 5'-GATCCCTTCTTATTGATTTTTTCTAATCATTGGCCCCTGGGCCCTGGGCCCCTGTTTTTTA-3'; bottom, 5'-CTAGTAAAAAACAGGGGCCCAGGGGCCCAGGGGCCAATGATTAGACAAAAT

CAATAAGAAGG-3'; hTra2β1, top, 5'-GATCCCTTCTTATTGATTTTGTCTAATCATTGAAGGAGGGAAGGAGGGAAGGAGGTTTTTTA-3'; bottom, 5'-CTAGTAAAAAACCTCCTTCCCTCCTTCCCTCCTTCAATGATTAGACAAAATCAATAAGAAGG-3'. Sequences for the 3'-bi-functional oligos are as follows; SF2/ASF, top, 5'-GATCCCACACGACACACGACACACGAATCATTCTTCTTATTGATTTTGTCTATTTTTTA-3', bottom, 5'-CTAGTAAAAAATAGACAAAATCAATAAGAAGAATGATTCGTGTGTCGTGTGTCGTGTGG-3'; SC35, top, 5'-GATCCGGCCCCTGGGCCCTGGGCCCCTGATCATTCTTCTTATTGATTTTGTCTATTTTTTA-3', bottom, 5'-CTAGTAAAAAATAGACAAAATCAATAAGAAGAATGATCAGGGGCCCAGGGCCCAGGGGCCG-3'; hTra2β1, top, 5'-GATCCGAAGGAGGAAGGAGGGAAGGAGGATCATTCTTCTTATTGATTTTGTCTATTTTTTA-3', bottom, 5'-CTAGTAAAAAATAGACAAAATCAATAAGAAGAATGATCCTCCTTCCCTCCTTCCTCCTTCG-3'. Plasmids were sequenced for verification.

**Virus production**

Plasmid DNA from each bi-functional clone was triple transfected with the previously described pXX6 (encodes: VA, E2A and E4) and pAD8 (encodes: AAV2 Rep and Cap proteins) helper plasmids into HEK 293 XDC cells (123, 124), using polyethyleneimine.

Transfections were done in a 1:1:2 molar ratio of plasmids pMU2 derived clones, pAD8, and pXX6 respectively. HEK 293 XDC cells were grown in 5% BGS and antibiotics. After 48 hrs, transfected cells were harvested and the viral samples were kept at -80$^{o}$C until needed. AAV titers were quantified by exposing HeLa cells to 10µl of either viral supernatant or the resuspended HEK 293 XDC pellet for 1 hour. HeLa cells were re-fed with DMEM + 5% BGS and antibiotics and incubated for 48 hours. Multiplicities of infection (MOI) for each viral preparation were quantified in triplicate wells from a 96 well dish based on three separate images of GFP expressing cells vs cell number and MOI is expressed as infectious particles/per cell.

**Immunofluorescence imaging**

For all immunofluorescence staining, sub-confluent Type 1 patient fibroblasts cells (3813 cells; Coriell Cell Repositories) were transfected with either plasmid bi-functional clones using Lipofectamine 2000 reagent (Invitrogen), or specified rAAV at an MOI of 100 for 16 days and grown in DMEM supplemented with 10% fetal bovine serum and antibiotics. Transfected cells were fixed with acetone/methanol (1:1), and washed with phosphate buffered saline (PBS). Cells were blocked in PBS and 5% BSA, washed with PBS. Cells were reacted with mouse anti-SMN monoclonal antibody 4B7 was diluted 1:10 in PBS with 1.5% BSA, washed in PBS, and reacted with the secondary monoclonal antibody (anti-mouse conjugated to Texas Red (Jackson Labs)) diluted at 1:200 in PBS with 1.5% BSA. After washing in PBS, DAPI was added to each coverslip for 5 minutes, and washed again. Cover slips were then loaded onto slides using mounting media (DABCO, 2.3% (w/v), 10% PBS, 87.7% glycerol) and sealed with nail polish.

**Western blot analysis**

Patient fibroblasts cells (3813) were infected with 5' and 3' bi-functional RNA vectors at MOI of 25 and grown in media as stated before. Cells were harvested 16 days post infection and resuspended in 20 µl of 8 M urea. The protein concentration of samples was normalized by measuring the OD at 595 using Bio-Rad protein assay dye reagent. SDS loading dye was added to the samples and were sonicated for 30 seconds on ice, boiled for 5 minutes, and resolved on by 12% SDS-PAGE. The gel was transferred to PVDF membrane and SMN was performed using 4B7, a SMN monoclonal antibody. Horseradish peroxidase-conjugated goat anti-mouse was used as the secondary antibody and complexes were detected by enhanced chemiluminescence (Pierce).

**Luciferase assays/RT-PCR**

Sub-confluent HeLa cells were plated in 12 well dishes and co-transfected with a previously described SMN2-luciferase plasmid(125) and the indicated bi-functional plasmids using the Lipofectamine 2000 reagent (Invitrogen). To establish baselines for SMN1 and SMN2 luciferase constructs, 0.75µg of pCI-SMN1-Luc or pCI-SMN2-Luc and 3 µg of sheared salmon sperm DNA were co-transfected for 48 hours. For the experimental samples, 3 µg of each bi-functional clone or pMU2 were co-transfected with 0.75 µg of pCI-SMN2-Luc for 48 hours. Transfected cells were collected by using the Luciferase Assay System (Promega) and luminescence was measured on a luminometer. RT-PCR experiments were performed to visualize splicing variations in both the high affinity hTra2β1 splice enhancer replacement in SE1 of the SMN1 and

SMN2 mini-genes, and the SMN2 sub-optimal poly-pyrimidine tract point mutations. For the both protocols HeLa cells were transfected with Lipofectamine 2000 reagent (Invitrogen) with their respective plasmids. Cells were harvested with Trizol (Invitrogen), and RNA was subsequently precipitated. First strand synthesis was done, and the SMN splicing variants were verified by using two pCI specific primers;

pCI Reverse Sequence 5' –AGCTCGTCTGTACTATTCTATGTAA- 3'

pCI Forward Sequence 5'- GCTAACGCAGTCAGTGCTTCTGAC -3'

**RNase protection assays**

An RNase protection assay was performed to detect the synthesis of the bi-functional RNAs in transfected HeLa cells. To generate the anti-sense RNA probes, the sequence of three 3' bi-functional RNA molecules were cloned into the pBluescript II KS(-) (Stratagene) vector into *Bam*HI and *Spe*I sites. The anti-sense plasmids were linearized with EcoRI and 1 μg of each template was transcribed with T7 RNA polymerase in the presence of $\alpha$-$^{32}$P UTP. 2 μg of each of the bi-functional plasmids were transfected into HeLa cells and total RNA was isolated using the TRIZOL reagent and used in RNase protection assays as previously described except for the following minor modifications. 10 μg of total RNA was incubated with the corresponding anti-sense probe overnight and then digested with the mixture of RNase A and RNase T1 for 45 minutes. The protected RNA samples were resolved in 8% sequencing gel and exposed to Kodak BioMax film. Total RNA from non-transfected HeLa cells was incubated with the 3' SC35 anti-sense probe and used as negative control.

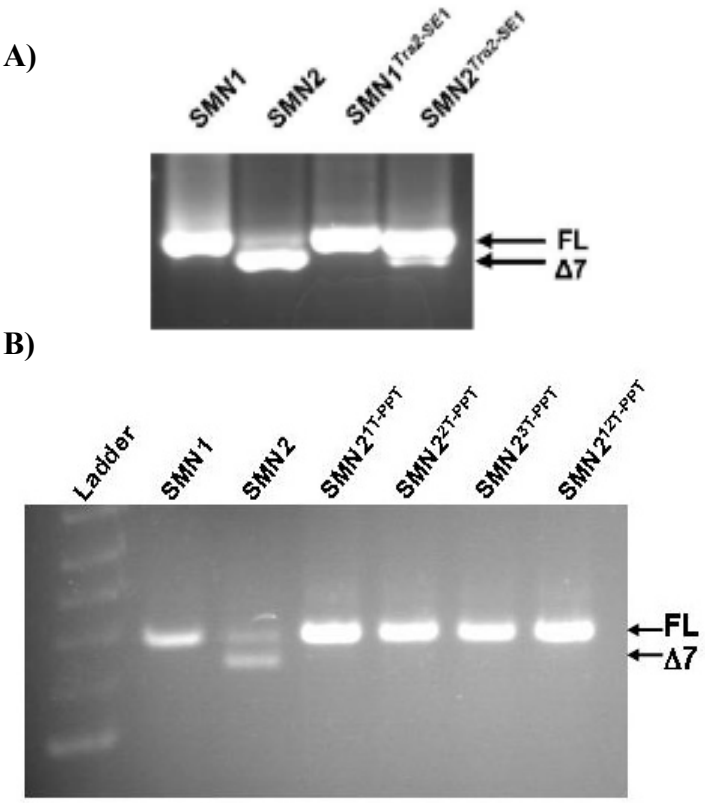


**Figure 1. Modulation of *SMN2* splicing**. **(A)** The native hTra2β1 splice enhancer was created within the previously described SF2/ASF splice enhancer in the SMN1 and SMN2 mini-gene contexts. Total RNA was isolated and used in RT-PCR reactions from HeLa cells transiently transfected with the plasmid-based mini-genes. Primers used in the PCR step anneal to a portion of the plasmid-derived transcript to specifically amplify the plasmid-derived transcripts. **(B)** Individual consensus basepair substitutions were introduced into the poly-pyrimidine tract upstream of SMN exon 7. Mini-genes were transfected into HeLa cells and RT-PCR was performed as described above. Experiments were performed in triplicate and representative results are shown.

A)

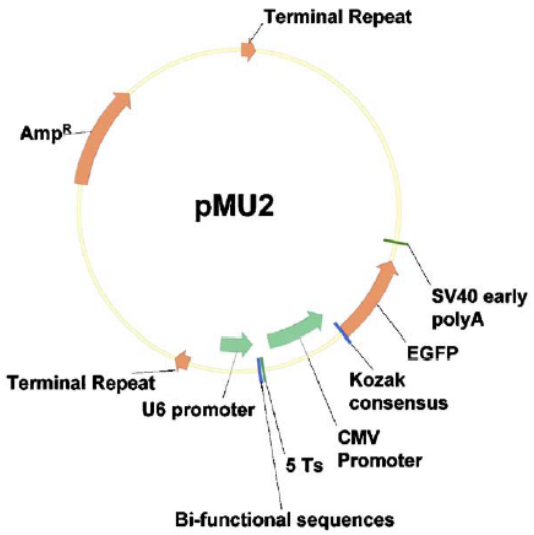


B)

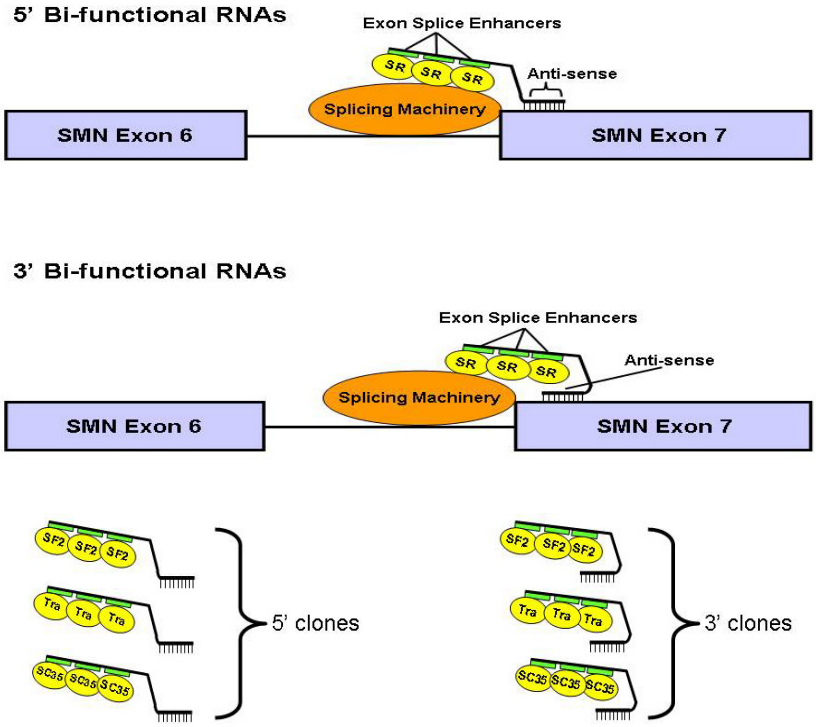


**Figure 2. Schematic of Delivery vector and Bi-functional RNAs (A)** Schematic of pMU2 vector. The plasmid includes the following characteristics: an ampicillin resistance gene (AmpR), AAV2 terminal repeats that allow excision from the plasmid and viral

replication, a U6 promoter that drives the expression of the bifunctional RNAs, a polymerase III transcriptional stop signal, a cytomegalovirus (CMV) promoter that drives expression of the eGFP gene, a Kozak consensus sequence for ribosomal entry, and a SV40 polyadenylation signal.

**(B)** Schematic of bi-functional molecules. The organization of the bi-functional RNA is illustrated with an anti-sense targeting domain specific to the 5' end of SMN exon 7, a short spacer region, and a domain comprised of three tandem repeats of exonic splice enhancers (SF2/ASF; hTra2β1; or SC35). The ESE regions serve to recruit cellular splicing factors that interact with the general splicing machinery which, in turn, promotes *SMN* exon 7 inclusion. The general composition of the 5' and 3' bi-functional RNAs are similar except that the orientation is altered: in the "5'" RNAs, the ESE sequences are 5' of the anti-sense region; in the "3'" RNAs, the ESE sequences are 3' of the anti-sense region.

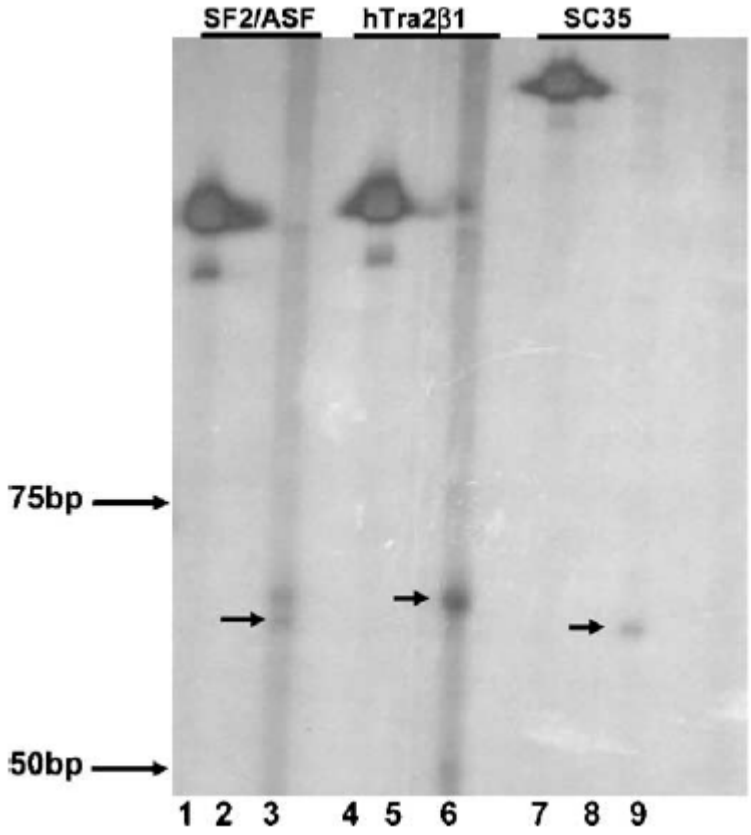


**Figure 3. Detection of bi-functional RNAs**. RNase Protection Assay of pMU2-derived bi-functional RNA. Total RNA from HeLa cells or HeLa cells transfected with pMU2 derivatives was isolated and hybridized with a radiolabeled in vitro synthesized RNA corresponding to the anti-sense of the various 3'-bi-functional RNAs. Arrows indicate where the 75bp and 50bp ladder ran. Lanes 1, 3, and 5 are the radiolabeled probes alone for the indicated bi-functional RNA. Lanes 2, 4, and 6 are the radiolabeled probes incubated with HeLa extract that had been transfected with the specified plasmid. Protected RNA species are indicated (arrows) and are not observed in the total RNA from untransfected HeLa cells (lane 7). Due to the difference in size of each 3'-bi-functional RNA produced we see the corresponding difference in the specie protected. 3'-SF/ASF is

64bp long (lane 2), 3'-hTra2β1 is 66bp long (lane 4), and finally, 3'-SC35 is 65bp long (lane6).

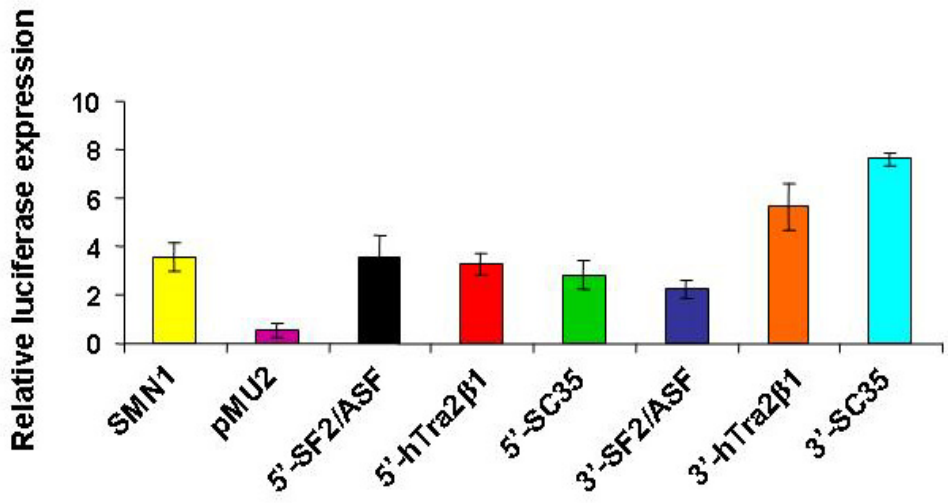


**Figure 4. Stimulation of SMN2 Exon 7 inclusion**. A SMN2-luciferase reporter construct was co-transfected with pMU2 derivatives for 48 hrs. Luciferase is out of frame when SMN exon 7 is excised and luciferase is in frame when SMN exon 7 is included in the transcript. The bars represent luciferase assays performed at least in triplicate. The x-axis represents the bi-functional plasmids co-transfected with the SMN2-luciferase construct. Lanes 2-8 were co-transfected with the SMN2-luc plasmid, and in excess with the specified pMU2 derived plasmid. The y-axis is shown in relative luminescent intensity over the baseline SMN2-luc relative luminescent intensity. The SMN1 expression plasmid is graphed to indicate potential levels of inclusion, however because this Luciferase is on a different plasmid comparing expression from any sample to SMN1 is impossible.

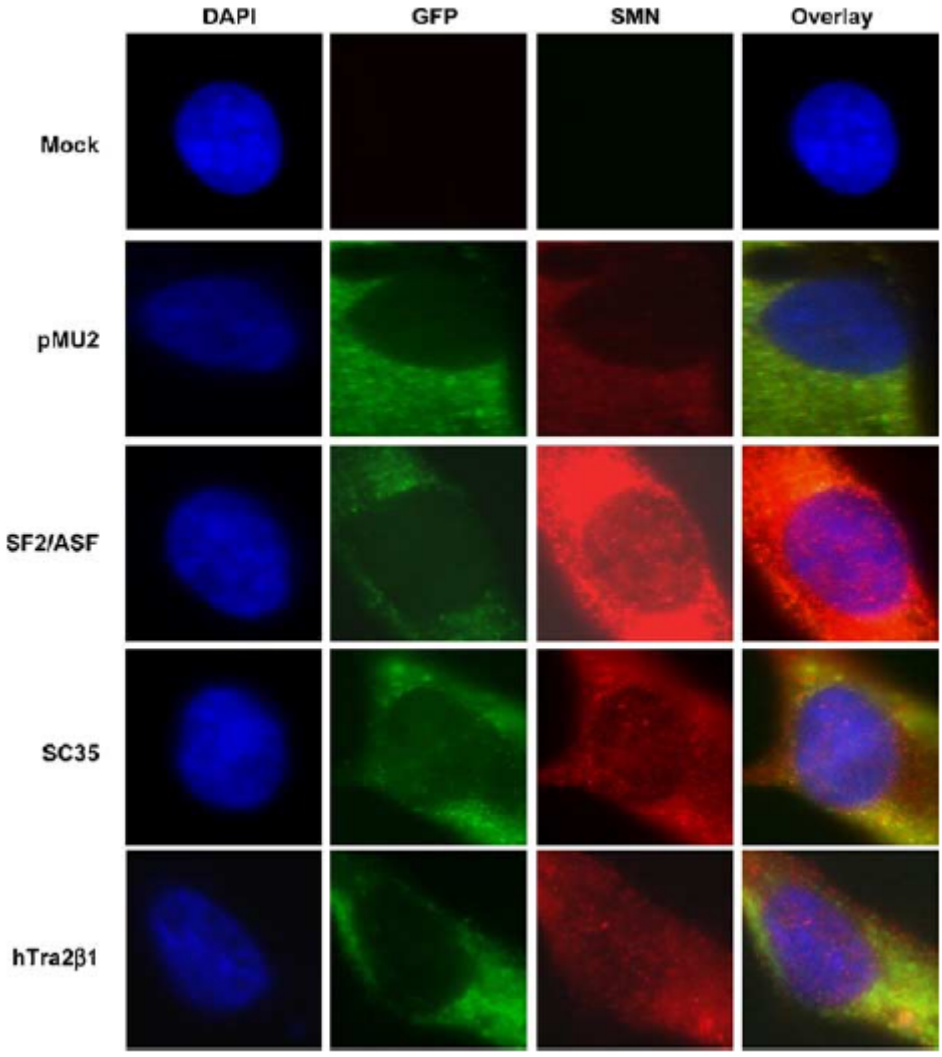


**Figure 5. Increase in SMN expression in Patient Fibroblasts.** SMA type I fibroblasts (3813 cells) were transiently transfected with pMU2 derivates of the 5'-bi-functional clones and indirect immunofluorescence was performed using an anti-SMN monoclonal antibody and visualized with a TRITC-conjugated secondary antibody (red). Transfected cells were initially identified by the expression of GFP. DAPI (blue) was used to stain nuclei.

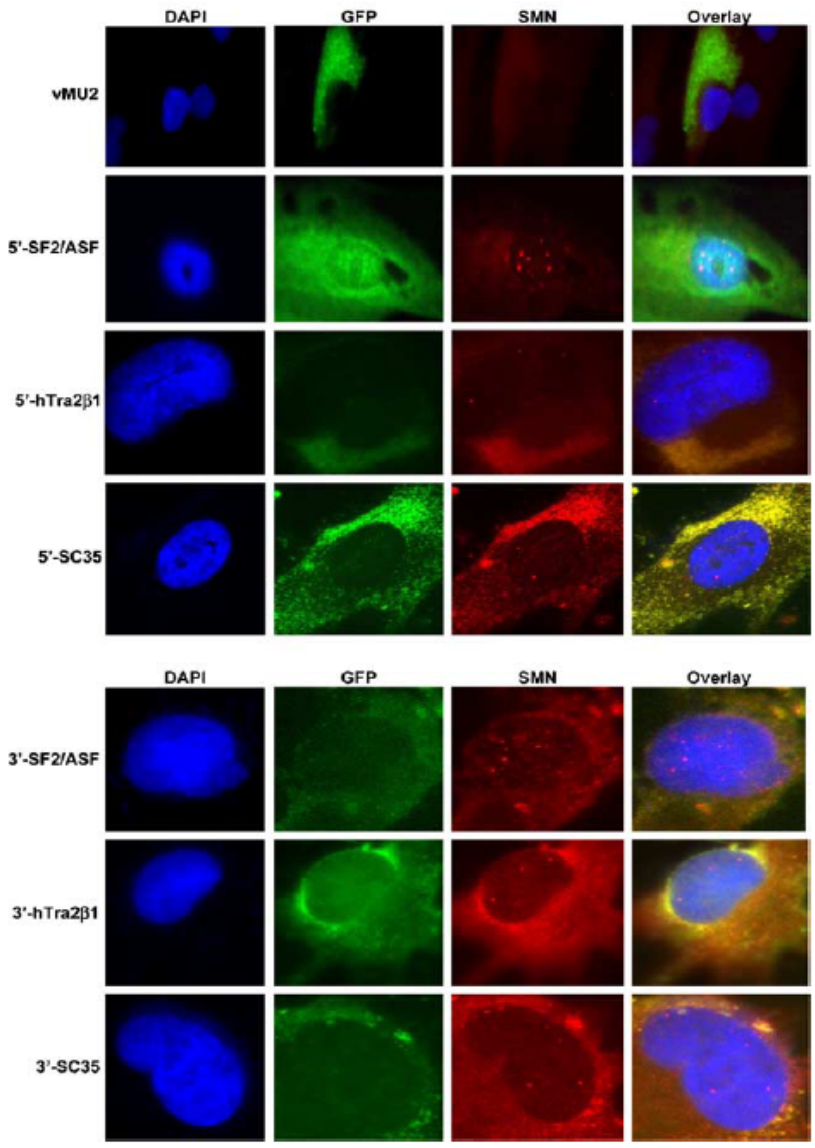


**Figure 6. rAAV infected Patient Fibroblasts show an increase in SMN levels**. SMA type 1 patient fibroblast cells were infected at an multiplicity of infection (MOI) of 100 for 4, 8, or 16 days at which time SMN-containing gem numbers were determined by indirect immunofluorescence staining using an anti-SMN monoclonal antibody and visualized with a TRITC-conjugated secondary antibody (red). Transfected cells were initially identified by the expression of GFP. DAPI (blue) was used to stain nuclei. This immunofluorescence is cells infected for 16 days.

A)

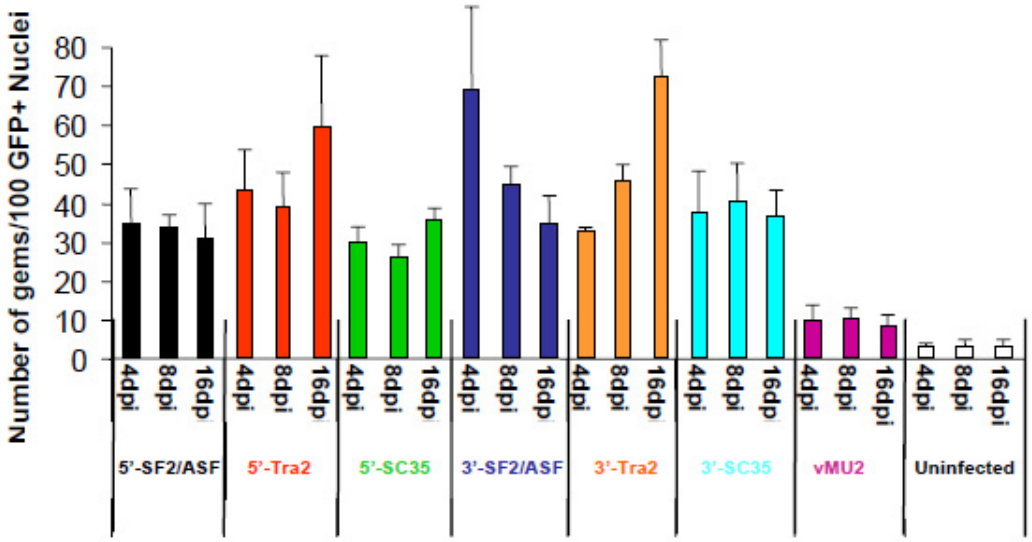
Number of gems/100 GFP+ Nuclei
80
70
60
50
40
30
20
10
0
4dpi
8dpi
16dpi
5'-SF2/ASF
5'-Tra2
5'-SC35
3'-SF2/ASF
3'-Tra2
3'-SC35
vMU2
Uninfected

B)

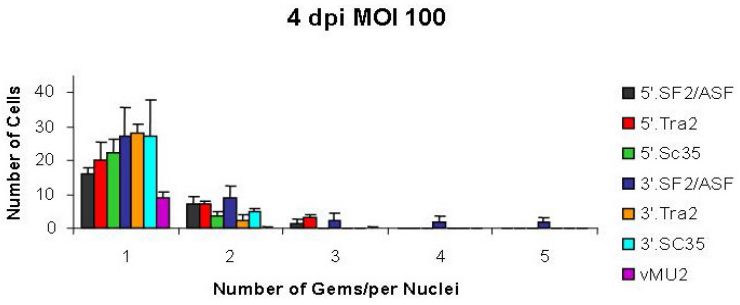
4 dpi MOI 100
Number of Cells
Number of Gems/per Nuclei
5'.SF2/ASF
5'.Tra2
5'.Sc35
3'.SF2/ASF
3'.Tra2
3'.SC35
vMU2

C)

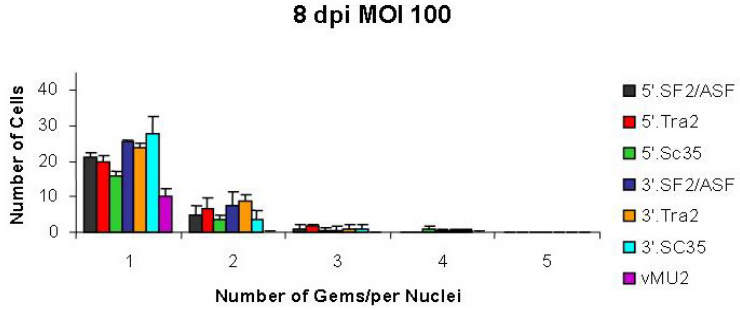
8 dpi MOI 100
Number of Cells
Number of Gems/per Nuclei
5'.SF2/ASF
5'.Tra2
5'.Sc35
3'.SF2/ASF
3'.Tra2
3'.SC35
vMU2

D)

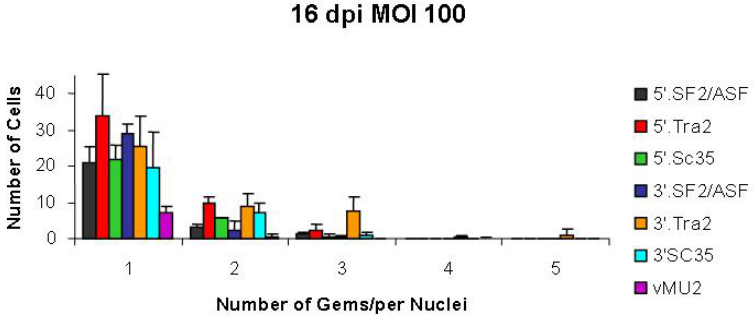
16 dpi MOI 100
Number of Cells
Number of Gems/per Nuclei
5'.SF2/ASF
5'.Tra2
5'.Sc35
3'.SF2/ASF
3'.Tra2
3'SC35
vMU2

**Figure 7. Gem analysis of rAAV infected 3813 cells. (A)** Type I fibroblasts cells were infected for 4, 8 or 16 days at an MOI of 100 and SMN-positive nuclear gems were counted in GFP positive cells. The x-axis indicates the virus used for transduction and the y-axis is the number of gems counted in 100 GFP-positive cells. Data presented represent at least three individual experiments in which 100 GFP-positive cells were analyzed per experiment. **(B-D)** The number of gems per nucleus was compiled from the previous gem counts, however, the data are now presented such that the y-axis depicts the number of cells, and the x-axis is the number of gems per nuclei

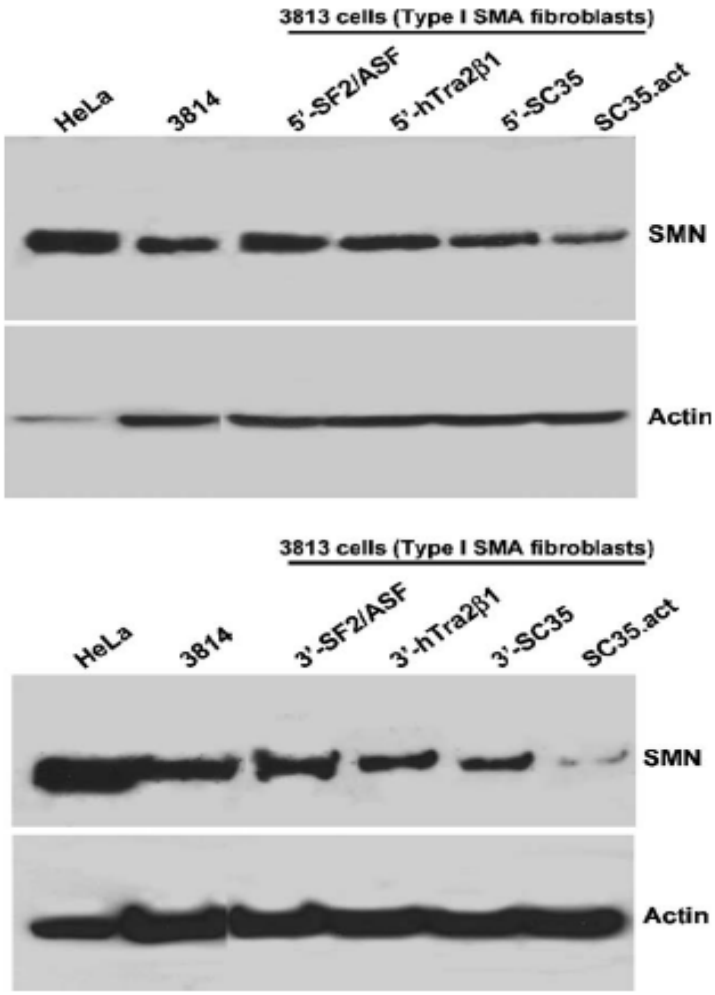


**Figure 8. rAAV transduction with bi-functional vectors increased total SMN protein levels.** SMN protein levels increased in sub-confluent 3813 cells were trasnduced for 13 days at an MOI of 100 (or mock infected) with each of the indicated rAAV vectors and relative SMN protein levels were determined by western blot. Cells were harvested in lysis buffer and resolved in a denaturing polyacrylamide gel. SMN and actin levels were visualized by chemiluminescence using anti-SMN and anti-actin monoclonal antibodies and a horseradish peroxidase conjugated secondary antibody. HeLa cell extract was included as a positive control for SMN mobility.

**Delivery of bifunctional RNAs that target an intronic repressor increase SMN levels in an animal model of spinal muscular atrophy**

## ABSTRACT

Spinal muscular atrophy (SMA) is a motor neuron disease caused by the loss of *survival motor neuron-1* (SMN1). A nearly identical copy gene called SMN2 is present in all SMA patients, which produces low levels of functional protein. Although the SMN2 coding sequence has the potential to produce normal, full-length SMN, approximately 90% of SMN2-derived transcripts are alternatively spliced and encode a truncated protein lacking the final coding exon (exon 7). SMN2, however, is an excellent therapeutic target since all SMA patients retain SMN2. Previously, we developed bi-functional RNAs that bound SMN exon 7 and modulated SMN2 splicing. To optimize the efficiency of the bi-functional RNAs, a different anti-sense target was required. To this end, we genetically verified the identity of a putative intronic repressor and developed bi-functional RNAs that target the inhibitory sequence. As a result, there is a two-fold mechanism for inducing full-length SMN: inhibition of the intronic repressor and recruitment of SR proteins via the SR-recruitment sequence of the bi-functional RNA. These new bi-functional RNAs effectively increased SMN in human primary SMA fibroblasts. Lead candidates were synthesized as 2'-O-methyl RNAs and were directly injected in the central nervous system of SMA mice. Single RNA injections were able to elicit a robust induction of SMN protein in the brain and throughout the spinal column of neonatal SMA mice. Additionally, in a smaller percentage of animals, a single injection of RNA resulted

in sustained SMN expression five days post-injection. Exposure of bifunctional RNAs in the CNS of a severe SMA mouse model resulted in significant increases of weight, and a trend of increased survival. This technology has direct implications for the development of a SMA therapy, but also lends itself to a multitude of diseases caused by aberrant pre-mRNA splicing.

## INTRODUCTION

Spinal Muscular Atrophy (SMA) is the second most common autosomal recessive disorder with an incidence of 1 in 6000 (79) and a carrier frequency of 1 in 40 (126). SMA is caused by the loss of motor neurons and the subsequent atrophy of voluntary muscle groups. Mutations in the gene SMN1 have been linked to SMA development. SMN is ubiquitously expressed in all tissues and is a critical factor in a variety of RNA pathways. The best characterized role for SMN involves its role in the UsnRNP maturation pathway (127).

In humans there is a copy gene called SMN2, which primarily produces an alternatively spliced isoform and low levels of full-length protein. The alternative splicing event is due to a silent C to T nucleotide transition 6 nucleotides within exon 7 (22), altering an important SF2/ASF enhancer sequence within this region (56). Though both SMN1 and SMN2 encode identical proteins, the silent nucleotide transition initiates an alternative splicing event which is the default splice variant for *SMN2*, resulting in a dysfunction and unstable truncated protein (24). Therefore in the case of SMA, patients have a loss of SMN1 gene with an increased reliance on the low functioning gene SMN2

as the source of SMN protein. Since SMN2 can not encode for 100% full length RNA and thus protein, SMN2 can not provide protection from disease development.

SMN2 exon 7 is alternatively spliced due to the silent C to T transition mentioned above, but why is under debate. One arena of thought is that this transition disrupts an exonic splice enhancer sequence (ESE) that is usually bound by an SR family protein SF2/ASF (56). On the other hand there is data supporting that this nucleotide change encourages an hnRNP protein to bind by creating an exonic splice silencer sequence (ESS) (57). Overall it is understood that SMN2 exon 7 loses/gains a signal that is crucial for exon inclusion. However this is not the only inter-play of known splice signals. There are numerous splicing factors affecting the splice decision of exon 7 in the SMN2 transcript found both in exonic sequences and intronic sequences making the region around exon 7 a very complex milieu of splice signals working together (48, 95, 97, 128).

Since nearly all SMA patients retain two or more copies of SMN2, and since this gene has the capacity to encode the identical protein to SMN1, the SMN2 gene is an attractive target for potential therapies. Many synthetic and botanical compounds have been used to increase SMN protein levels by modulating SMN2 at any one of the steps from gene transcription to protein expression (99, 103, 115, 119, 129, 130). In addition there have been many antisense technologies used to specifically increase SMN protein expression from the SMN2 transcript (46, 48, 104, 108, 121, 131-134). Targeting the SMN2 transcript has been a growing trend with antisense technology for many reasons, but one of the most obvious is that of safety. These technologies remain very safe because targets to manipulate are only present when, where, and at what level the transcript is normally expressed. Recent antisense targets have been identified flanking

SMN2 exon 7 (46, 48), which adds to the number of regulating signals that work in unison resulting in the overall splice decision. One negative regulator was identified 10 nucleotides downstream of exon 7 called ISSN1 (46), while another was found to be upstream of exon 7 between nucleotides -67 and -112 designated Element 1 (48).

There has been a surge of interest in gene therapies involving small molecules, one example being antisense RNA. As the evolution of these varied therapies continue researchers are devising ways to increase the number of activities that one can commandeer or manipulate with the same short RNA. In our previous work we demonstrated the use of bi-functional RNAs in cell culture, and presented data suggesting this could be used in a rAAV vector delivery system (135). The term bi-functional RNA simply means an RNA that has two distinct functions, although those functions can be highly variable (136). In this case the bi-functional RNAs derive their name from two distinct regions of sequence, an antisense sequence linked by a non-specific 6 nucleotide domain to a high affinity exonic splice enhancer sequences (ESE) in triplicate (107, 135). These ESEs were designed to recruit positively acting SR or SR-like proteins. We improved upon our previous work by the creation of a bifunctional RNA targeting element 1 upstream of exon 7. Furthermore we identified two novel negatively acting proteins that bind specifically to Element 1 called PTB and FUSEBP, which have been shown to be negative regulators in other transcripts previously identified (52, 53, 137-139). These are the candidate proteins we are proposing that are displaced by the Element 1 target bi-functional RNAs. In continuation we show that the addition of 2'-O-methyl bifunctional RNAs to the CNS of SMA mice result in an increase in SMN protein induction, increase in weight gain and represent a novel gene therapy for SMA.

## RESULTS

### Deletion of Element 1 increases full length expression from SMN2

In the previously described bifunctional RNAs, the anti-sense component overlapped a critical regulatory region within exon 7 (135). As a means to enhance the effectiveness of a new class of bi-functional RNAs, we hypothesized that targeting an intronic regulatory element that inhibited the inclusion of SMN2 exon 7 with the anti-sense component of a bifunctional RNA would result in enhanced full-length expression. The two mechanisms of action that could lead to an enhanced full-length expression are: inhibition of the repressor via the anti-sense component, and increasing the local concentration of positively acting SR protein via the SR binding motifs. A previous report identified a potential negative regulatory element 67 nucleotides 5' of SMN exon 7, referred to as Element 1 (E1) (48). As E1 was only characterized in a heterologous exon-trapping vector system, we first sought to confirm the activity of this region in a more native genetic context. A small deletion was engineered into a SMN2 mini-gene that includes genomic SMN2 sequences from Exon 6 to Exon 8. RNA expression patterns of this mini-gene were analyzed by RT-PCR. Deletion of the E1 regulatory region dramatically altered SMN2 splicing such that the majority of SMN2-derived transcripts were full-length compared to the normally low levels of full-length transcript (Fig. 1A). Quantitation of RT-PCR confirmed an approximate 2-fold increase of exon 7 inclusion when E1 was deleted (Fig. 1B).

**PTB and FUSE-BP interact with Element 1**

To extend the genetic analysis and identify potential regulatory proteins that mediate the repressive activity of E1, RNA affinity chromatography was performed with a biotinylated synthetic RNA consisting of the entire E1 region. E1 RNA or a similarly sized control RNA was incubated in vitro with splicing competent HeLa nuclear extract, bound fractions were washed extensively, and RNA-associated factors were resolved on a denaturing gel (Fig. 2A). Two bands were specifically enriched in the E1 reactions compared to control reactions that used a similarly sized control RNA (Fig. 2A). The two specific bands were excised and analyzed by MALDI-TOF. Two previously described RNA binding proteins were identified: PTB and FUSEBP (Fig. 2A). As a confirmatory measure for this complex, an additional RNA affinity chromatography was performed and the gel was probed with an anti-PTB antibody, confirming the MALDI-TOF results (Fig. 2B). These results are consistent with E1 functioning as a negative regulator as PTB has been shown to function as a potent repressor of splicing in a variety of cellular contexts (137, 140). Additionally, FUSE-BP has been implicated in the regulation of mRNA expression including GAP-43 (138) , c-myc, and TF-IIH (141-143). Collectively, these results provide genetic and biochemical evidence that E1 is a bona fide negative regulator of SMN2 exon 7 inclusion. This evidence validates the strategy of targeting E1 with bi-functional RNAs as a means to further enhance SMN2 exon 7 inclusion.

**Development of Element 1 targeted bi-functional RNAs**

To identify an optimal anti-sense region that would effectively block E1 activity, a series of overlapping anti-sense RNAs ranging from 19-24 nucleotides in length were generated that sequentially progressed through the entire E1 sequence. However, none of the sequential anti-sense RNAs effectively inhibited E1 activity extensively (data not shown). An additional anti-sense RNA was designed that consisted of two non-sequential target sequences that effectively flank the entirety of the E1 region (Fig. 3). This strategy is similar to RNAs that were developed to functionally inhibit splice site recognition and to promote exon skipping in the dystrophin gene (144). Unlike the initial E1 anti-sense RNAs, the non-sequential anti-sense RNA effectively stimulated SMN protein levels (Fig. 6). Based upon this anti-sense sequence, two bi-functional RNAs were generated that contained binding platforms for SF2/ASF or hTra2β. These are well-described splicing factors that promote SMN2 exon 7 inclusion (56, 58) and functioned efficiently in the first generation of bi-functional RNAs. Additionally, a U7 stem-loop was included within the bi-functional RNA sequences since it has been shown that antisense effects can be increased by including a U7 snRNA-derived stem loop (104, 144-146). The bi-functional RNA sequences were cloned into the pMU2 vector under the expression control of a U6 or CMV promoter (135). A separate CMV-driven green fluorescent protein (GFP) is present on the vector and allows the detection of transfected cells.

**Plasmid derived Element 1 bi-functional RNAs increase SMN levels in patient fibroblasts**

In a first step towards the development of E1-targeted bi-functional RNAs, we transfected primary SMA type 1 patient fibroblasts, 3813 cells, with our pMU2 based

plasmids expressing the various E1 RNAs. These cells are a valuable model for assessing bi-functional RNA activity since they lack SMN1 and consequently express very low levels of SMN and contain very few nuclear gems (83). Plasmids were transfected into the 3813 patient fibroblasts and transfected cells were visualized 48 hours cells later by indirect immunofluorescence. Plasmid entry was identified by CMV-driven GFP expression and representative pictures are shown (Fig. 4A). Bi-functional RNAs were expressed under the control of the U6 promoter or the CMV promoter (as indicated). In addition to the bi-functional RNAs, control RNAs were also generated, including a similarly sized irrelevant RNA that was expressed from CMV-pMU2-U7 and an antisense RNA that targeted a region approximately 600 nucleotides upstream relative to exon 7. As expected, neither of these control RNAs increased SMN levels.

Expression of the E1-bi-functional RNAs or the E1 antisense RNA consistently increased SMN staining in the cytoplasm and in nuclear gems (Fig. 4A). Consistent with these observations, analysis of 100 transfected cells, as determined by GFP expression, demonstrated that gem numbers were significantly increased in cells treated with the bi-functional RNA vectors (Fig. 4B). Control RNAs did not increase the SMN positive gem numbers above the background of non-transfected cells (all E1 specific RNAs were statistically higher than controls; 1way ANOVA $p<0.0001$). However the antisense alone RNA did increase the gem number to about 70 nuclear gems in 100 cells (Fig. 4B). The E1 bi-functional RNAs increased gem numbers further than the gem numbers produced from the E1 antisense alone (Fig. 4B), the average of all bifunctional RNAs are approximately 30% higher than antisense alone (1way ANOVA of U6 driven bi-functional RNAs and antisense RNA $p=0.0005$). This suggests a potential dual mode of

action from the E1 bi-functional RNAs: 1) blocking a negative regulatory element in cis (E1) and recruiting positive regulatory factors, SR proteins. Interestingly the RNAs expressed by a U6 promoter increased gem numbers that were approximately 15-30% higher than the gem numbers from the CMV-driven counterparts (Fig. 4B). These results were also tabulated as "gems per nucleus" to exclude the possibility that a small population of cells had an aberrantly high number of gems, thus skewing the results. From these results, the majority of transfected cells expressing the E1 RNAs contained 1 or 2 gems per nucleus, consistent with numbers observed with carrier fibroblasts, 3814 cells (Fig. 4C).

**2'-O-methyl modified bi-functional RNAs increase SMN protein levels in primary patient fibroblasts**

As it is not currently practical to deliver plasmid-derived bi-functional RNAs as a SMA therapeutic, the previous qualitative analysis of bi-functional RNAs served as a proof-of-concept screen to determine whether E1 bi-functional RNAs could increase SMN levels. 2'-O-methyl RNAs are a more tractable therapeutic candidate and were therefore selected as the chemistry to analyze in the subsequent generation of bi-functional RNAs. The addition of the 2'-O-methyl chemistry stabilizes the RNA and allows for sustained activity *in vivo*. Manufactured RNA/DNA homologues have been used extensively in other disease models with encouraging results (131, 132, 147, 148). To initially verify that the 2'-O-methyl RNAs exhibited similar activities compared to the plasmid-derived RNAs, 2'-O-methyl bi-functional RNAs were transfected into 3813 cells and SMN protein was visualized by indirect immunofluorescence after 48 hours. Following

transfection of the bi-functional RNAs or E1 antisense RNA, SMN protein levels increased in the cytoplasm and gems were more readily detectable (Fig. 5A). Gem counts were performed on cell populations transfected with the various RNAs, however, in these experiments, it was not possible to identify the transfected cells since the RNA molecules were not tagged with a fluorescent moiety. Therefore, a larger number of cells were examined in each transfected population. 500 cells were counted in at least three separate experiments and the tabulated results demonstrate that E1 and the E1 bi-functional RNAs significantly increased SMN containing gems (Fig. 5B, 1way ANOVA $p<0.0001$) and that the majority of gem-positive cells contained 1-2 gems (Fig. 5C). In addition the bi-functional RNAs increased gems numbers above E1 antisense alone (Fig. 5B, 1way ANOVA $p=0.015$) The negative control RNA, D2-Selex, did not induce SMN protein (Fig. 5A). Consistent with these results, analysis of steady-state levels of SMN protein by western blot in extracts from transfected 3813 cells demonstrates that the 2'-O-methyl bi-functional RNAs elevate total SMN protein levels above untransfected and control transfected levels (Fig.6). These data identify RNAs that are capable of elevating SMN levels in a variety of cell-based assays and suggest that these molecules may be capable of increasing SMN levels in the more complex environment of the SMA mouse model.

**CNS delivery of 2'-O-methyl RNA into SMA mice increase SMN protein levels**

The subsequent experiments utilize a well described animal model of SMA (149). These animals lack endogenous murine Smn, but express transgenes for human SMN2 and a SMNΔ7 cDNA ($Smn^{-/-}$;$SMN2^{+/+}$; $SMN\Delta7^{+/+}$). These mice express an SMA phenotype that is very similar to the human form of the disease. This is categorized by low levels of

SMN protein which results in loss of motor neurons post-natally, a severe muscle atrophy and death at PND ~15. To deliver the RNAs to the central nervous system, we performed intra-cerebralventricular injections (ICV) on 2 day old SMA mice with the 2'-O-methyl RNAs (150, 151). Twenty four hours after ICV delivery of the RNAs, tissues were collected and SMN protein levels were analyzed (Fig. 7A). Delivery of either modified bifunctional RNA increased SMN protein levels in the brain (Fig. 7A). Additionally, this delivery procedure also likely allowed for transportation of the RNAs throughout the spinal column as evidenced by the increase in total SMN levels in extracts generated from the cervical, thoracic, and lumbar segments of treated mice (Fig. 7A). Analysis of 33 injected animals demonstrated that tissue extracts from 8/13 (Tra2-E1) or 5/10 (SF2-E1) treated animals exhibited a two-fold or greater increase in SMN protein levels (throughout the CNS, data not shown). Delivery of non-specific RNA or the injection procedure did not contribute to the SMN induction as evidenced by the low levels of SMN in control RNA/PBS treated animals (Fig. 7B).

To examine the sustainability of the SMN increase from a single injection, similar single ICV injections were performed on PND 2 SMA mice, however, tissues were collected 5 days post-injection. Subsequently SMN protein levels were detected by western blot (Fig. 8). Although not as reproducible, in all animals, we observed an SMN increase in tissue from 1 of 3 animals injected with the Tra2-E1 RNA such that levels were comparable to the unaffected heterozygote animal (Fig. 8). A lower percentage of animals examined at the 5 day time point exhibited a two-fold or greater increase in SMN levels, however, 2/9 animals did exhibit a two-fold increase (data not shown). Similar to the previous injections, bifunctional activity is detected distal from the injection site as

evidenced by the increase in SMN levels in various spinal cord sections, including the lumbar section (Fig.8). These results suggest that modified RNAs can have a sustained effect on the SMN protein levels. Furthermore we have shown an increase in the SMN protein in the tissue that is affected by SMA and this increase can be sustained for a period of time.

**CNS delivery of 2'-O-methyl bi-functional RNA increases weight gain in a more severe model of SMA mouse**

To examine the potential for physiological changes in the SMA mice we used a more severe mouse model for two reasons; 1) The severe mouse model experimental duration is much shorter than the Δ7 mice 2) The severity of the model could potentially be a benefit because a small change would be measurable rather than in a less severe model. The severe mouse model $SMN2^{+/+}Smn^{-/-}$(17) has an average life span of roughly 5 days with a very severe form of SMA that phenotypically coincides with the human form. These mice usually do not gain weight after birth and progressively lose weight until death. To examine a potential change in phenotype of these mice, ICV injections were performed on PND 2, and 4 with 6 μg of RNA delivered for Tra2-E1 or negative control Selex act. The Selex act RNA is a high affinity ESS in triplicate that is specific for hnRNPA1 but without an antisense domain. Thus this control has no targeting domain. After the first injection mice were weighed daily and data compiled (Figure 9A). Through random selection Tra2-E1 mice were born lighter than the negative control group however reached a higher average peak weight on PND 5 than negative control injection or non-injected (Figure 9A). A Kaplan-Meier curve shows a trend towards increased life span for the mice ICV injected with Tra2-E1 (Figure 9B, Mantel-Cox p=0.08). The

phenomenon of increased weight gain becomes clear when graphing the percent weight gain from PND 2 until peak weight. Mice injected with Tra2-E1 show a significant increase in weight gained from PND 2 to peak weight than both non-injected, and Selex act. injected mice (Figure 9C, 1way ANOVA $p=0.0015$, and t-test Tra2-E1:Selex act $p=<0.0001$). This data is in agreement with western blot data in the Δ7 mouse model where the Selex act did not increase SMN protein levels. This suggests that the action of both Tra2-E1 and the negative control is similar in both mouse models.

## DISCUSSION

In this study we verified the negative activity of Element 1 in a more natural context than previously published. In addition we identified two new proteins as the possible candidates to explain why Element 1 has a negative effect on SMN2 exon 7 splicing, PTB and FUSE-BP. We used this data as a rational for a new antisense technology directed to disrupt Element 1. We showed that these RNAs can increase a nuclear hallmark of natural SMN protein distribution both by plasmid and 2'-O-methyl RNA transfections. Furthermore upon ICV injection of the 2'-O-methyl bi-functional RNAs into SMA mice we observed an increase of the SMN protein to levels similar to heterozygous mice throughout the entire length of the spinal cord, and have the possibility to sustain this affect as long as five days after injection with the Tra2-E1 RNA.

The proteins FUSEBP and PTB identified to bind to Element 1 RNA have been implicated in de-regulating other transcripts. PTB has been identified as a repressor of splicing for α-tropomyosin (152), c-src (53), and FGFr-2 (52) among others. Additionally FUSEBP has been identified to inhibit TF-IIH (142), and plays a role in c-myc expression (141, 153). This supports the data shown here that both FUSEBP and PTB police RNA expression with implication for both being negative regulators.

The use of antisense RNAs in potential therapies is expanding to include many different diseases like Duchenne Muscular Dystrophy (DMD) (104, 131, 132, 154-158), and Amyotrophic Lateral Sclerosis (ALS) to name a few (148). These works are moving towards human gene therapy trials (159) and are examples of future directions for other

genetic diseases such as SMA. In the SMA field work has recently been done that shows use of antisense RNA (104, 131, 132) and negative bi-functional RNA (151) can increase SMN protein levels. The latter increased SMN protein levels in the brain of SMA mice via ICV injection. The work presented here furthers this work showing that the use of positive bi-functional RNAs can increase SMN protein levels in the CNS at a region distal to the injection sight.

ICV delivery has previously been described in a variety of genetic contexts, and this strategy has been used successful to deliver several viral-based gene vectors (160-162). Additionally, negatively acting bi-functional RNAs have been used in the SMA mouse model and were shown to increase SMN 24 hrs post-injection in brain extracts (151). This delivery paradigm represents an intriguing possibility for direct delivery to the central nervous system for therapeutic oligonucleotides, small molecules and viral vectors. As a means to determine the functionality of SMN inducing compounds in a relevant in vivo context, ICV delivery provides an excellent platform. The severe mouse model data suggests that ICV delivery of bi-functional RNAs can increase the weight gained from birth to peak in a severe model of SMA, and suggests a trend towards increasing the life span of these mice. The mouse data is in accord with the Δ7 western blot data where the Selex act. RNA did not have an affect on the SMN protein levels in the brain, and in the severe mouse model it did not increase weight gain or life span. However, it is clear that additional experimentation will be needed to determine whether the physiology of neonatal SMA animals is a tractable model that can be used to predict the potential clinical efficacy in human trials for ICV delivery.

With the viciousness of SMA affecting 1:6000 live births it is advantageous that we purse all types of potential therapies. This is one of the reasons why this paper presents data based both in a viral vector platform and modified oligonucleotide context. As of yet it is unknown where, when, or for how long the SMN protein is needed by the α-motor neurons to retain function and integrity. It is interesting that recent data suggests the SMN protein is needed in neurons for amelioration in a model of *C. elegans* (163) , and not skeletal muscle. Contrastingly, in a Drosophila model of SMA there appears to be a role for SMN in the muscle (164). This presents an interesting situation where it is imperative to study a wide range of therapies with different tropisms and pharmokinetics, because it is yet unknown what traits an ideal SMA therapy would need.

## MATERIAL AND METHODS

### Cloning

The Element 1 deletion construct was derived from the SMN2 minigene plasmid and the following primers (IDT, Coralville, IA, USA) were used to delete E1 by overlapping PCR. The orientation of the Element 1 region deletion is indicated by a **Δ** symbol. SMN E1 deletion: 5'-CTT AAT TTC TGA TCA TAT TTT GTT GAA TAA AAT AAG T**Δ**CT ATC TAT ATA TAG CTA TCT ATG TCT ATA TAG C-3' and 5'-GCT ATA TAG ACA TAG ATA GCT ATA TAT AGA TAG **Δ**ACT TAT TTT ATT CAA CAA TAA ATG ATC AGA AAT TAA G-3'. The U7-Opt-sm sequence was cloned into the pMU2 vector by overlapping PCR with DNA primers (IDT, Coralville, IA, USA); Frw, 5'-CCG CGG TCC TAG GAG CAT GCT AAA AAA AGG GGT TTT CCG ACC GAA GTC AGA AAA CCT GCT CCA AAA ATT ACT AGT TAA GCT GAT ATC TGA GC-3', Rev, 5'-GC TCA GAT ATC AGC TTA ACT AGT AAT TTT TGG AGC AGG TTT TCT GAC TTC GGT CGG AAA ACC CCT TTT TTT AGC ATG CTC CTA GGA CCG CGG-3' paired with plasmid specific primers previously published (133). pMU2-U7 plasmid was subsequently used in the cloning of the U6-promoter driven bi-functional clones. To make the CMV driven bi-functional RNAs the U6 promoter from the pMU2-U7 plasmid was digested with Pme1 and Sal1, then using CMV specific primers from the parent EGFP promoter CMV was subsequently cloned into the sites to make a CMV-pMU2-U7 parent plasmid. The bi-functional clones were generated with annealed complementary pairs of DNA oligonucleotides (IDT, Coralville, IA, USA) that were cloned into the pMU2-U7 vector between the BamHI and Spe1 sites.

Sequences for the E1 targetting clones are as follows: E1, top, 5'-GAT CCC TAT ATA TAG ATA GTT ATT CAA CAA AA-3', bottom, 5'-CTA GTT TTG TTG AAT AAC TAT CTA TAT ATA GG-3'; Tra2-E1, top, 5'-GAT CCG AAG GAG GGA AGG AGG GAA GGA GGA GAT CTC TAT ATA TAG ATA GTT ATT CAA CAA-3', bottom, 5'-CTA GTT TTG TTG AAT AAC TAT CTA TAT ATA GAG ATC TCC TCC TTC CCT CCT TCC CTC CTT CG-3'; SF2-E1, top, 5'-GAT CCC ACA CGA CAC ACG ACA CACG AAG ATC TCT ATA TAT AGA TAG TTA TTC AAC AAA A-3', bottom, 5'-CTA GTT TTG TTG AAT AAC TAT CTA TAT ATA GAG ATC TTC GTG TGT CGT GTG TCG TGT GG-3'.

**2'-O-Methyl Bi-functional RNA**

The following modified oligos were modified at every base with 2'-O-methyl groups (IDT, Coralville, IA, USA); Tra2-E1, 5'-GAA GGA GGG AAG GAG GGA AGG AGG CUA UAU AUA GAU AGU UAU UCA ACA AA-3', SF2-E1, 5'-CAC ACG ACA CAC GAC ACA CGA CUA UAU AUA GAU AGU UAU UCA ACA AA-3', and negative control RNAs; D2Selx 5'-AAG AUU AAA GAG UAA ACG UCC GGU ACC UAG GGA UAG GGA UAG GGA-3', Selex-act 5'-UAG GGA UAG GGA UAG GGA-3'. The modified oligos differ from the plasmid expressed bi-functional RNAs by the lack of a non-specific 6 nucleotide spacer sequence between the antisense domain and the SR recruitment domain, and furthermore do not have the U7-opt-sm sequence.

**Element 1Δ RT-PCR**

In vivo splicing assays were performed essentially as described previously. In brief, subconfluent HeLa cells were plated on a 60-mm dish and transfected with 1.0 μg of minigene plasmid using Lipofectamine 2000 per manufacturer's directions (Invitrogen). Total RNA was isolated 24 hours post transfection using TRIzol reagent (Invitrogen) and first-strand cDNA synthesis was performed using Super Script II (Invitrogen). To ensure only transfected minigene template was amplified, PCR primers that specifically anneal to the plasmid backbone common to all *SMN* minigene plasmids were used in the subsequent PCR amplification.

**RNA affinity chromatography**

The following 5'-biotinylated RNA corresponding to element 1 and a negative control RNA, respectively, were ordered(IDT, Coralville, IA, USA): 5'-GUA AAA UGU CUU GUG AAA CAA AAU ACU UUU UAA CAU CCA UAU AAA-3' , 5'-AGU CCU CAA CUU AGC CUC UAA CUU-3'. Control RNA was obtained (IDT, Coralville, IA, USA) with 5' biotinylation. This control was utilized as a negative control for interaction with PTB, and was composed of entirely purines: 5'-GAA GAA AGA GAA GAA AGA GAA GAA AGA -3'. RNA affinity chromatography was done as previously shown(132), but briefly the biotinylated RNAs were incubated with splicing competent HeLa cell nuclear-extract and avidin-agarose beads under splicing conditions, in the presence of heparin as a nonspecific competitor. The RNA and any interacting proteins were immunoprecipitated and washed. The proteins were then resolved on a 10% SDS-PAGE gel.

**Protein identification**

The Element 1 interacting proteins were visualized utilizing coommassie blue stain. Two specific bands were excised from the gel and sequenced using MALDI-TOF (University of Missouri Charles W. Gehrke Proteomics Center).

**Immunoflurescence imaging**

For all immunofluorescence staining, subconfluent type 1 pateint fibroblasts cells (3813 cells, Coriell Cell Repositories) were transfected in 8 chambered slides (BD Biosciences, Bedfored, MA, USA) with first plasimd clones using Lipofectamine 2000 reagent (Invitrogen) or 2'-O-methyl-RNA oligos using the same reagent, incubated for 48 hours in DMEM supplemented with 10% fetal bovine serum and antibiotics. Transfected cells were fixed with a solution of acetone/methanol (1/1 by volume) and then washed with phosphate-buffered saline (PBS) (Gibco). Fixed and washed cells were then blocked in PBS + 5% BSA and then washed again in PBS. A pooled group of three previously described anti-SMN monoclonal antibodies was added, diluted 1:10 in PBS + 1.5% BSA (119). Cells were washed again in PBS and a secondary mAB, an anti-mouse conjugated to Texas red (Jackson), or conjugated to FITC (Sigma) for either the plasmid or 2'-O-methyl transfected cell respectfully, diluted 1:200 in PBS + 1.5% BSA. After washing in PBS, DAPI was added to each chamber for 5minutes, and samples were washed again. Chambers were then fitted with coverslips using mounting media (DABCO, 2.3% (w/v), 10% PBS, 87.7% glycerol) and sealed with nail polish. Microscope images were captured using a Nikon Eclipse E1000 using Meta-Morph software. Cells for gem counting were

chosen at random. Each randomly-chosen nuclei was examined for nuclear gem accumulation and gems were counted.

**Western Blots**

For the PTB western blot proteins were transferred to PVDF membranes (Millipore), blocked overnight in 3% NFDM in TBST and probed with α-hnRNPI (PTB) antibody (Santa Cruz Biotechnology).

For the 2'-O-methyl RNA western blot, sub-confluent patient fibroblast cells (3813) plated on 60mm dishes were transfected with 100 ng of each indicated RNA using Lipofectamine 2000 reagent (Invitrogen). After 48 hours of transfection the cells were collected and proteins were resolved on a 12% SDS-PAGE gel. The gel was transferred to PVDF membrane (Millipore) and SMN immunoblot was performed using a SMN monoclonal antibody. A goat anti-mouse secondary antibody-conjugated to Horseradish peroxidase was used to detect the presence of the target protein by chemiluminescence (Pierce). The western was performed in triplicate and representative results are shown.

For the SMA mouse western blots, injected mice were handled by Animal Care and Use Committee (ACUC) regulations and tissues indicated were collected at selected time points and immediately placed in liquid nitrogen. Tissue was placed at -80$^{o}$C until ready for analysis. Roughly 100 mg of tissue was isolated and homogenized in JLB buffer (50 mM Tris-HCl ph 7.5, 150 mM NaCl, 20 mM $NaH_2(PO_4)$, 25 mM NaF, 2 mM EDTA, 10% glycerol, 1% Triton x-100, and 1x PIC ((Roche, Indianapolis, IN, USA)) and equal amounts of subsequent protein was loaded onto 12% SDS-PAGE gel. The SMN immunoblot was performed using a mouse SMN specific monoclonal antibody (BD

Biosciences, San Jose, CA, USA) diluted 1:3000 in TBST in 1.5% Dry Milk. Then blots were visualized by chemilumnescence on a Fujifilm imager, LAS-3000 and the corresponding LAS-3000 Image Reader software. To verify loading the westerns were then stripped using $H_2O_2$ for 30 minutes at room temperature and re-probed with anti-β-actin rabbit and anti-rabbit HRP. Western blots were done in quadruplicate or more and representative blots are shown.

**Animal Injections**

All animals were housed and treated in accordance with ACUC guidelines. $SMN2^{+/+}$, $SMN\Delta7^{+/+}$, $Smn^{-/-}$ mice (149) or $SMN2^{+/+}$, $Smn^{-/-}$ mice (17) were genotyped at day of birth, designated as day 1, and injected on day 2. A single intracerebralventricular (ICV) injections were performed on PND 2 neonates as previously described (150, 151, 162) for the Δ7 mice (Figure 7-8). For the Severe mouse model mice were ICV injected on PND 2, and 4 (Figure 9). Briefly, mice were immobilized via cryo-anesthesia and injected using μL calibrated sterilized glass micropipettes. The injection sight was approximately 0.25 mm lateral to the sagittal suture and 0.50-0.75 mm rostral to the neonatal coronary suture. The needles were inserted perpendicular to the skull surface using a fiber-optic light (Boyce Scientific Inc.) to aid in illuminating pertinent anatomical structures. Needles were removed after 15 seconds of discontinuation of plunger movement to prevent backflow. Mice recovered in 5-10 minutes in a warmed container until movement was restored. Single injections of 4μg of each 2'-O-methyl oligonucleotides were delivered via ICV described above for Δ7 mice, and severe mice were injected on PND 2 and 4 with 6μg of RNA (Figure 9).

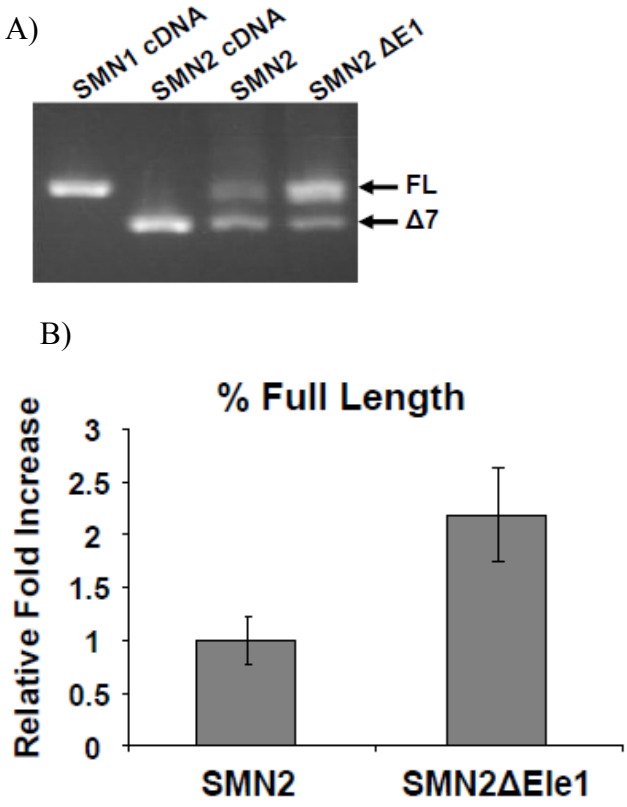


**Figure 1. Element 1 is a negative regulator of SMN 2 Exon 7 inclusion. (A)** RT-PCR of SMN minigenes transfected (1 μg) into HeLa cells and total RNA was isolated after 24hr of transfection. Bands of exon 7 and Δ7 are shown by use of previously published SMN minigene specific primers. **(B)** Quantification of RT-PCR performed in triplicate on transfected cells utilizing a Cy3 fluorescent primer pair specific to SMN minigene; independent experiments repeated 3 times. This quantification shows an approximately 2 fold increase of splicing to exon 7 when element 1 is deleted. P value ≤ 0.009.

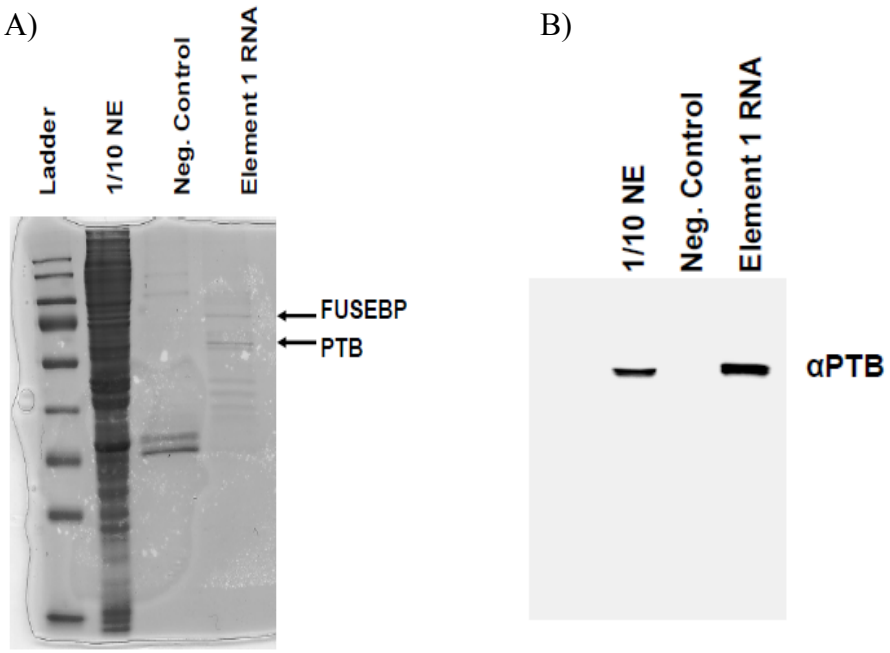


**Figure 2. Identification of PTB and FUSE-BP proteins bound to Element 1. (A)** RNA affinity chromatography with subsequent coommassie stain identified at least two specific proteins interacting with Element 1 but not control RNA. The bands were excised from the gel and MALDI-TOF identified PTB and FUSE-BP as the two unique bands. **(B)** Confirmation of PTB interaction with element 1. RNA-protein affinity chromatography was performed and the Western blot was developed using an anti-PTB specific antibody. PTB specifically interacts with element 1 RNA and not with the negative control RNA.

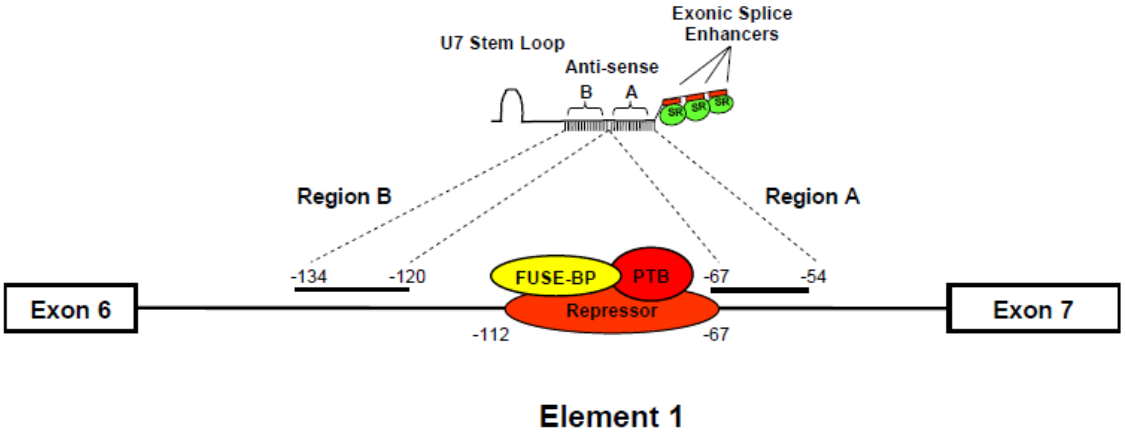


**Figure 3. Schematic of Element 1 specific Bi-functional RNAs**. The organization of the bi-functional RNA is illustrated with the split antisense domain targeting the sequences flanking Element 1, with the non-specific linker sequence and 3 tandem repeats of high affinity exonic splice enhancer sequences for either hTra2b1 or SF2/ASF. In addition the cartoon shows the orientation of the U7-sm-opt sequence found on the plasmid derived bi-functional RNAs.

A)

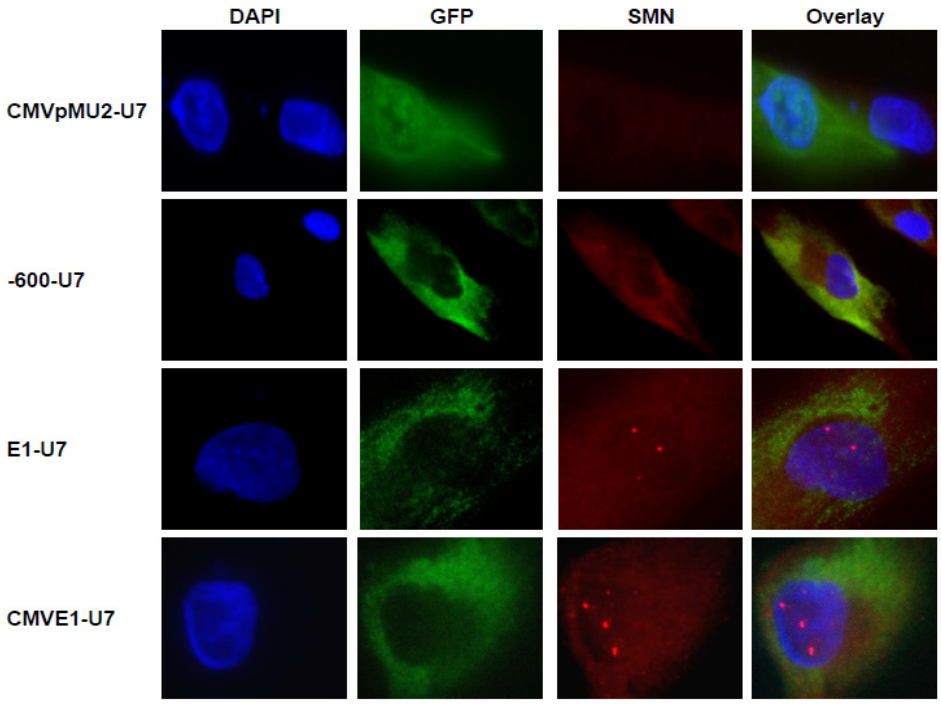
DAPI
GFP
SMN
Overlay
CMVpMU2-U7
-600-U7
E1-U7
CMVE1-U7

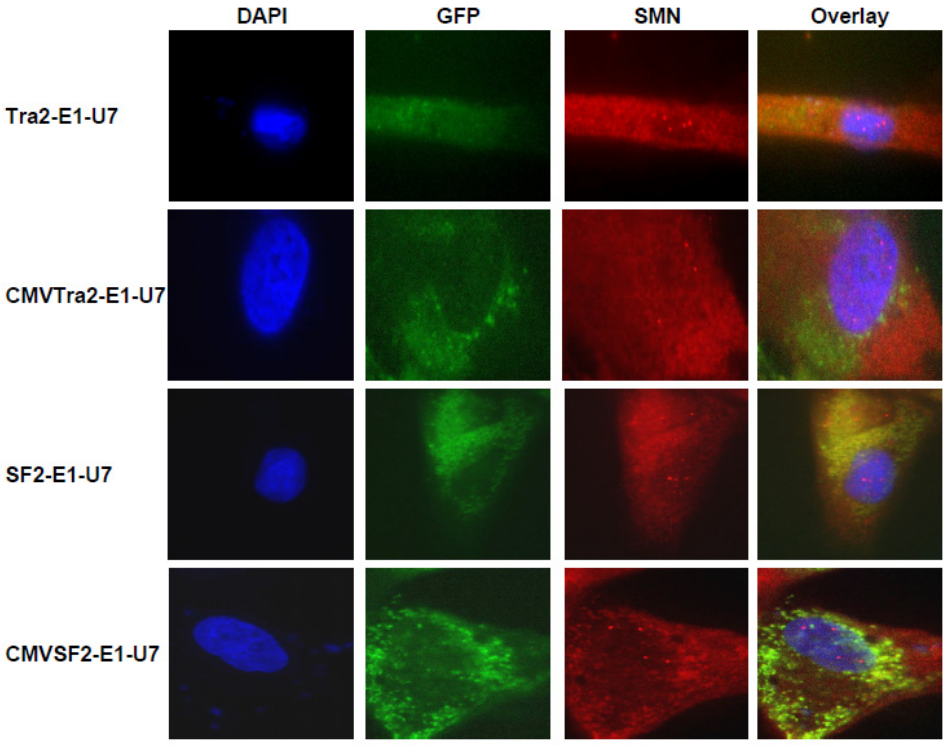
DAPI
GFP
SMN
Overlay
Tra2-E1-U7
CMVTra2-E1-U7
SF2-E1-U7
CMVSF2-E1-U7

B)

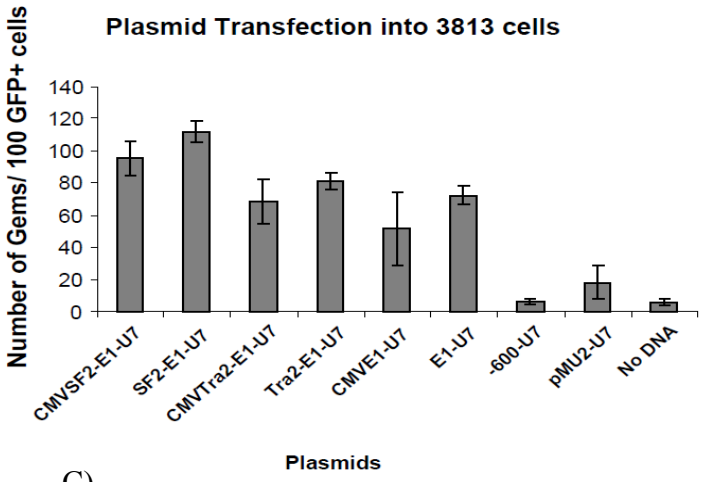


C)

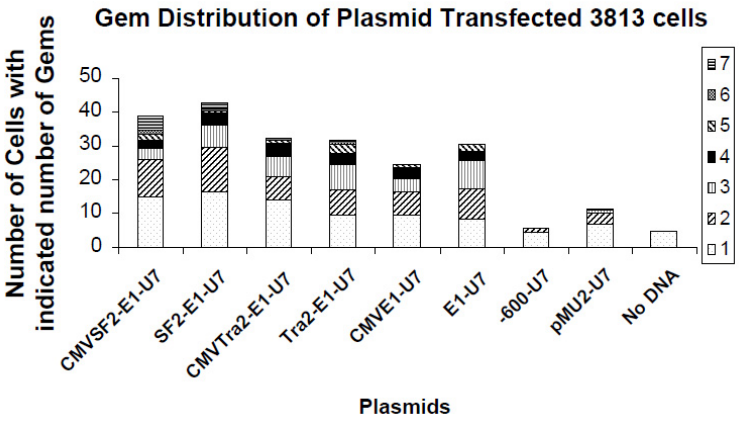


**Figure 4. Increase in SMN protein in presence of plasmid expressed Bi-functional RNAs**. **(A)** SMA type 1 fibroblasts (3813 cells) were transiently transfected with 1µg of plasmid DNA producing the indicated RNAs. Cells were incubated for 48 hours and an IMF was performed. Unless otherwise indicated the U6 promoter is driving expression. Transfected cells are identified by GFP expression. Pictures are of representative cells found for each sample. **(B)** 3813 cells transfected with plasmids were randomly selected and gem numbers compiled. 100 GFP positve cells were observed and SMN positive foci in the nucleus were counted.( n=3 and error bars are $^{\pm}$ STD) (all E1 specific RNAs were statistically higher than controls; 1way ANOVA $p<0.0001$) (1way ANOVA of U6 driven

bi-functional RNAs and antisense RNA p=0.0005) **(C)** Gem data compiled and now expressed as number of SMN positive gems per nucleus. (n=3)

A)

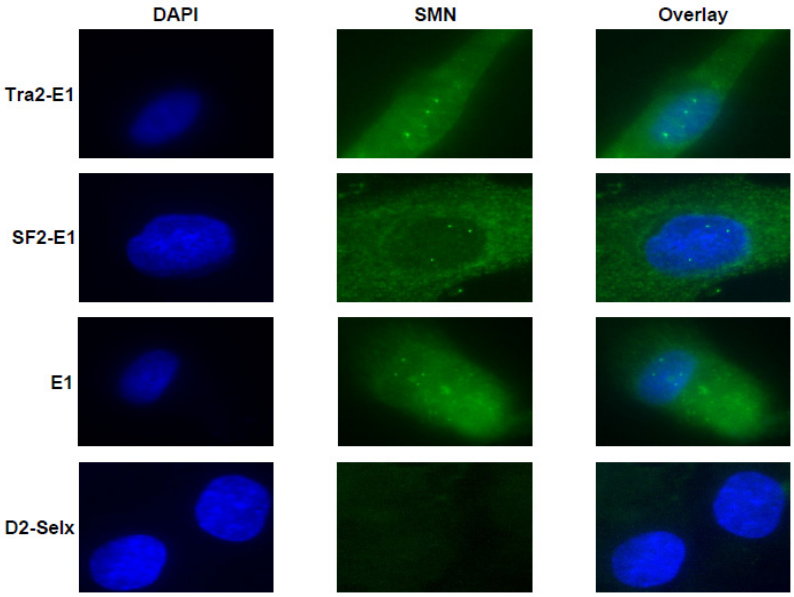
DAPI
SMN
Overlay
Tra2-E1
SF2-E1
E1
D2-Selx

B)

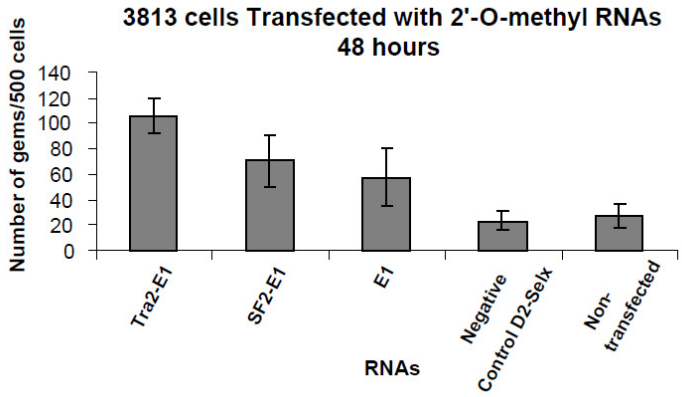
3813 cells Transfected with 2'-O-methyl RNAs
48 hours
Number of gems/500 cells
140
120
100
80
60
40
20
0
Tra2-E1
SF2-E1
E1
Negative Control D2-Selx
Non-transfected
RNAs

C)

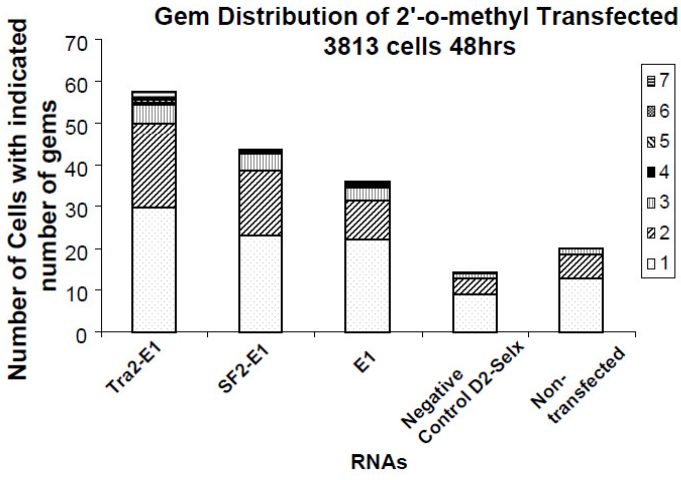
Gem Distribution of 2'-o-methyl Transfected
3813 cells 48hrs
Number of Cells with indicated number of gems
70
60
50
40
30
20
10
0
7
6
5
4
3
2
1
Tra2-E1
SF2-E1
E1
Negative Control D2-Selx
Non-transfected
RNAs

**Figure 5. Increase in SMN expression after transfection of 2'-O-Methyl-modified Bi-functional RNAs. (A)** SMA type 1 fibroblasts (3813 cells) were transiently transfected with 100 ng of 2'-O-methyl bifunctional RNAs for 48 hours. IMF staining was performed and images are of representative cells. **(B)** 500 3813 cells were randomly counted (n=4) and total gem number shown (error bars $^{\pm}$ STD) (all E1 targeted RNA show higher gems than negative control; 1way ANOVA $p<0.0001$) (bi-functional RNA is better than E1 alone, 1way ANOVA $p=0.015$). **(C)** Gem data compiled and expressed as the number of gems per nucleus (n=4).

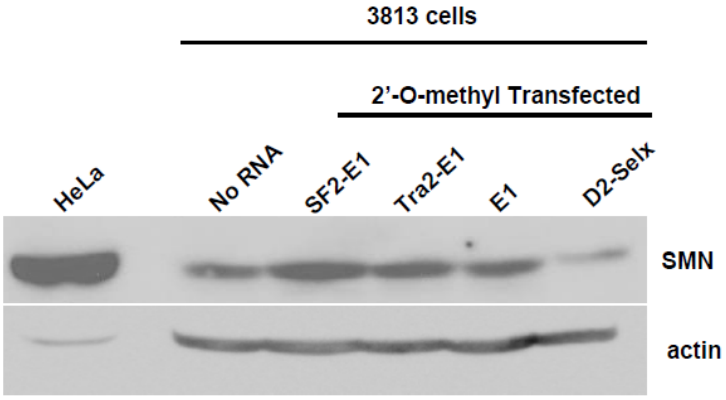


**Figure 6. 2'-O-Methyl Bi-functional RNAs increased total SMN protein levels in SMA fibroblasts.** Subconfluent 3813 cells were transfected with 100 ng of the indicated RNAs and subsequently incubated for 48 hours. Relative SMN protein levels were determined by western blot. HeLa cellular extracts were included as a size control.

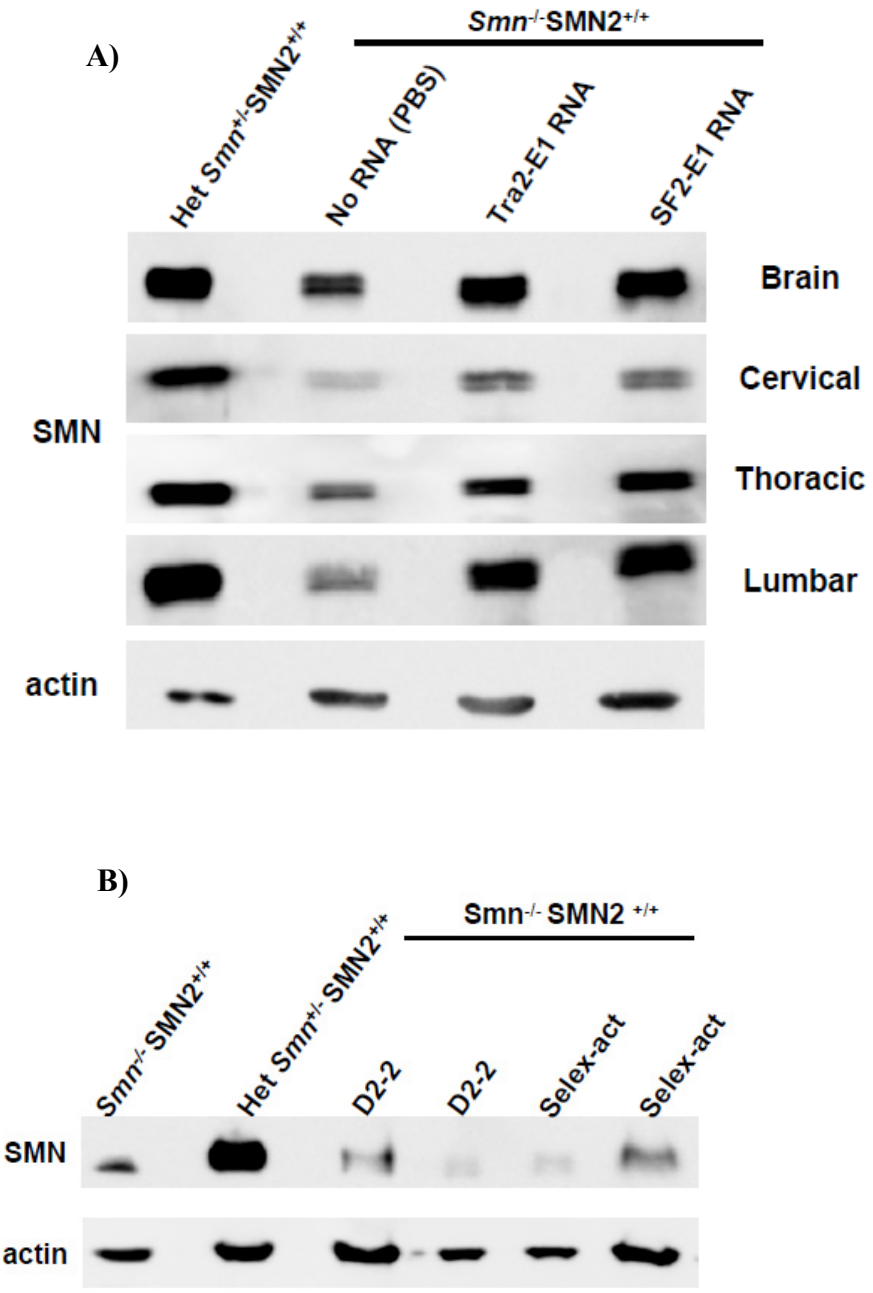


**Figure 7. ICV injection of 2'-O-Methyl Bi-functional RNAs increase SMN protein levels throughout the CNS. (A)** 2 DPN SMA mice were ICV injected with 4 µg of the modified bi-functional RNAs, SF2-E1 and Tra2-E1. Indicated tissues were isolated 24 hr after injections. RNAs were able to increase SMN protein levels all the way to the lumbar

region of the spinal cord. Western blots were done in quadruplicate, and representative blot is shown. Multiple mice were injected and tested data not shown. (Tra2-E1 (n=13) SF2-E1 (n= 10)) **(B)** 2 DPN SMA mice were ICV injected with 4 ug of modified control RNAs and brain tissue was isolated 24 hr post injection. SMN protein levels were observed by western blot which were done in triplicate, and a representative blot is shown.

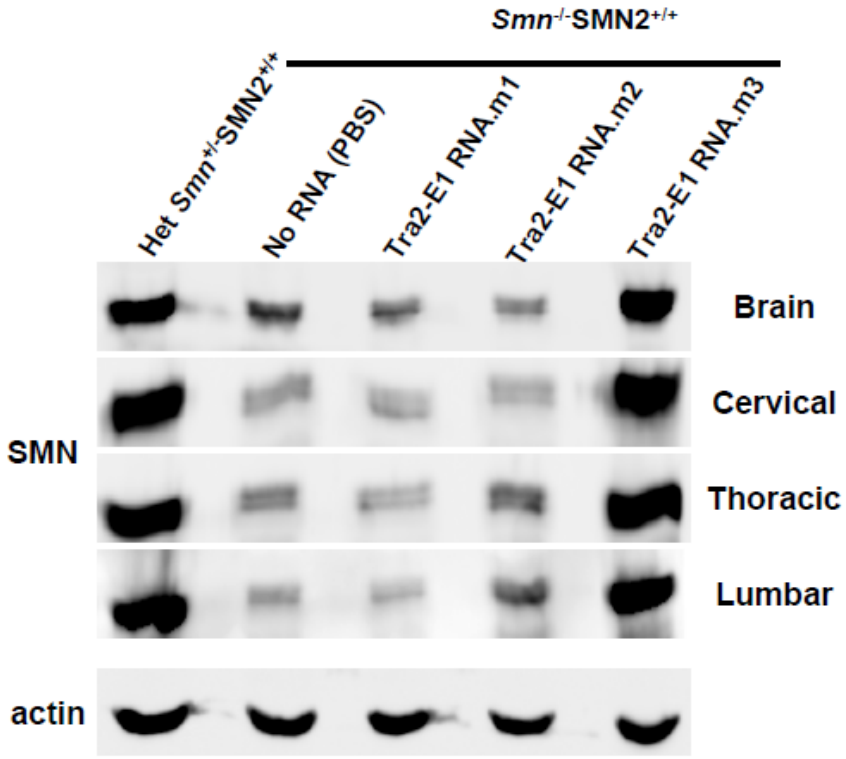


**Figure 8. ICV injection of Tra2-E1 modified Bi-functional RNA increase SMN protein levels 5 days after a single injection**. 2 DPN SMA mice were ICV injected with 4 µg of Tra2-E1 RNA. (The RNA that increased SMN levels more often (data not shown)) Five days following injection the indicated tissues were harvested and SMN western blot performed. Western blots were done in quadruplicate and representative blot is shown. One Tra2-E1 RNA injected mouse shows a dramatic increase in protein levels, suggesting SMN specific bi-functional RNAs have the ability to have a sustained effect.

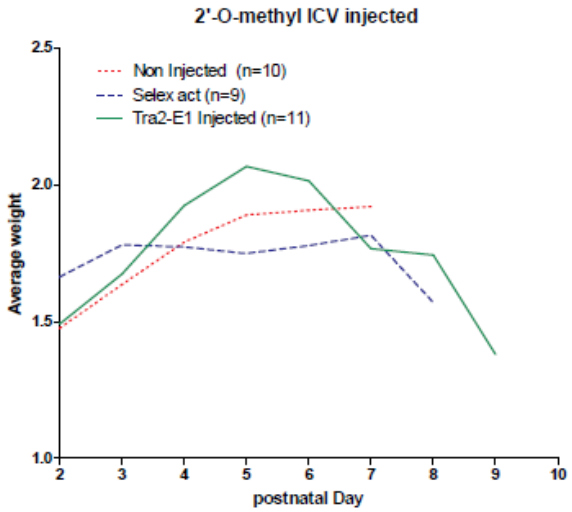
2'-O-methyl ICV injected
Non Injected (n=10)
Selex act (n=9)
Tra2-E1 Injected (n=11)
Average weight
2.5
2.0
1.5
1.0
2
3
4
5
6
7
8
9
10
postnatal Day

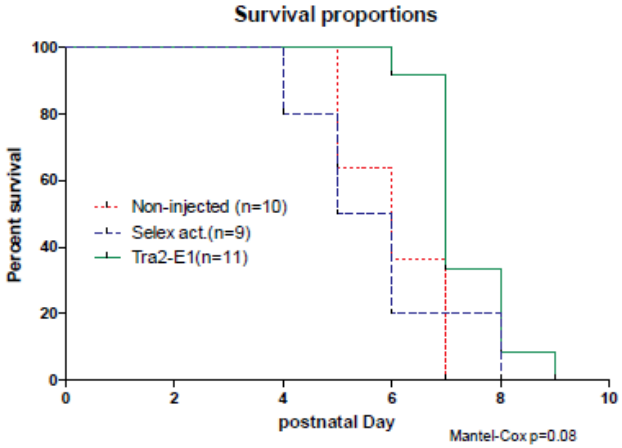
Survival proportions
Percent survival
100
80
60
40
20
0
Non-injected (n=10)
Selex act.(n=9)
Tra2-E1(n=11)
0
2
4
6
8
10
postnatal Day
Mantel-Cox p=0.08

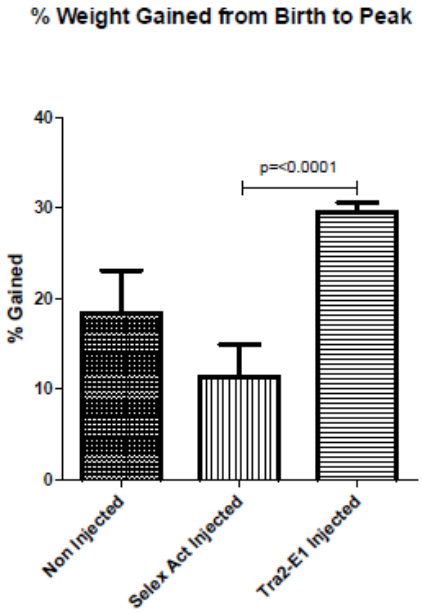
% Weight Gained from Birth to Peak
% Gained
40
30
20
10
0
p=<0.0001
Non Injected
Selex Act Injected
Tra2-E1 Injected

**Figure 9. ICV injection of 2'-O-methyl bi-functional RNA increases weight in a severe mouse model of SMA. (A)** 2 DPN severe mice were ICV injected on DPN 2, 4 with 6 μg of either Tra2-E1, or Selex activation RNA. Mice were weighed everyday post first injection and graphed. **(B)** Kaplan-Meier survival curve depicts a trend towards increased life expectancy for Tra2-E1 injected mice (Mantel-Cox p=0.08). **(C)** Percent weight gained from birth to peak weight. Tra2-E1 injected mice showed a significant weight gain from birth to peak over non-injected and Selex act. injected (1way ANOVA p=0.0015). There is a significant difference between Tra2-E1 and Selex act. injected mice as well (t-Test p=<0.0001).

**Bi-functional RNAs relieve repression of the ISSN-1 and lessen disease severity in a mouse model of SMA**

## ABSTRACT

Spinal muscular atrophy (SMA) is a progressive proximal motor neuron disease caused by the loss of *survival motor neuron-1* (SMN1). A nearly identical mirror copy gene called SMN2 is present in all SMA patients. Although the SMN2 coding sequence has the potential to produce normal, full-length SMN, roughly 90% of SMN2-derived transcripts are alternatively spliced and encode a truncated protein lacking the final coding exon (exon 7). SMN2 is an excellent therapeutic target since all SMA patients retain two or more copies of SMN2. Previously, we developed bifunctional RNAs that bound SMN exon 7, or a negative acting intronic splice silencer and increased SMN protein levels in patient fibroblasts and an SMA animal model. Recently a new splice silencer has been identified 10 nucleotides downstream of exon 7. We developed bi-functional RNAs that target the inhibitory sequence, and recruit positively acting splice signals. As a result, there is a two-fold mechanism for inducing full-length SMN expression: inhibition of the intronic repressor and recruitment of SR proteins via the SR-recruitment sequence of the bifunctional RNA. These new bifunctional RNAs increase a hallmark of SMN localization called gems in patient fibroblasts. Lead candidates were synthesized as 2'-O-methyl RNAs and were directly injected in the central nervous system of SMA mice. Double RNA injections were able to elicit increases in weight gain in a severe model of SMA mouse, however seemed to have no effect on the Δ7 mouse

model. This technology has direct implications for the development of a SMA therapy, but also lends itself to a multitude of diseases caused by aberrant pre-mRNA splicing.

## INTRODUCTION

Spinal muscular atrophy (SMA) is a devastating disease of children throughout the world. It is the 2nd most common autosomal recessive disorder (6), and the leading cause of infantile death. This is due to a proximal muscle atrophy that progresses radially until the diaphragm eventually can not function (165). However, the phenotype of muscle atrophy is not due to an inherent deficiency found in the muscles but rather a loss of functional motor neurons, starting with the degeneration of the ventral horn motor neurons (2). SMA has been linked to the loss of a single gene called Survival Motor Neuron 1 gene, or SMN1 (6-8). A nearly identical mirror copy gene called SMN2 is found in every human (166), and has been linked to a decrease in disease severity (16). The non-polymorphic nucleotide change found 6 nucleotides within a required exon (12), exon 7, causes an alternative splicing event (22). SMN2 represents a unique therapeutic target and it is reasonable to believe that modalities designed to increase exon 7 inclusion and thus full length (functional) protein could potentially decrease disease severity.

It is known that exon 7 has a weak 3' ss (105), possibly due to a suboptimal polypyrimidine tract, which was shown in chapter one. Furthermore exon 7 relies on alternative splice signals to obtain a basal level of exon retention (56, 58). These are examples indicating that exon 7 is highly regulated and requires additional auxiliary

signals for exon inclusion. Yet another factor that influences splice decision; a group recently identified a new ISS (intronic splice silencer) found 10 nucleotides downstream of exon 7 and continuous for 14 more nucleotides (46). This ISS was termed ISSN1. It was observed that moving the inhibitory region further away from exon 7 decreased the negative affect by ISSN1, suggesting that this regulator can lose its effect on exon 7. To help deregulate this region we developed bifunctional RNAs that were specific for ISSN1 and designed to recruit the positive splicing SR proteins SF2/ASF or SR like protein hTra2β1.

## RESULTS

### Development of ISSN1 targeted bi-functional RNAs

Similar to the previously described bi-functional RNAs we constructed RNAs that contained a sequence specific for ISSN1 to which we added in triplicate high affinity ESEs for either hTra2b1, or SF2/ASF. Both of these SR proteins have been previously shown to be positive splice signals in the SMN context (56, 58) and based on previously developed bifunctional RNAs had been shown to function in a positive manner in *trans* (135). In addition the bi-functional RNAs retained a U7 stem-loop sequence that mimics a natural U7 snRNA for enhanced nuclear retention and cellular stability (104, 144-146). Each RNA was cloned into the pMU2 vector described previously and were placed under the expressional control of either the CMV promoter or a U6 promoter (Figure 1).

### Plasmid derived ISSN1 bi-functional RNAs increase SMN levels in patient fibroblasts

To determine potential activity in a disease-relevant context we cloned the bifunctional RNA sequences into pMU2 (135, 151) plasmid and transfected them into type 1 primary patient fibroblasts (3813). These are a reasonable model to assess bi-functional RNA activity because they have no copies of SMN1, two copies of SMN2, and very low levels of SMN protein and SMN positive gems. Cells transfected with antisense RNA directed against ISSN1, or their bi-functional counterparts both increased SMN protein levels in the cytoplasm and nuclear gems (Figure 1A). Transfected cells can be readily identified due to the plasmid-derived expression of GFP. Therefore, in the initial screening of the bi-functional expressing plasmids, we were interested in identifying GFP-positive cells. Since gem number is an accepted method for indirect measurement of SMN protein levels semi-quantitative gem counts were performed. We quantified 100 GFP expressing cells and compiled the number of gems in those cells (Figure 1B, n=3 or more, with error bars as $\pm$STD). We show that overall gem numbers are increased after transfection of the plasmids producing the antisense RNA (1way ANOVA p=0.0002). In addition the bi-functional RNAs increased the gem numbers further (1 way ANOVA p=0.0354), and our negative controls do not show an appreciable increase in gems per 100 cells. To ensure that the overall gem profile was normal the data is expressed as gem per nuclei which describe the number of cells with indicated number of nuclei in them (Figure 1C). Distribution numbers suggest that transfection reaches a fairly large population and the majority of cells gain 1 to 2 gems per cell, similar to carrier primary fibroblasts (3814 cells) (Figure 1C).

**2'-O-methyl modified bifunctional RNAs increase SMN protein levels in primary patient fibroblasts**

2'-O-methyl RNAs are a more attractive therapeutic candidate compared to plasmid derived transcripts and were therefore selected as the modification to analyze in the subsequent generation of bifunctional RNAs. Even though the pMU2 plasmid has the capacity to be packaged into rAAV vectors modified oligos are still a very attractive therapeutic when considering the severity of mouse models that will be eventually used. Severe SMA mice do not survive past PND 5 and rAAV vectors have a variable expression profile in vivo with the majority of expression not being turned on until after 4-6 days. This could mean that rAAV production of RNA would not be early enough in the disease progression to have a beneficial affect. The addition of the 2'-O-methyl chemistry stabilizes the RNA and allows for sustained activity *in vivo*. Manufactured RNA/DNA homologues have been used extensively in other disease models with encouraging results (131, 132, 147, 148). As a proof of principle experiment primary patient fibroblasts were transiently transfected with the modified RNAs; Tra2-ISSN1 or SF2-ISSN1. After 48 hours cells were visualized by indirect immunofluorescence against the SMN protein (Figure 3A). From this figure it is apparent that cells transfected with the synthetic oligos have an increase in cytoplasmic SMN and gain nuclear gems similar to the carrier fibroblasts (3814 cells) (Top Row Figure 3A). Semi-quantitative analysis indicates that cells transfected with bi-functional RNAs show a increase in gem number in 500 randomly selected cells (Figure 3B, n=3 or 4).

**2'-O-methyl modified bifunctional RNAs do not have a positive effect in the Δ7 SMA mouse model**

The experiments in this section utilize a well described animal model of SMA (149). These animals lack endogenous murine Smn, but express transgenes for human SMN2 and a SMNΔ7 cDNA ($Smn^{-/-}$;$SMN2^{+/+}$; $SMN\Delta7^{+/+}$) these mice live longer than the severe mouse model roughly PND 13. Placement of the modified oligos are the highest priority. Though it is still unknown why there is a specific loss of motor neurons seen in the mouse model it is reasonable to theorize it will be of some benefit to increase SMN protein levels in the CNS. Localization to the CNS was achieved by ICV injection on PND 2 of SMA mice (150, 151). A routine of an injection every other day for the first six days of life was implemented for the following experiments. Injections were on PND 2, 4, and 6 which delivered 6 ug of RNA per injection. RNAs tested for these experiments were Tra2-ISSN1 and Scramble. Tra2-ISSN1 is the bifunctional RNA designed to bind to ISSN1 and recruit hTra2β1 to the region down stream of exon 7. Scramble RNA is a previously published RNA that has no sequence homology in either mouse or human genomes (148). Total weights of mice were measured everyday and graphed (Figure 4A). There is not an increase in body weight between PBS injected (n=6), Scramble injection (n=8), or Tra2-ISSN1 (n=5) injected. Furthermore there was no statistical significance in the percent of weight gained from birth to peak between the RNA injected mice and PBS injected mice (student t-test p=0.106) (Figure 4B). To asses overall gain of mobility within experimental mice we performed time to right experiments and graphed the percentage of mice that can right themselves after being placed in a prone position. A positive time to right requires the mice do so within 60 seconds of being placed on their

back and maintain all four limbs on the ground for at least 2 seconds. Though we see a higher percentage of Tra2-ISSN1 injected animals able to right between 10 and 13 days, this effect was lost, and is not significant (Figure 4C, 1way ANOVA p=0.48). Even though the Scramble injected mice have an increase in ability to right this was also not significant over PBS injected (t-test p=0.219). Finally a Kaplan-Meier survival curve shows no significant difference between any groups of experimental mice tested (Mantel-Cox p=0.29) (Figure 4D). These experiments indicate that an ISSN1 directed bi-functional RNA does not have the ability to significantly change the mouse model by the assay we tested. Similar to the other project however we wanted to assess the RNAs ability to affect the severe mouse model, which could be more amenable to 2-O-methyl RNA therapy.

**2'-O-methyl modified bi-functional RNAs increase weight and life span in the severe mouse model**

Differing from the previous experiments this section employs the use of a severe animal model of SMA (17). These animals lack endogenous murine Smn, but express the transgenes for human SMN2 ($Smn^{-/-}$;$SMN2^{+/+}$). The following results are preliminary and there are future plans to increase the experimental number. Since this mouse model has an average life span of around 6-7 days (17), the injection routine has been modified. The mice received 6 ug of RNA at PND 2 and 4 ICV followed by continued monitoring for the duration of the experiment. Total weights are graphed and Tra2-ISSN1 (n=1) injected mouse shows an increase in weight gain compared to control mice (non-injected n=8, Scramble injected n=8) (Figure 5A). Furthermore the mouse showed an increase in

percent weight gained and survival (Figure 5B, 5C).Though this is still very preliminary data it is encouraging to speculate that the severe mouse model is tractable to modified oligo therapies.

## DISCUSSION

Alternative splicing is a complex event in which many *cis*- and *trans*- elements work congruently in a dynamic fashion to ultimately lead to a splice competent pre-mRNA and eventually an mRNA. It has been shown previously that SMN2 exon 7 predominately travels along an alternative splicing path that leads to a majority of transcripts skipping the required exon. Its predominance for alternative splicing adds an even greater burden on alternative splice signals to enhance the overall splice fidelity. It has been previously shown there are a multitude of alternative splice signals within and flanking exon 7. Compared to exonic *cis* elements the role of intronic *cis* elements is less understood (167), and there has yet to be a method to predict intronic *cis* sequences (168).

Previously it has been shown that SMN2 exon 7 has a weak 5'ss (96) possibly due to a non-consensus U1 snRNA binding site found with in that region. In the effort to fully understand the splice signals in that area Singh et. al. determined that there was a unique silencer adjacent to the U1 binding site found within intron 7 that can modulate exon 7 fate in splicing (46). This region was named ISSN1, for intronic splice silencer N1. They showed that moving this 14 base pair region further away from exon 7 (from +10 bp, to +35) abolished its negative effect on exon 7 inclusion. In an attempt to investigate the

exact region of inhibition they reported that the use of an antisense oligo nucleotide directed against ISSN1 could restore exon 7 inclusion, but not an oligo just 5 nucleotides removed (46). This became part of the impetus for the creation of a bi-functional RNA directed against ISSN1. In addition to ISSN1's known silencing action and our previous results with other bi-functional RNAs that target negative regions we developed a group of bi-functional RNAs that target ISSN1 and presumably recruit positive splice factors. In this study plasmid-derived and 2'-O-methyl modified bi-functional RNAs directed against ISSN1 increased SMN positive nuclear structures (gems) found in patient fibroblasts. In addition the application of 2'-O-methyl bi-functional RNAs into the Δ7 SMA mouse model did not result in a significant change in weight, weight gain, time to right, nor life span. However in a severe mouse model Tra2-ISSN1 oligo increased overall weight, percent weight gain, and life span. Though the experimental number is too low to perform statistics this represents an encouraging result and further investigation is warranted. The severe mouse model represents a potential avenue that will allow measurement of physiological changes that are perhaps too small in the Δ7 model. This initial data is the basis of continued research toward a potential SMA therapy using a ISSN1 directed bifunctional RNA.

## MATERIALS and METHODS

### Cloning

The U7-Opt-sm sequence was cloned into the pMU2 vector as previously described. Briefly overlapping PCR was performed with DNA primers (IDT, Coralville, IA, USA); Frw, 5'-CCG CGG TCC TAG GAG CAT GCT AAA AAA AGG GGT TTT CCG ACC GAA GTC AGA AAA CCT GCT CCA AAA ATT ACT AGT TAA GCT GAT ATC TGA GC-3', Rev, 5'-GC TCA GAT ATC AGC TTA ACT AGT AAT TTT TGG AGC AGG TTT TCT GAC TTC GGT CGG AAA ACC CCT TTT TTT AGC ATG CTC CTA GGA CCG CGG-3' paired with plasmid specific primers previously published(133). pMU2-U7 plasmid was subsequently used in the cloning of the U6-promoter driven bi-functional clones. To make the CMV driven bi-functional RNAs the U6 promoter from the pMU2-U7 plasmid was digested with Pme1 and Sal1, then using CMV specific primers from the parent EGFP promoter CMV was subsequently cloned into the sites to make a CMV-pMU2-U7 parent plasmid. The bi-functional clones were generated with annealed complementary pairs of DNA oligonucleotides (IDT, Coralville, IA, USA) that were cloned into the pMU2-U7 vector between the BamHI and Spe1 sites. Sequences for the ISSN1 targetting clones are as follows: ISSN1, top, 5'-GAT CCG ATT CAC TTT CAT AAT GCT GGA-3', bottom, 5'-CTA GTC CAG CAT TAT GAA AGT GAA TCG-3'; Tra2-ISSN1, top, 5'-GAT CCG AAG GAG GGA AGG AGG GAA GGA GGT GAT CAG ATT CAC TTT CAT AAT GCT GGA-3', bottom, 5'-CTA GTC CAG CAT TAT GAA AGT GAA TCT GAT CAC CTC CTT CCC TCC TTC CCT CCT TCG -3'; SF2-ISSN1, top, 5'-GAT CCC ACA CGA CAC ACG ACA CAC GAT GAT CAG ATT CAC TTT CAT AAT GCT GGA-3', bottom, 5'-CTA GTC CAG CAT TAT GAA AGT GAA TCT GAT CAT CGT GTG TCG TGT GTC GTG TGG-3'.

**2'-O-Methyl Bi-functional RNA**

The following modified oligos were modified at every base with 2'-O-methyl groups (IDT, Coralville, IA, USA); Tra2-ISSN1, 5'-GAA GGA GGG AAG GAG GGA AGG AGG GAU UCA CUU UCA UAA UGC UGG-3', SF2-ISSN1, 5'-CAC ACG ACA CAC GAC ACA CGA GAU UCA CUU UCA UAA UGC UGG-3', and negative control RNAs; D2Selx 5'-AAG AUU AAA GAG UAA ACG UCC GGU ACC UAG GGA UAG GGA UAG GGA-3', Selex-act 5'-UAG GGA UAG GGA UAG GGA-3', Scramble 5'-CCU UCC CUG AAG GUU CCU CC-3'. The modified oligos differ from the plasmid expressed bi-functional RNAs by the lack of a non-specific 6 nucleotide spacer sequence between the antisense domain and the SR recruitment domain, and furthermore do not have the U7-opt-sm sequence.

**Immunoflurescence imaging**

For all immunofluorescence staining, subconfluent type 1 pateint fibroblasts cells (3813 cells, Coriell Cell Repositories) were transfected in 8 chambered slides (BD Biosciences, Bedfored, MA, USA) with first plasimd clones using Lipofectamine 2000 reagent (Invitrogen) or 2'-O-methyl-RNA oligos using the same reagent, incubated for 48 hours in DMEM supplemented with 10% fetal bovine serum and antibiotics. Transfected cells were fixed with a solution of acetone/methanol (1/1 by volume) and then washed with phosphate-buffered saline (PBS) (Gibco). Fixed and washed cells were then blocked in PBS + 5% BSA and then washed again in PBS. A pooled group of three previously described anti-SMN monoclonal antibodies was added, diluted 1:10 in PBS + 1.5% BSA (119). Cells were washed again in PBS and a secondary mAB, an anti-mouse conjugated

to Texas red (Jackson), or conjugated to FITC (Sigma) for either the plasmid or 2'-O-methyl transfected cell respectfully, diluted 1:200 in PBS + 1.5% BSA. After washing in PBS, DAPI was added to each chamber for 5 minutes, and samples were washed again. Chambers were then fitted with coverslips using mounting media (DABCO, 2.3% (w/v), 10% PBS, 87.7% glycerol) and sealed with nail polish. Microscope images were captured using a Nikon Eclipse E1000 using Meta-Morph software. Cells for gem counting were chosen at random. Each randomly-chosen nuclei was examined for nuclear gem accumulation and gems were counted.

**Animal Injections**

All animals were housed and treated in accordance with ACUC guidelines. $SMN2^{+/+}$, $SMN\Delta7^{+/+}$, $Smn^{-/-}$ mice(149) or $SMN2^{+/+}$, $Smn^{-/-}$ mice (17) were genotyped at day of birth of, designated as day 1, and injected on day 2. Intracerebralventricular (ICV) injections were performed on PND 2, 4 and 6 neonates of Δ7 mice as previously described (150, 151, 162). In the severe mouse ($SMN2^{+/+}$, $Smn^{-/-}$) studies mice were ICV injected on PND 2, and 4 only. Briefly, mice were immobilized via cryo-anesthesia and injected using μL calibrated sterilized glass micropipettes. The injection site was approximately 0.25 mm lateral to the sagittal suture and 0.50-0.75 mm rostral to the neonatal coronary suture. The needles were inserted perpendicular to the skull surface using a fiber-optic light (Boyce Scientific Inc.) to aid in illuminating pertinent anatomical structures. Needles were removed after 15 seconds of discontinuation of plunger movement to prevent backflow. Mice recovered in 5-10 minutes in a warmed container

until movement was restored. Injections of 6 μg of each 2'-O-methyl oligonucleotides were delivered via ICV described above for all mice.

**Figures**

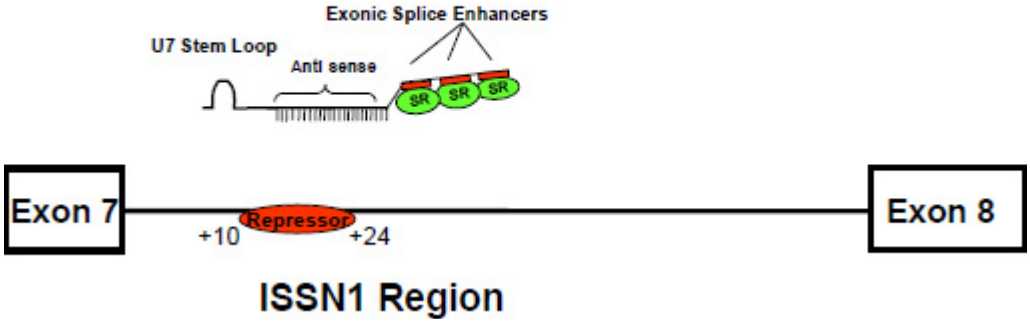


**Figure 1. Schematic of ISSN1 targeting bifunctional RNA.** The ISSN1 bifunctional RNAs have a uninterrupted antisense specific for ISSN1 with an additional 6 nucleotides downstream to ensure coverage of the negative region. In addition the RNA has a linked domain that contains in triplicate ESE high affinity enhancer region that is a recruitment domain. The U7 stem-loop has an optimized sm core binding domain for improved nuclear localization (above natural U7snRNA) and concentration in that sub-cellular compartment.

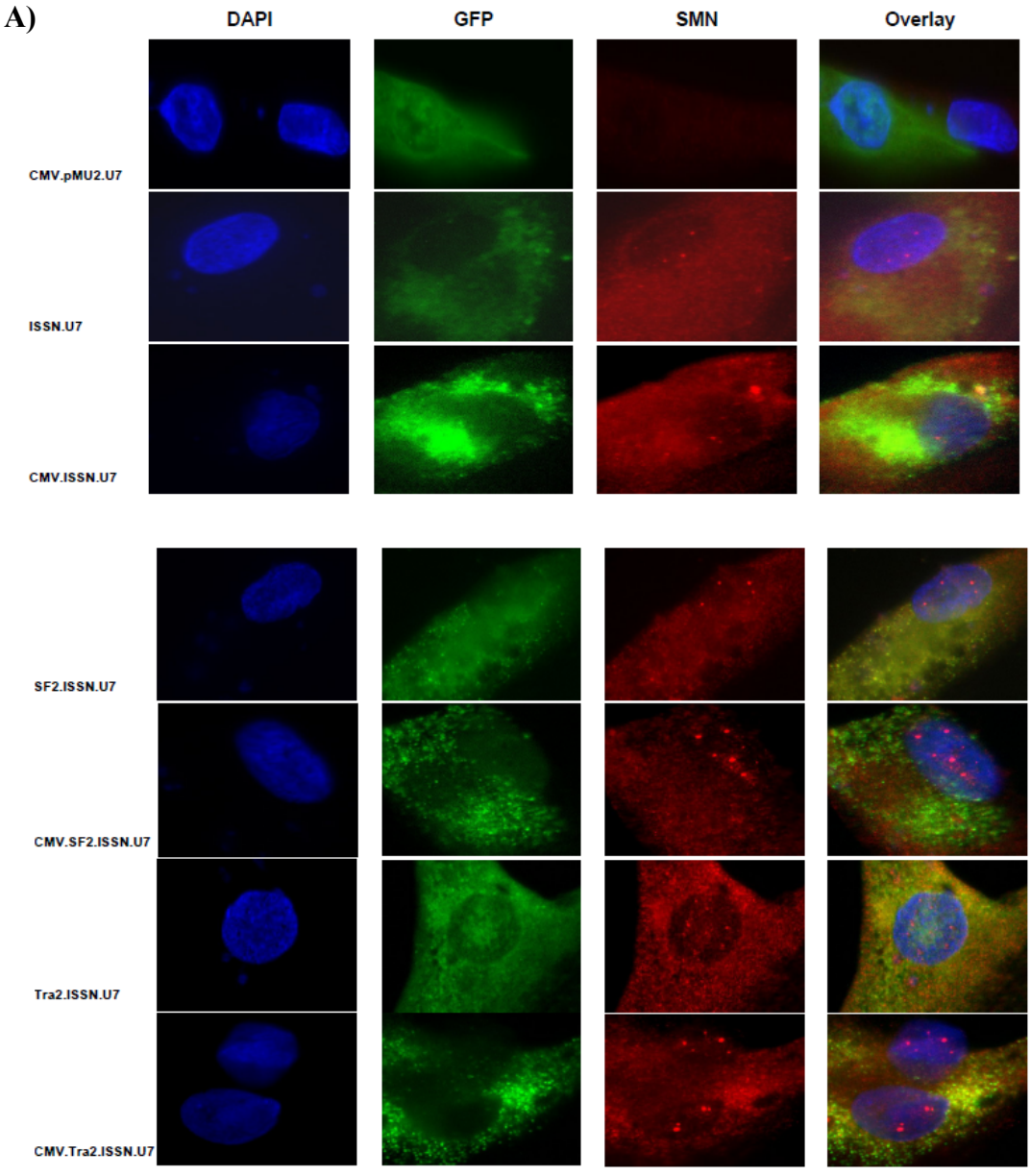
A)
DAPI
GFP
SMN
Overlay
CMV.pMU2.U7
ISSN.U7
CMV.ISSN.U7
SF2.ISSN.U7
CMV.SF2.ISSN.U7
Tra2.ISSN.U7
CMV.Tra2.ISSN.U7

**B)**

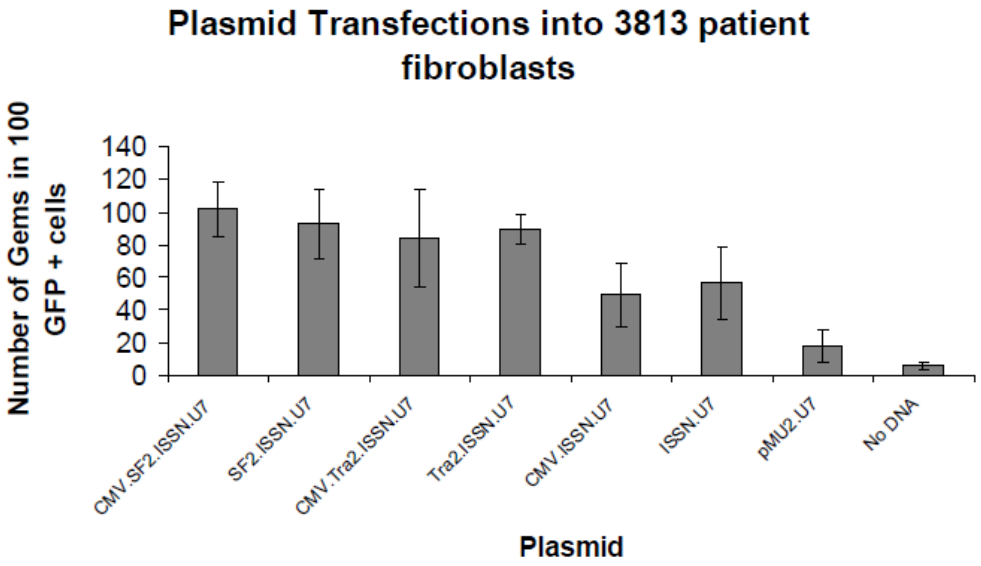


**C)**

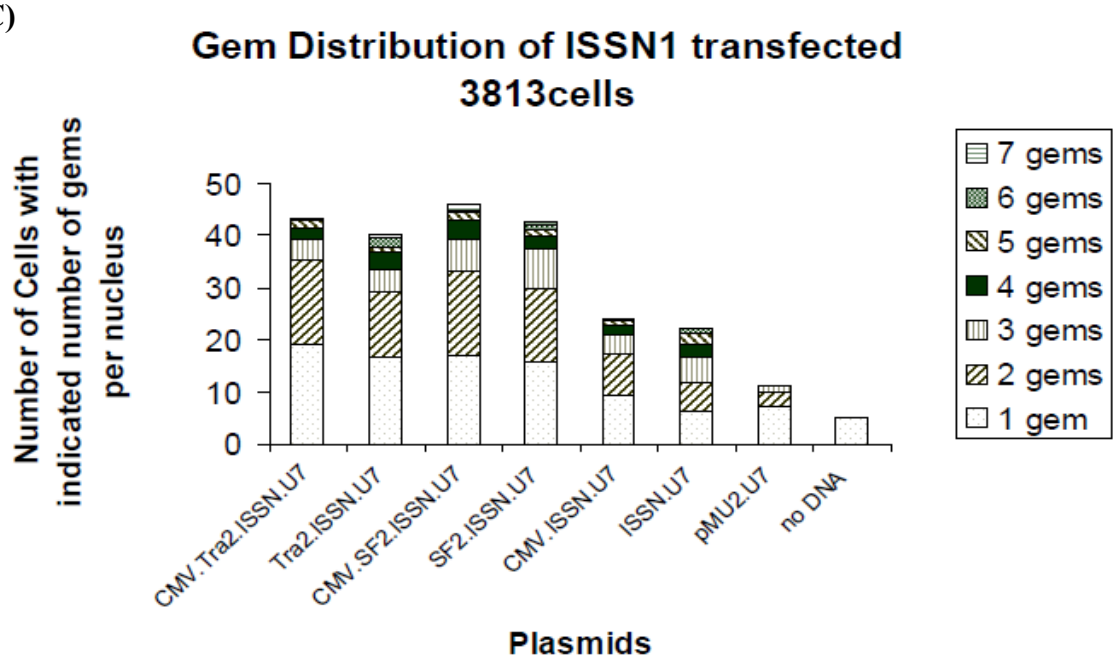


**Figure 2. ISSN1 Plasmid Transfection increases SMN protein levels in primary patient fibroblasts. (A)** SMA type 1 fibroblasts (3813 cells) were transiently transfected with 1 µg of plasmid DNA producing the indicated RNAs. Cells were incubated for 48 hours and an IMF was performed. Unless otherwise indicated the U6 promoter is driving expression. Transfected cells are identified by GFP expression. Pictures are of

representative cells found for each sample. **(B)** 3813 cells transfected with plasmids were randomly selected and gem numbers compiled. 100 GFP positve cells were observed and SMN positive foci in the nucleus were counted.( n=3 or more, and error bars are $\pm$ STD) (all RNA specific for ISSN1 showed an increase in gems, 1 way ANOVA p= 0.0002) (Bi-functional RNA increased Gem number above antisense alone, 1way ANOVA p=0.0354) **(C)** Gem data compiled and now expressed as number of SMN positive gems per nucleus. (n=3)

**A)**

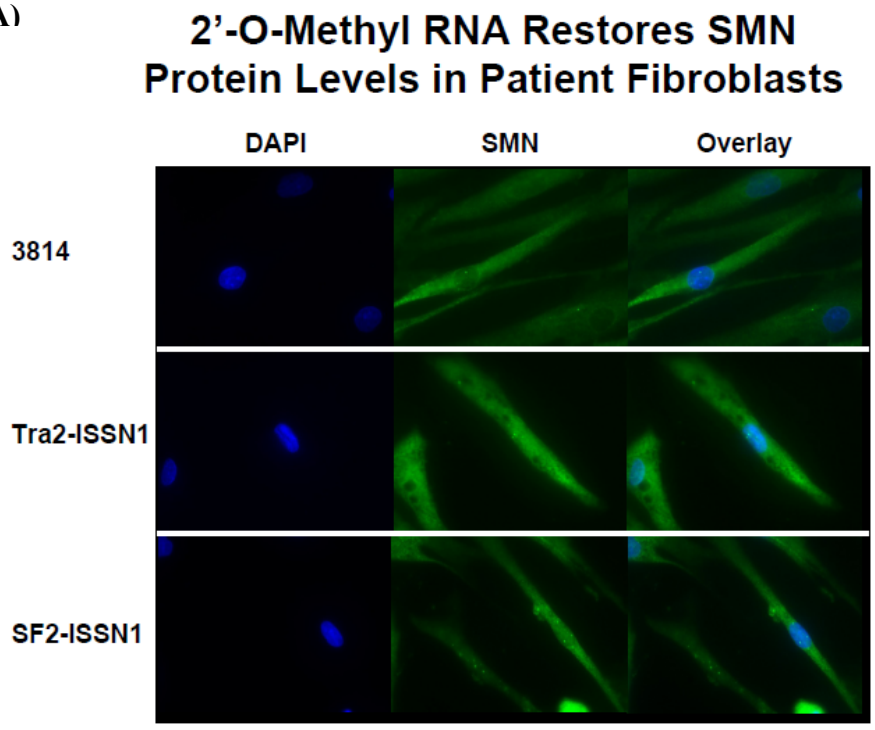

**B)**

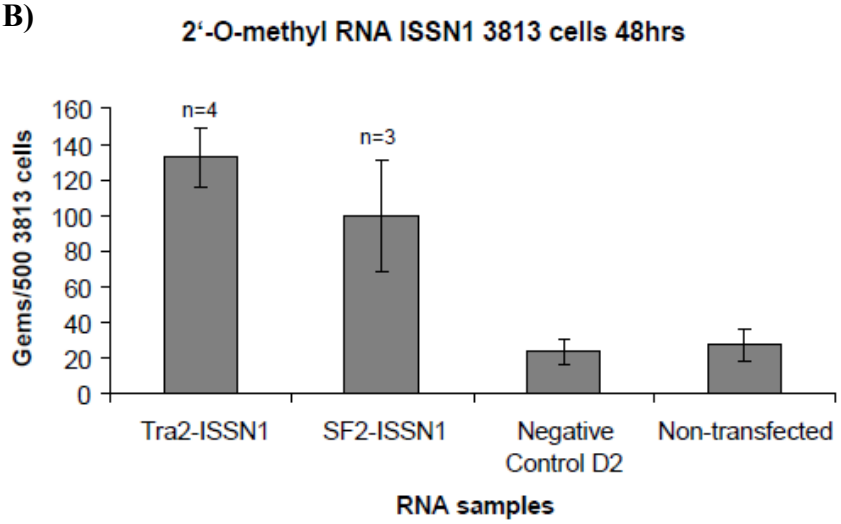


**Figure 3**. **2'-o-methyl RNA increases SMN protein and gem number in patient fibroblasts. (A)** SMA type 1 fibroblasts (3813 cells) were transiently transfected with 100ng of 2'-O-methyl bifunctional RNAs for 48 hours. IMF staining was performed and images are of representative cells. 3814 cells are shown in the top row as positive control staining **(B)** 500 3813 cells were randomly counted (n=4 or n=3) and total gem number shown (error bars $^{\pm}$ STD).

**A)**

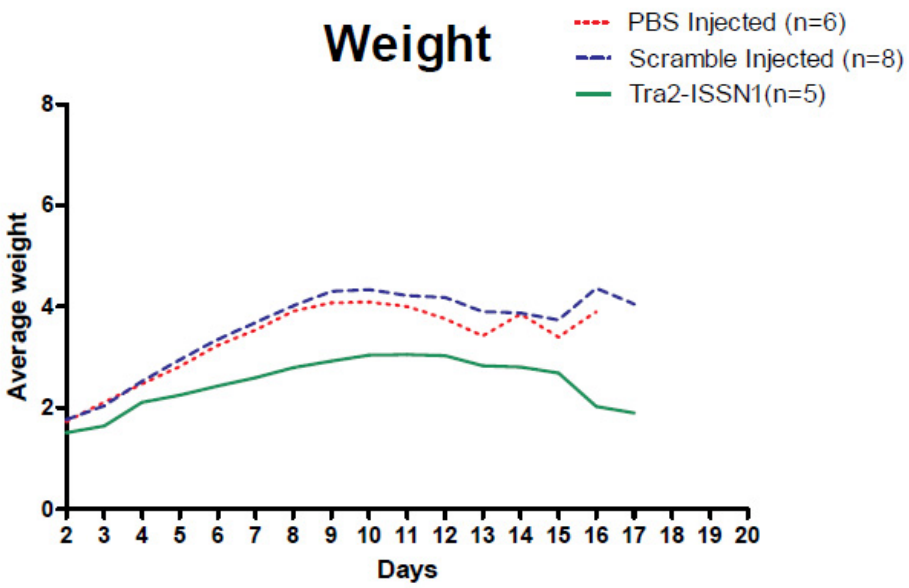
Weight
PBS Injected (n=6)
Scramble Injected (n=8)
Tra2-ISSN1(n=5)
Average weight
0
2
4
6
8
2 3 4 5 6 7 8 9 10 11 12 13 14 15 16 17 18 19 20
Days

**B)**

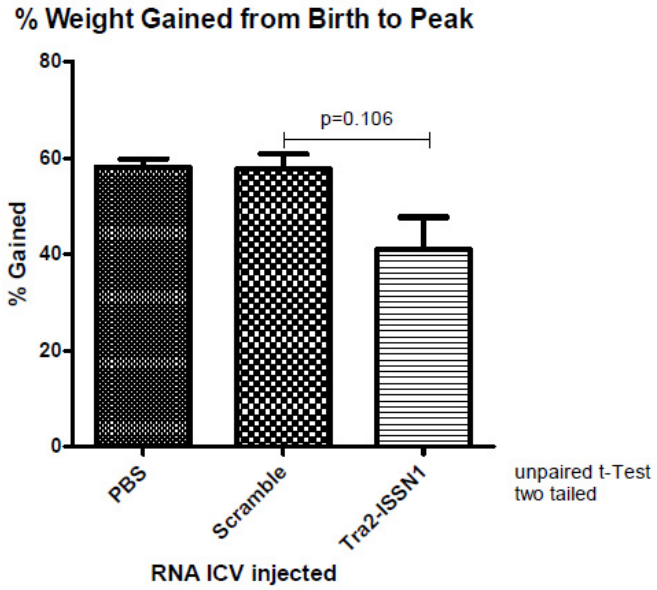
% Weight Gained from Birth to Peak
% Gained
0
20
40
60
80
p=0.106
PBS
Scramble
Tra2-ISSN1
unpaired t-Test
two tailed
RNA ICV injected

C)

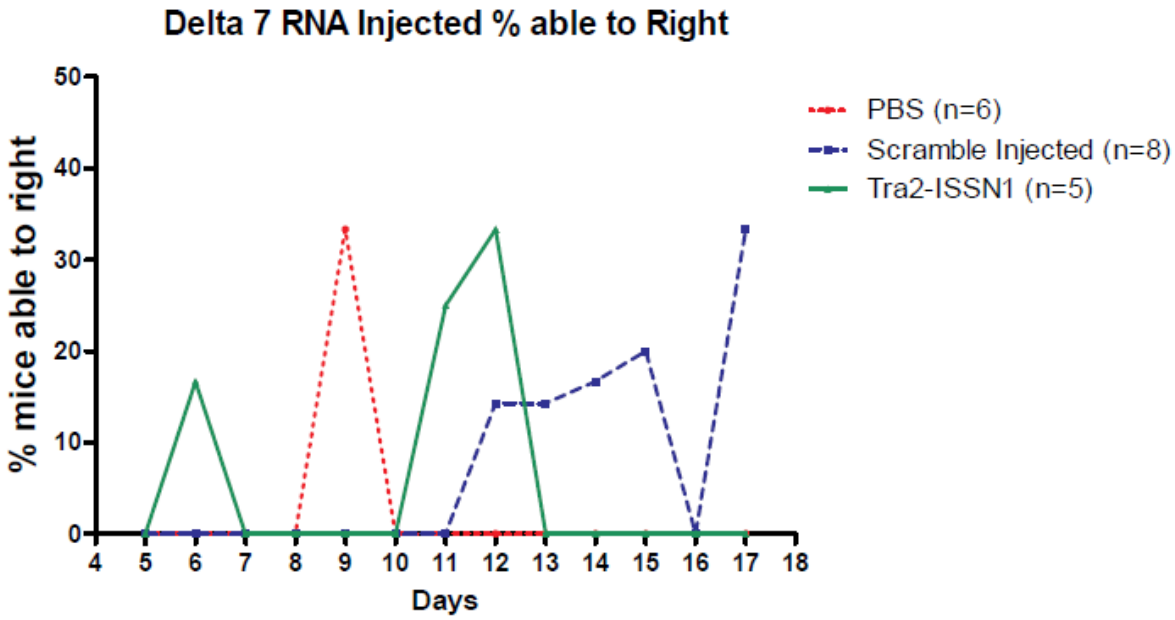


D)

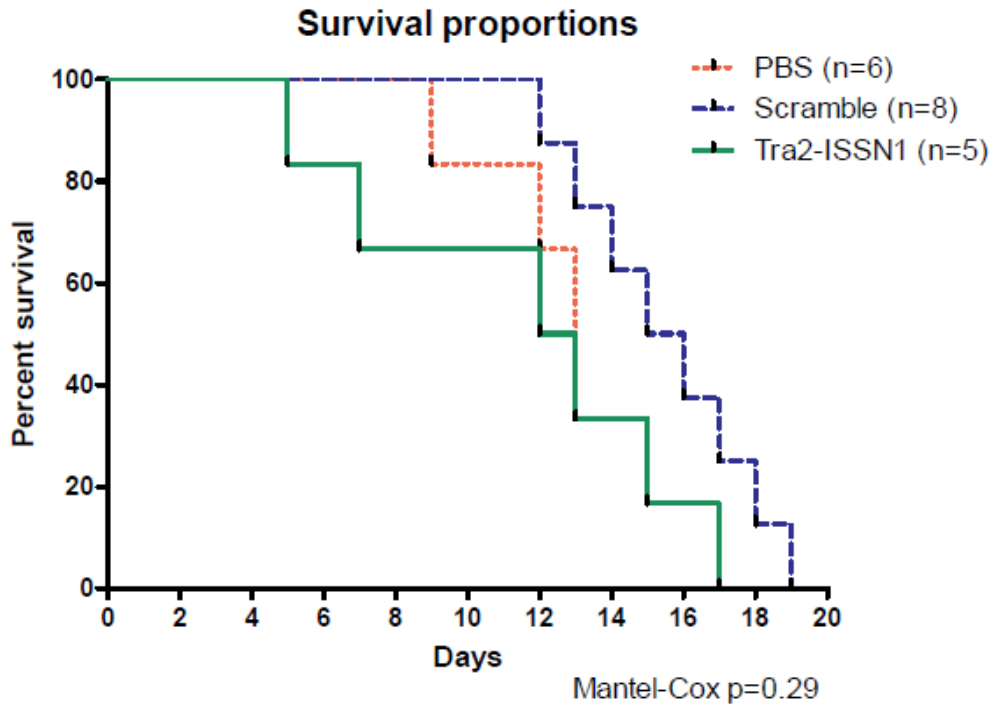


**Figure 4. Δ7 mice ICV injection of 2'-O-methyl ISSN1 Bi-functional RNAs. (A)** Total body weight was measured daily for PBS, Scramble, and Tra2-ISSN1 injected mice **(B)** The weight gained from birth to peak was also compared between mouse populations (unpaired student t-test p=0.106) **(C)** Overall fitness was assessed by the ability of the mice to right themselves from a prone position. (1way ANOVA p=0.48) Scramble RNA increase is not significant over PBS (t-test p=0.219). This graph is representing the

percentage of mice able to right themselves with in 60 seconds **(D)** Kaplan-Meier survival curve of bifunctional RNA injected mice, PBS, or Scramble RNA (Mantel-Cox p=0.29).

**A)**

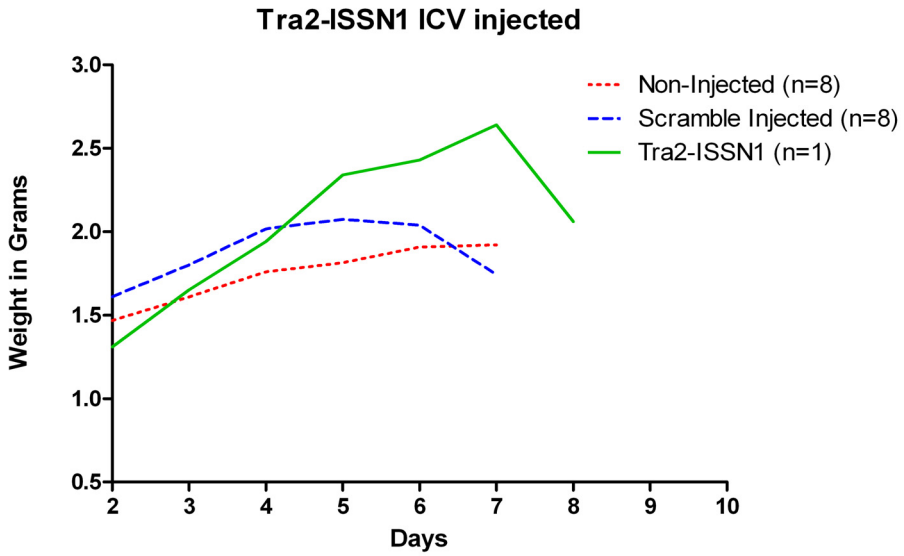


**B)**

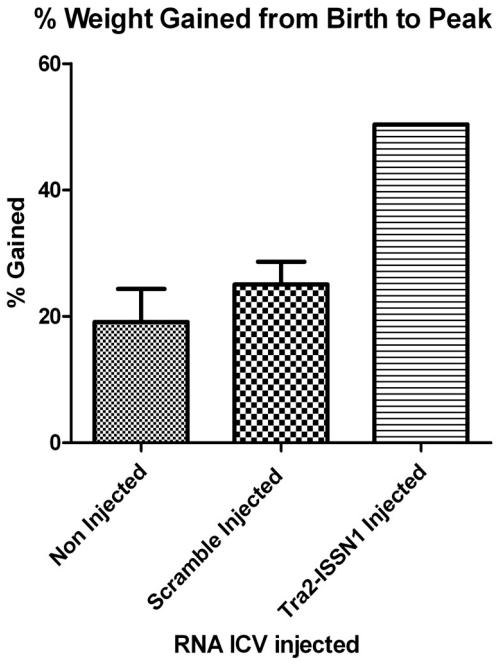

C)

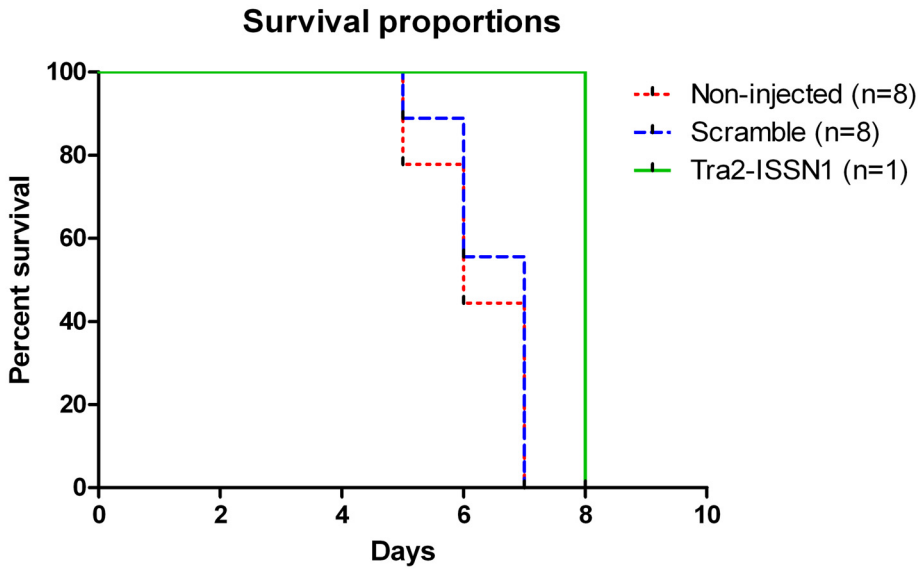


**Figure 5. Severe mice ICV injection of 2'-O-methyl ISSN1 Bi-functional RNAs. (A)** Total body weight was measured daily for non-injected, Scramble, and Tra2-ISSN1 injected mice **(B)** The weight gained from birth to peak was also compared between experimental mice **(C)** Kaplan-Meier survival curve of bifunctional RNA injected mice, PBS, or non-injected.

**Development of a dual therapeutic approach; antisense oligonucleotide can enhance trans-splicing of SMN2 transcripts**


## ABSTRACT

RNA modalities are developing as a powerful means to re-direct pathogenic pre-mRNA splicing events. Improving the efficiency of these molecules *in vivo* is critical as they move towards clinical applications. Spinal muscular atrophy (SMA) is caused by loss of SMN1. A nearly identical copy gene called SMN2 produces low levels of functional protein due to alternative splicing. We previously reported a *trans*-splicing RNA (tsRNA) that re-directed SMN2 splicing. Here we show that reducing the competition between endogenous splices sites enhanced the efficiency of *trans*-splicing. An antisense oligo nucleotide (ASO) was developed that bound to the downstream splice decision to competitively inhibit downstream ligation. This in turn increases the inclusion of the tsRNA splicing event. The ASO-tsRNA vector significantly elevated SMN levels in primary SMA patient fibroblasts. This dual therapeutic technique increased SMN-dependent *in vitro* snRNP assembly, in addition to increasing SMN protein levels within the central nervous system of SMA mice, though a detailed description of the *in vivo* work is beyond the scope of the chapter. These results demonstrate that the ASO-tsRNA strategy provides insight into the *trans*-splicing mechanism and represents a means of significantly enhancing *trans*-splicing activity *in vivo*.


## INTRODUCTION

*Trans*-splicing has recently been used as a potential therapeutic intervention for a multitude of genetic diseases. The potential effectiveness of this strategy has been demonstrated in a variety of diseases including spinal muscular atrophy, cystic fibrosis, hyper-IgM X-linked immunodeficiency, hemophilia A, Alzheimer's disease, and epidermolysis bullosa simplex with muscular dystrophy (122, 169-172). *Trans*-splicing is a natural, albeit infrequently utilized process in mammals, therefore, maximizing efficiency is central to developing *trans*-splicing therapeutics (173). Conceptually, this strategy relies upon nuclear pre-mRNA splicing occurring between two different molecules: 1) the mutant endogenous RNA and 2) the exogenous therapeutic RNA that provides the correct RNA sequence via a *trans*-splicing event.

Spinal Muscular Atrophy (SMA), a neurodegenerative disorder, is caused by the homozygous loss of *survival motor neuron 1* (SMN1) and is the leading genetic cause of infantile death (79, 174). In humans two copies of the *SMN* gene exist, SMN1 and SMN2 (8). The critical distinction between the two genes occurs at the RNA processing level: SMN1 produces full-length transcripts, while SMN2 primarily produces an alternatively spliced transcript lacking the final coding exon (8). A single silent C to T non-polymorphic nucleotide difference is responsible for disrupting a critical splice enhancer element in SMN2 exon 7 (22, 56).

SMN2 is retained in essentially all SMA patients and is a primary target for SMA therapeutic development (175). In addition to the identification and development of small molecules that stimulate full-length SMN2 expression, RNA modalities such as antisense oligonucleotides (ASO), TOES/bi-functional RNAs and *trans*-splicing RNAs have shown

promise in SMA cell-based models (104, 131-135, 176). ASOs have also been shown to modulate SMN2 expression *in vivo* in an unaffected transgenic mouse expressing the human SMN2 gene (132).

In this report, we demonstrate that *trans*-splicing efficiency is enhanced by competitively disabling a downstream splice site. As a means to develop a tractable molecular therapy, a series of antisense RNAs were screened to identify a sequence that would disable SMN exon 8 and promote *trans*-splicing. *In vitro* assays identified an enhancing antisense RNA and which was constructed into a novel single vector system individually expressing the *trans*-splicing RNA and the antisense RNA. Cell-based assays identified a highly efficient vector system that resulted in high levels of trans-splicing and correspondingly high SMN protein levels.

## RESULTS

### Competitive inhibition of downstream splice site enhances *SMN trans*-splicing

The key to introducing *trans*-splicing *in vivo* and in clinical settings is by developing efficient *trans*-splicing systems. We have previously described a SMN *trans*-splicing system that significantly elevated full-length SMN protein levels in SMA patient fibroblasts (133). However, initial *in vivo* experiments failed to achieve similar levels of activation (data not shown). Therefore, we initially examined SMN2 *trans*-splicing with the goal of devising strategies to enhance *trans*-splicing efficiency *in vivo*.

In SMN2 *trans*-splicing, there are three potential splicing outcomes: full length (FL), truncated (Δ7) and *trans*-spliced mRNA (TRANS*) (Figure 1A). Since pre-mRNA

splicing is a highly dynamic process, we hypothesized that competition exists between the *trans*-splicing event and the naturally strong SMN2 exon 8 splice site. Thus, competitive inhibition of the exon 8 splice site would enhance *trans*-splicing efficiency. To address this possibility, two complementary experiments were performed. A previously described slow-polymerase encoding plasmid was co-transfected with the SMN2 mini-gene and the plasmid expressing the SMN *trans*-splicing RNA (177). Under these experimental conditions, the exon 8 splice site approximately 2 kb downstream from exon 7, should not be synthesized as quickly compared to the rate of the natural polymerase. Therefore, the inclusion of exon 7 from the tsRNA tethered to intron 6 should potentially be favored. Consistent with the hypothesis, in the presence of the slow transcribing polymerase, *trans*-splicing was substantially increased over the typical level of *trans*-splicing previously observed (Figure 1B). Additionally, a SMN2 mini-gene was used in a separate experiment in which the intervening intron between SMN2 exons 7 and 8 was deleted. In the absence of an intact acceptor site at the intron 7/exon 8 junction, SMN *trans*-splicing was again elevated several fold over the standard SMN2 mini-gene (Figure 1C). Collectively, these results demonstrate that competitively disabling the downstream splice site can lead to enhanced *trans*-splicing efficiency, either through a biochemical means or by a genetic alteration.

**Identification of anti-sense RNA that enhances SMN *trans*-splicing**

The previous experiments provided the impetus to identify a more tractable molecular mechanism to enhance SMN *trans*-splicing, such as antisense molecules. Antisense oligonucleotides (ASO) have proven to be an effective molecular means to modulate pre-mRNA splicing, primarily by inhibiting splice site selection. A panel of plasmids

expressing short 18-22 nt ASOs complementary to the intron 6 region and intron 7/exon 8 splice site were constructed and used to determine whether any of the SMN antisense RNAs could enhance *trans*-splicing (Figure 2A). The ASO-expressing plasmids were co-transfected into HeLa cells with the SMN2 mini-gene and the plasmid pM13 which expresses the SMN *trans*-splicing RNA. Evaluation of Intron 7 ASOs identified a single lead candidate that significantly elevated *trans*-splicing levels: ASO pIn7[11] (Figure 2B, C). ASO In7[11] overlaps the intron 7/exon 8 boundary (Figure 3A). Other ASO did not increase *trans*-splicing from the SMN2 mini-gene, or in some instances, even inhibited *trans*-splicing (Figure 3B, 3C). These results confirm the genetic experiments that ASO inhibition of a downstream splice site can significantly enhance *trans*-splicing efficiency in a mini-gene context.

To determine whether ASO-enhanced *trans*-splicing occurred in a more complex context of endogenous SMN gene expression, pIn7[11] and pM13 were co-transfected into HeLa cells to examine *trans*-splicing with endogenous SMN transcripts. HeLa cells express SMN1 and SMN2 genes and provide a robust level of target RNA. Consistent with the mini-gene analysis, endogenously derived *trans*-spliced SMN increased in a dose dependant manner with increasing amounts of pIn7[11] (Figure 4A). To examine *trans*-splicing in a more disease-specific context, similar co-transfections were performed in primary SMA patient fibroblasts, 3813 cells. The cells are derived from a severe type I SMA patient and lack endogenous SMN1, and consequently contain very low levels of SMN-enriched nuclear structures called gems and express very low levels of full-length SMN protein. Extracts generated from 3813 cells co-transfected with pM13 and increasing concentrations of ASO pIn7[11] were analyzed for SMN levels using a SMN

monoclonal antibody. Western blots demonstrated an ASO dose-dependent protein induction greater than control-treated 3813 cells as well as pIn7$^{11}$ alone treated cells (Figure 4B). SMN levels in the co-transfected cells were comparable to SMN levels detected in the unaffected control fibroblasts, 3814 cells. These results demonstrate that endogenous *SMN* transcripts can be re-directed by *trans*-splicing and that SMN levels can be significantly increased by the ASO/*trans*-splicing strategy in a relevant disease context.

## DISCUSSION

This is the first demonstration of a technique designed to enhance *trans*-splicing efficiency by blocking downstream splice site selection. While the initial *trans*-splicing RNA alone showed considerable activity in cell-based models of SMA in terms of significantly increasing SMN levels and increasing snRNP activity (133), these results did not translate to the *in vivo* context. Our research highlights a key finding that low dose *trans*-splicing is enhanced by the co-expression of the ASO and resulted in detectable levels of SMN expression *in vivo*.

As a therapeutic approach, *trans*-splicing offers the advantage over gene replacement in that expression is intrinsically controlled by the endogenous promoter (173). Consequently, temporal and spatial constraints on gene expression are retained. As SMN expression has previously been shown to be significantly down-regulated from embryogenesis to adulthood, this additional restraint may prove beneficial for long-term exposure to a SMN *trans*-splicing vector, because the requirement of higher levels of

SMN diminish after birth. Avenues of research directed to the reduction of tsRNA vector dosage would inhibit the negative effects of off-target *trans*-splicing, because the most efficient tsRNA vector could result in protein expression high enough to be phenotypically beneficial while at the same time being at very low dosages.

The genetic context of SMA represents an intriguing target for a number of therapeutic strategies, including *trans*-splicing. In the SMN2 gene, the intrinsic quality of the exon 7 splice acceptor site is reduced due to the C/T transition. Therefore, the competition between SMN2 *cis*-splicing and *trans*-splicing is likely reduced, providing a potential advantage to *trans*-splicing in the *SMN* context compared to other alternatively regulated exons that retain fully functional splice sites.

In general, the field of *trans*-splicing therapeutics can benefit from the discovery of combined ASO-tiling and tsRNAs. ASO-tiling increases the potential of tsRNA by modulating *cis*-splicing signals within the target transcript. The combination of ASO-tsRNA mechanism and a novel single vector platform produces a potent enhancement of basal *trans*-splicing. In the case of *trans*-splicing RNAs designs such as, 5' or 3' versions would require examination of beneficial upstream and downstream sequences to merge with ASO RNA. In other words each tsRNA platform will have to be evaluated with potential ASO RNAs to verify whether or not an increase in *trans*-splicing could occur.

The use of AAV vectors for the delivery of gene therapies would provide a substantial longevity to ASO-tsRNA expression and thus SMN2 redirection. Future studies could examine the role of expression of the virus vectors in the SMA CNS. We conclude that the combined effects of ASO-tsRNAs enhanced *trans*-splicing in the context of SMN2 alternative *cis*-splicing.

## MATERIALS AND METHODS

### Plasmids and cloning

The pMU2-tsRNA$^{M13}$ clone reported previously is now written as pM13(133). The SMN1 and SMN2 mini-genes (pSMN1, pSMN2) have been previously described (22). Mini-gene pSMN2$^{\mathbf{\Delta In7}}$ was created by using overlapping PCR primers which anneal the 5' splice donor of exon 7 to the 3' splice acceptor of exon 8. SMN In7 DEL FWD (5'-TCCTTAAATTAAGGAGAAATGCTGGCATAGAGC-3'). This PCR product was then gel purified and cloned into the pCI minigene using 5'-NheI and NotI-3'. The plasmid pAT7-*Rpb1*- (N792D) (R749H) expresses the mutant RNA polymerase (177). The Antisense Oligonucleotides (ASO) were cloned into the previously reported pMU2 plasmid context driven by a U6 promoter (135). Sequences were chosen with intron 6 denoted as In6$^{X}$ (with X indicated the number the ASO is in order relative to the others) and intron 7 as In7$^{X}$. Upper case and lower case letters in the primers depict the intronic versus exonic sequences found in the SMN2 transcript. Listed below are the binding domains for the ASO as read 5' to 3' in the SMN pre-mRNA **[*SMN* EXON6]5'**-(In6$^{1}$-5'-uucugaucauauuuuguugaauaaa-3')

(In6$^{2}$-5'uuuguugaauaaaauaaguaaaaug) (In6$^{3}$-5'auaaguaaaaugucuugugaaacaaa)

(In6$^{4}$-5'gucuugugaaacaaaaugcuuuuuaa) (In6$^{5}$-5'aaugcuuuuuaacauccauauaaag)-**3' [*SMN* EXON7]5'**- (In7$^{1}$-5'auaugggaauaaccuaggcauacugca)

(In7$^{2}$-5'cuaggcauacugcacuguacacucug) (In7$^{3}$-5'cacuguacacucugacauaugaagug)

(In7$^{4}$-5'acauaugaagugcucuagucaa) (In7$^{5}$-5'gcucuagucaaguuuaacuggugucca)

(In7$^{6}$-5’uuuaacugguguccacagaggacau) (In7$^{7}$-5’acagaggacaugguuuaacugga) (In7$^{8}$-5’gguuuaacuggaauucgucaagcc) (In7$^{9}$-5’ggaauucgucaagccucugguucuaauuu) (In7$^{10}$-5’ugguucuaauuucucauuugcagG) (In7$^{11}$-5’ucucauuugcagGAAAUGCUGGCAUA) -**3’[*SMN* EXON8]** (In$^{712}$-5’AAUGCUGGCAUAGAGCAGCACUAAA) (In7$^{13}$-5’AUGACACCACUAAAGAAACGAUCA) (In7$^{14}$-5’AAGAAACGAUCAGACAGAUCUGGAA) The pMU3 construct produces three gene products, tsRNA, eGFP protein and ASOs. ASO-In7$^{11}$ was subcloned by PCR by Platinum *Pfx* DNA Polymerase (Invitrogen) amplification according to the manufacture instructions. The U6 promoter and the antisense RNA were cloned by flanking restriction sites 5’-BlpI and AsiSI-3’(NEB). pMU3$^{KO}$ is a substitution of the In7$^{11}$ anti-sense RNA with a random sequence of RNA created by overlapping PCR and cloned using the same restrictions sites above. The pMU2-tsRNA$^{EX4}$ intron 3 binding domain was amplified from HeLa genomic DNA using primers (Int3 Rev 5’-ATCAAGCTTGAGCTCAAAAAGAAAAAATATGCAGGTTTT-3’) and (Int3 Fw 5’-ATCACCGCGGTTCAATTTCTGGAAGCAGAGACTA-3’) and cloned into HindIII-SacII of pcDNA3/PTM2 replacing Int6 binding domain. Exons 4-7 were amplified from a SMN1 cDNA clone using primers (Ex4 Fw 5’-TCAGATATCCTGCAGAGAATGAAAATGAAAGCCAAGTTT-3’) and (Ex7 Rev 5’-CATTCTCGAGGGGCCCGTCATAGCTGTTTCCTGCGACTCCTTAATTTAAGGAA TGTGAGCA-3’) and cloned into EcoRV and XhoI sites of pMU2.

***In vitro* transfections**

The transfections were performed using linear PEI (Polysciences, Inc.) with pH adjusted to 8.3 using 20 μL aliquots of HCl or NaOH. Stock linear 250 kDa PEI for HeLa in vitro transfections were snap frozen in liquid nitrogen and thawed 5 times at 37°C. Triple transfections in HeLas required "mean-low molecular weight PEI," stock PEI was sonicated on ice at 30% total power for 30 seconds three times. Plasmids were transfected into HeLa or HEK293 cells (Coriell Cell Repositories) grown to 80% confluence before transfection. Plasmids were diluted in a 150 mM NaCl solution before adding filtered linear 7.5 mM 250 kDa PEI. Cells were incubated with plasmid overnight and replenished with fresh Dulbecco's Modified Eagle Media High Glucose 1X $DMEM^+$ (D-glucose 4.5g/L, +L-glutamine, 1% penicillin/streptomycin 10000 units/mL, 3% fetal bovine serum-endotoxin free) and harvested 48 hours post-transfection. Salmon sperm DNA (ssDNA) (Invitrogen) was added to adjust for differences in plasmid DNA input. SMA patient fibroblasts (GM3813) were transfected with Lipofectamine™2000 in serum free $DMEM^-$ for 4 hours then washed via media and replaced with $DMEM^+$ for 2 hours. Finally complete media $DMEM^+$ was added back for the remaining incubation. Cells were harvested 24 hours later in PBS (137 mM NaCl, 2.7 mM KCl, 10 mM $Na_2HPO_4$, 2 mM $KH_2PO_4$) pH 7.5-8.0. ASO-tsRNA co-transfections used ssDNA to control for total amount of DNA. Post-transfection harvested cells were counted on a hemacytometer and viability was determined using trypan dye exclusion.

**RT-PCR**

48 hours post-transfection or transduction, total RNA was harvested from cells using TRIzol Reagent (Invitrogen) according to the manufacturer's instruction. Total RNA concentration was determined using a Nano-drop spectrophotometer and normalized before cDNA synthesis. RT-PCR was performed as previously described (135). The *trans*-splicing product was amplified using a reverse primer M13 (5'-GTCATAGCTGTTTCCTGCGAC-3') 5' Cy3 labeled (564 nm peak emission) (Intergrated DNA Technologies, Inc.) and a mini-gene specific primer, pCI-Fwd (22). The SMN1 and 2 mini-gene transcripts were amplified using pCI-Fwd#1 and pCI-Rev (22). The primers used in endogenous PCR amplifications were SMN Exon 6 -Forward (5'-CCCCCACCACCTCCCATATGT-3') and *SMN* Exon 8-Reverse (5'-AGTGGTGTCATTTAGTGCTGC-3'). The endogenous *trans*-spliced product was amplified by SMN Exon 6 (+7) Forward and M13 Reverse. Reactions without RT polymerase were included as controls (not shown). Semi-quantitative determinations of Cy3 labeled *trans*-splicing products were achieved using a laser Fuji-Imager FLA5000 at 550 nm excitation range. RT-PCRs were repeated in triplicate, and relative abundance of *trans*-SMN mRNA were compared using 2-tail Student t-test. To normalize within experiments, *trans-SMN* induction was determined as (*trans-SMN:GAPDH*) and between experiments levels were normalized to basal pM13 *trans*-splicing values (set to 1). SMN *trans*-splicing was expressed as fold change over pM13 which was set to 1.

**Western blot**

HeLa cell pellets were prepared in RSB100 lysis buffer (20 mM Tris-HCl pH 7.4, 100 mM NaCl, 25 mM $MgCl_2$, Triton X100 0.5%) and centrifuged at 10,000 g for 5 min at 4°C. Samples were sonicated and boiled in loading dye and resolved in a 10% SDS-PAGE using 20 cm x 10 cm glass plates and the BioRad Protean 2000 apparatus. Resolved proteins were then transferred to PVDF (Immoblion) at 200 mA for 400 minutes in Towbins (24 mM Tris base, 192 mM glycine, 20% methanol (v/v)). Western blots were blocked overnight in 5% casein and Tris-buffered Saline (TBS) (90 mM Tris-HCl, 10 mM KCl, 547 mM NaCl, 2% Tween (v/v) (Acros)) pH 7.5. Primary patient fibroblast western blots were probed with 1:100 dilution of mouse anti-SMN monoclonal antibody, 4B7 (119), and visualized with a HRP-conjugated secondary mouse antibody. Murine western blots were probed with 1:1000 dilution of mouse anti-SMN (BD Biosciences) and were produced using 1:1 mixture of Pierce West Pico reagent. Cross reaction with endogenous mouse heavy and light chain antibody Mouse TrueBlot™ ULTRA HRP anti-mouse IgG (eBioscience) was used at 1:10000 in 5% skim milk. Images were captured and quantitated using a Fuji Imager LAS 3000 at 75% of total resolution (10-30 second exposure) and Multi-Gauge V2.3 software. To control for loading error the westerns were then stripped using $H_2O_2$ for 15-20 minutes at room temperature and re-probed with anti-β-actin rabbit and anti-rabbit secondary antibody conjugated to HRP. Western blots were repeated in quadruplicate and mean relative abundance were compared using 2-tailed Student t-test. To normalize within experiments, SMN induction was determined as (SMN:β-actin) and between experiments SMN levels were normalized to GM3813 values (set to 1). SMN protein induction was measured

using pIn7[11] ASO as baseline, and fold change over pM13 alone to express *trans*-splicing efficiency.

**Figures**

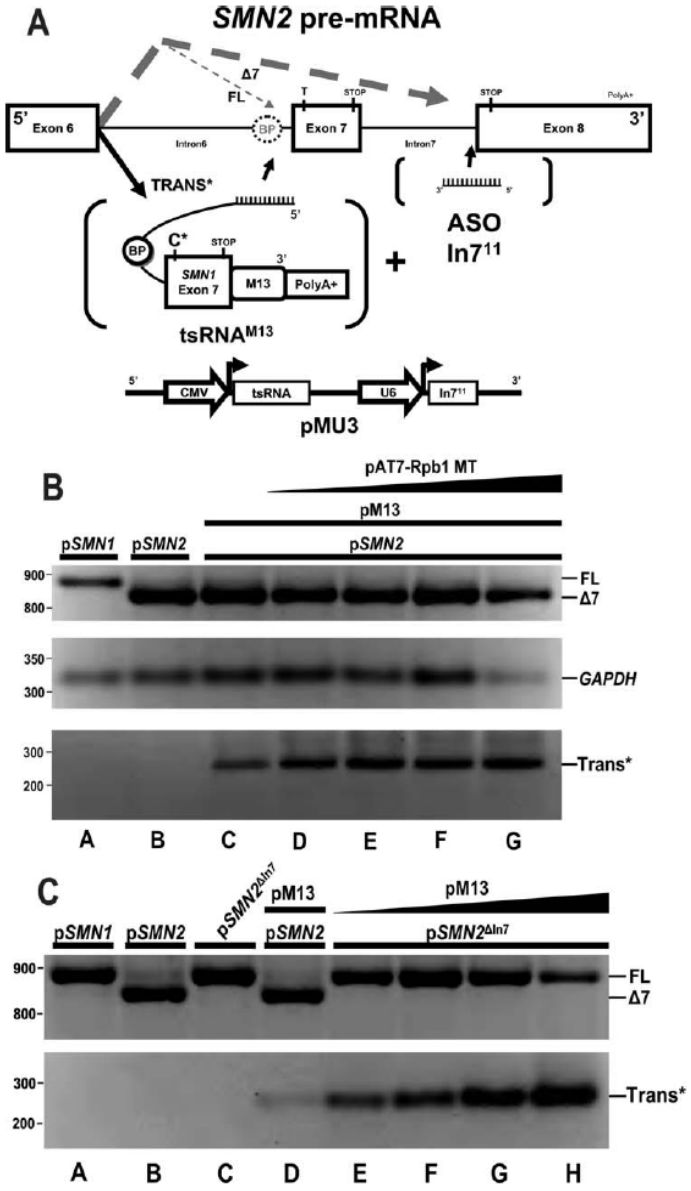


**Figure 1 Development of a single plasmid vector enhances SMN based *trans*-splicing.** (**A**) Proposed ASO-tsRNA mechanism. SMN2 transcripts alternative splice

producing two mRNA products. The alternative splicing pathway is represented by gray dashed lines, SMN2 mRNA products: "Δ7"- Exon 7 skipped "FL"- full length. *Trans*-splicing RNA identifies SMN2 pre-mRNA specifically in intron 6 and contains overlap of sequences that include the endogenous branch point. Circles surrounding symbol "BP" identify known branchpoints in the model. We demonstrate a novel mechanism of disrupting downstream intron 7 splicing elements causes enhancement of *trans*-splicing. (Bold "TRANS*" and large black arrow indicate enhanced *trans*-splicing pathway). The effect is accomplished via Antisense Oligonucleotides "ASO $In7^{11}$" targeted to the distal intron and exon boundary. The stop codons "STOP" and SMN2 "C-T" or tsRNA "C*" nucleotide changes are denoted with vertical line marking approximate RNA position. Bracketed objects indicate promoters and gene products produced from pMU3 plasmid pictured below by a black line. (**B**) Increasing concentrations of transcription mutant RNA polymerase promotes *trans*-splicing. HeLa cells were transfected with static amounts mini-gene pSMN1 (lane a) or pSMN2 (lanes b-g) 1.25 μg , pM13 (lanes c-g) 0.75 μg, and increasing amounts of mutant Rpb1 RNA Polymerase subunit (pAT7-Rpb1MT) at 0.25, 0.75, 1.0 and 2.0 μg were harvested at 48 hrs post transfection. A representative reverse transcriptase PCR gel is displayed with *GAPDH* normalization control. (**C**) A genetically disabled SMN2 intron 7 deletion mini-gene displays enhances trans-splicing at reduced tsRNA plasmid concentrations. HeLa cells were co-transfected with p*SMN1* (lane a), p*SMN2* (lanes b,d) $pSMN2^{\Delta In7}$ (lanes e-h) 1.25 μg each and increasing concentrations of pM13 (lane d) 0.25 μg, (lanes e-h) 0.10, 0.25, 1.0 and 2.0 μg. RNA harvested 48 hrs later. A representative reverse transcriptase PCR gel is displayed.

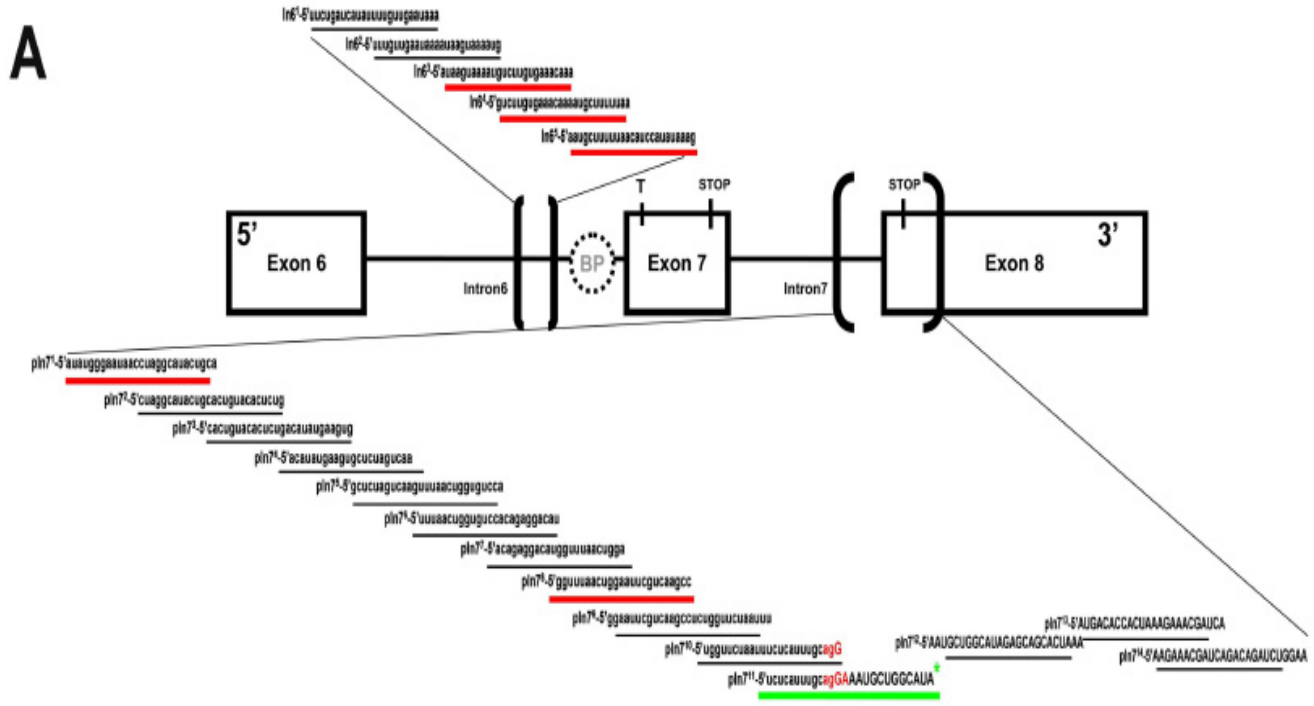
A
5'
Exon 6
Intron6
BP
T
STOP
Exon 7
Intron7
STOP
Exon 8
3'

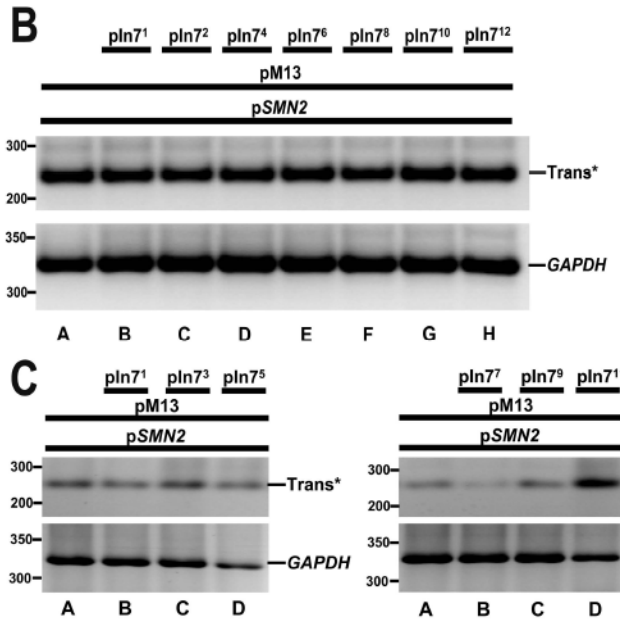
B
pIn7¹ pIn7² pIn7⁴ pIn7⁶ pIn7⁸ pIn7¹⁰ pIn7¹²
pM13
pSMN2
300
200
Trans*
350
300
GAPDH
A B C D E F G H


C
pIn7¹ pIn7³ pIn7⁵
pIn7⁷ pIn7⁹ pIn7¹¹
pM13
pSMN2
300
200
Trans*
350
300
GAPDH
A B C D

**Figure 2 Summary of SMN2 trans-splicing and intron 7 ASO-tiling screen demonstrates specificity of ASO-In7$^{11}$ effect. (A)** Graphical depiction of intron 7 ASO targets. ASO sequences are identified at the beginning of the individual string, written 5′-3′. Capitalized sequence indicates exon 8 sequences with the 3′ splice site defined in red. The bars located directly below illustrate the effects on the trans-splicing product by the respective colors. Black lines indicate neutral effects, red lines indicate negative influences, and green lines represent increased trans-splicing. **(B)** Summary of even numbered intron 7 ASO screen demonstrates no effect. HeLa cells were triple-transfected with plasmids expressing pM13 1.0 μg, a minigene SMN2 (lanes a–h) 1.25 μg and ASO pIn7$^{2}$-pIn7$^{12}$ (lanes c–h) 1.0 μg and RNA harvested 48 hrs later. RT-PCR gel is displayed with GAPDH normalization control. pIn7$^{1}$ negative control serves to normalized between ASO experiments. **(C)** Summary of odd numbered intron 7 ASO screen identifies pIn7$^{11}$ ASO as a potent enhancer of trans-splicing. HeLa cells were triple-transfected with plasmids expressing pM13 1.0 μg, a minigene pSMN2 (lanes a–d) 1.25 μg and ASO pIn7$^{1-5}$, pIn7$^{7-11}$ (lanes b–d) 1.0 μg for blots respectively and RNA harvested 48 hrs later. RT-PCR gel is displayed with GAPDH normalization control. pM13 controls depict a basal *trans*-splicing sample.

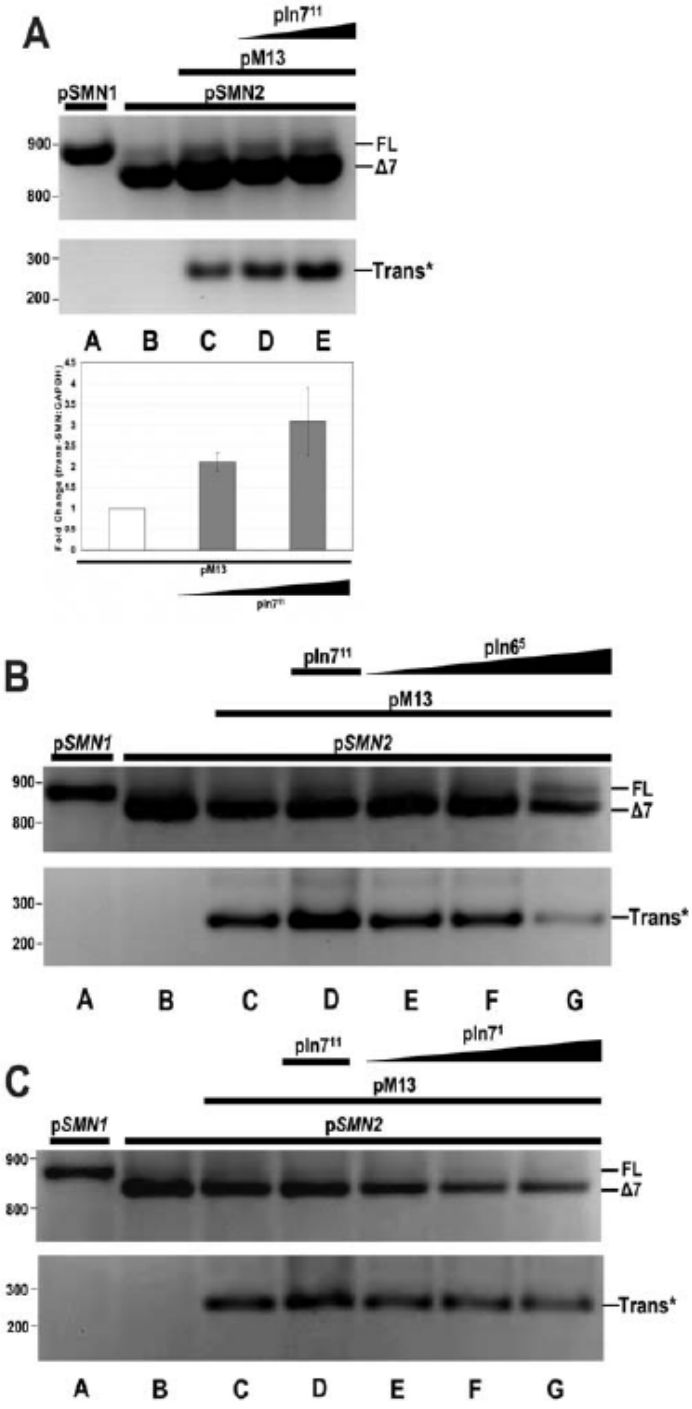


**Figure 3 ASO mediated inhibition of downstream splicing increases SMN2 *trans*-splicing.** (**A**) HeLa cells transfected with static amounts of pSMN1 (lane a), pSMN2 1.25 µg (lanes b-e) and pM13 (lane c-e) 0.75 µg were co-transfected with increasing

concentrations of pIn7[11] (lane d, e) 0.25, 1.0 μg and RNA harvested 48 hrs later. RT-PCR gel is displayed with GAPDH normalization control. Graph represents independent triplicate repeats using a quantitative M13-Cy3 labeled primer and linear-range PCR amplification. Inset graph represents the average of triplicate repeats and error bars indicate ±s.d. (**B**) SMN intron 6 ASO controls contribute to a reduction of *trans*-splicing because they are specific for the region that the tsRNA binds to in the SMN2 transcript. HeLa cells were triple transfected with static amounts of mini-gene pSMN1 (lane a) pSMN2 (lane b-g) 1.25 μg and pM13 (lane c-g) 0.75 μg with increasing amounts of pIn6[5] (lane e-g) 0.25, 0.75 and 1.0 μg and RNA harvested 48 hrs later. RT-PCR gel is displayed with *GAPDH* normalization control. pIn7[11] (lane c) 1.0 μg serves as a positive ASO-tsRNA control. (**C**) ASOs targeted internally to *SMN* intron 7 reduce *trans*-splicing. HeLa cells were triple transfected with static amounts of mini-gene pSMN1 (lane a) pSMN2 (lanes b-g) 1.25 μg and pM13 (lanes c-g) 1.0 μg with increasing amounts of pIn7[1] (lanes e-g) 0.25, 0.75 and 1.0 μg and RNA harvested 48 hrs later. RT-PCR gel is displayed with GAPDH normalization control. pIn7[11] (lane c) at 0.25 μg serves as a positive ASO-tsRNA control.

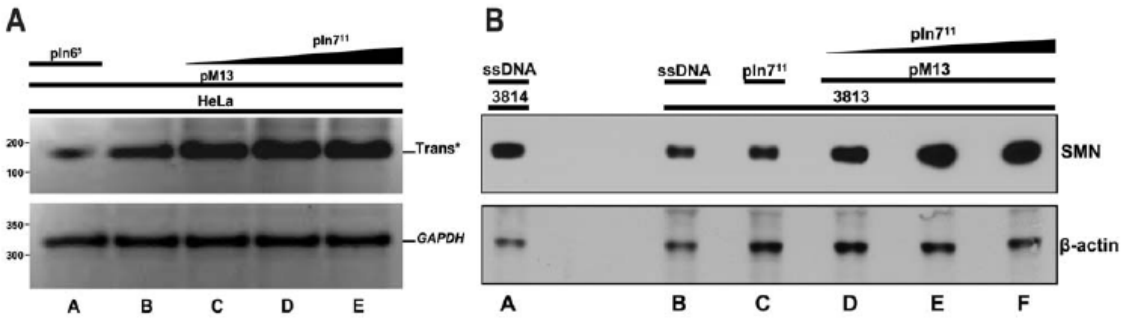


**Figure 4. Endogenous enhancement of *trans*-splicing utilizing combined delivery of ASO and tsRNA.** (**A**) Dose dependant ASO $In7^{11}$ enhancement of endogenous SMN *trans*-splicing. HeLa cells were co-transfected with pM13 (lanes a-e) 1.0 μg and increasing concentrations of ASO $pIn7^{11}$ (lanes c-e) 0.25, 2.0 and 5.0 μg and RNA harvested 48 hrs later. RT-PCR gel is displayed with GAPDH normalization control. $pIn6^{5}$ (lane a) 2.0 μg serves as a negative control. (**B**) Dose dependant ASO $pIn7^{11}$ enhancement of pM13 mediated SMN protein induction. 3813 SMA patient fibroblasts were co-transfected with pM13 (lanes d-f) 0.75 μg and increasing concentrations of $pIn7^{11}$ (lanes d-f) 0.50, 1.0 and 2.0 μg. Cells were harvested 24 hrs later and protein extracts were separated by SDS-PAGE. $pIn7^{11}$ alone (lane c) 2.75 μg and ssDNA (lanes a, b) 2.75 μg serve as negative controls. The β-actin antibody panel serves as a normalization control.

**Development of a multi-antisense therapy that targets three separate regions of SMN2 pre-mRNA splicing**

**Introduction**

Antisense oligonucleotides are primarily known for their ability to hybridize to a sense target sequence, which can lead to activation and cleavage by RNase H and knockdown of targeted sequences (178). At first most antisense RNAs were used as a therapy to knockdown specific genes in control of various diseases including cystic fibrosis, Hutchinson-Gilford progeria, and certain types of cancers (179-181). In the vast majority of these types of therapeutics antisense molecules are used in an attempt to skip exons (154, 157, 182, 183). This is especially true in Duchenne's muscular dystrophy, and has shown promise. The strategy is the use of multiple antisense RNAs in unison to skip multiple exons within the dystrophin transcript. By the use of 8 different antisense RNAs it has been shown to increase functional protein levels in cells, mice, and human muscle biopsies and this lends itself applicable to over 50% of all DMD patients. In fact, antisense-mediated exon skipping is currently in human trials with no obvious adverse effects so far, and a second trail appears to be on the horizon (184). This is quite exciting and led us to devise a similar technique directed at the SMN2 transcript. Though we do not want to skip multiple exons in the SMN2 transcript here we propose to use multiple antisense RNAs congruently to target multiple regulatory regions in hopes to increase the inclusion of exon 7 over therapies using singular antisense. This is a completely novel way to use a multi-ASO technique; targeting multiple splice signals tailored specifically for the SMN transcript in hopes of increasing an exon inclusion, not exclusion.

## RESULTS

### Schematic of multi-antisense strategy of SM2 modulation

In an effort to increase our effect seen in previous therapeutic approaches in lab, we devised a multi-antisense method for increasing SMN2 full length expression. In a concerted effort three antisense RNA specific for different regions of the SMN2 transcript will presumably help increase full-length expression albeit through different effects. One, an antisense directed against a negatively acting region called Element1 (48) two, a different inhibitory element down-stream of exon 7 called ISSN1(46) and three, a short antisense moiety designed to competitively inhibit the 3' splice site of exon 8. All are designed to funnel all splice decisions to include exon 7 in the SMN2 transcript in hopes of increasing full-length expression from this transcript.

### ICV injection of multi-antisense cocktail does not change weight profile of Δ7 mice

As a proof of principle to the validity of multi-antisense therapy in SMA, we injected Δ7 SMA mice and determined the weight profile throughout the life span of the animals. The onset of weight loss is the first detectable and most sensitive means of identifying a change in disease progression in this model of SMA (17). No significant difference was found in overall weight or the amount of weight gained between mice injected with 'pool' or control groups (Figure 2). Each mouse received 6 μg total of the RNA pool once every other day, starting at PND 2 and ending on PND 6. Control mice, received either 6 μg of Scramble RNA, or PBS. There was no difference between the weight curve of 'pool' injected mice and the other controls (Figure 2).

**Delivery of multi-antisense cocktail does not significantly increase the percent weight gained from birth to peak**

In examination of overall fitness we measured the percent of weight gained from birth to peak weight for the mice. This percentage is relative to each mouse, and is graphed as percent weight gained from birth to peak. As before mice were injected on PND 2, 4, and 6 with 6 μg of total RNA per injection. The mice were weighed every day; we did not observe significant difference between the experimental groups percent weight gained from birth to peak (Figure 3; 1way ANOVA p=0.58). This suggests that 'pool' treated mice did not have a measurable affect on the ability of the Δ7 mice to gain weight from birth to peak. There could be a multitude of reasons, and further experimentation is required.

**No appreciable change in survival of ICV injected mice**

In order to determine if the administration of the multi-antisense cocktail affected life span we graphed survival days for each group. The Kaplan-Meier curve showed no statistical significant change in life span from negative control injected and 'pool' injected mice (Mantel-Cox p=0.366 Figure 4). This suggests that multi-antisense therapy does not increase survival time in SMA Δ7 mice, or the beneficial effect that 'pool' injections could be achieving is not measurable in this model/assay.

**Multi-antisense injected mice showed early and sustained gross motor function**

Additionally, an established measure of gross motor function in the SMA Δ7 mice is their ability to right from a prone position; SMA mice are unable to right themselves

efficiently when placed on their backs (17). Starting PND 8, mice were tested for their ability to right themselves. Mice recorded a positive result if they could right themselves within 60 seconds, and maintained the upright posture for at least two seconds thereafter. The graph in Figure 5 is portraying the percentage of mice able to right themselves from each experimental group. A greater percentage of mice were able to right themselves after three injection of the multi-antisense cocktail throughout their lifespan as compared to the control injected mice (1way ANOVA p=0.04). Furthermore the increase observed with the scramble injected above PBS injected was not significant (t-test p=0.206). The 'pool' injected mice attained this ability sooner, and a greater proportion maintained that ability through the study. This suggests that even though life span and weight of 'pool' injected mice did not significantly increase their overall fitness was statistically improved.

**DISCUSSION**

The use of multiple antisense RNAs targeting a single transcript is not a novel idea, as it has been performed extensively in different models, like DMD (154, 157, 182). This type of strategy has been adapted for use against the SMN2 transcript with pronounced variations. In the DMD approach each different antisense was designed to induce skipping of an exon that either induced or created a truncated/mutant form of the protein thus leading to a partially functional protein. In this model we are targeting multiple splice regulatory sights and one splice acceptor sight in a concerted effort to increase inclusion of a single exon (SMN2 exon 7). The first two antisense molecules used in this study were designed to competitively inhibit or disrupt negative splice regions found

surrounding SMN2 exon 7 called, Element 1 or ISSN1 (46, 48). In addition to manipulating the overall auxiliary splice signal surrounding SMN2 exon 7 we are trying to inhibit the conserved splice acceptor sight downstream of exon 7 found at exon 8 with the use of the antisense called In7[11]. This antisense was previously shown to help increase trans-splicing in a SMA mouse model presumably by controlling the general splicing machinery's splice decision masking the exon 8 acceptor site, and there by blocking recognition (150). All three were employed in this project to cooperatively modulate SMN2 pre-mRNA splicing. Weight gain and life span remained unaltered. However, the overall functionality of the 'pool' injected mice were significantly higher than the control mice. This becomes obvious in the time to right graph showing that a larger percentage of 'pool' injected mice were able to right themselves sooner and throughout the disease progression (Figure 5, 1way ANOVA p=0.04). The data suggests that the multi-antisense technology used in the Δ7 mouse model, with the routine outlined here, had no measurable effect on life span, or weight (total, or percent increase). However this therapy did have an affect on the overall muscle function in 'pool' injected mice. This could be due to an increase in motor neuron functionality allowing for better muscle function, or it could be due to a coordination increase. Both attributes need to be examined in future studies. Future experiments will look at dosage changes, SMN protein levels, mRNA splicing and other molecular assays that can unveil a better understanding of the underlying mechanism.

## MATERIALS and METHODS

### 2'-O-Methyl Bi-functional RNA

The following oligos were modified at every base with 2'-O-methyl groups (IDT, Coralville, IA, USA); E1, 5'- CUA UAU AUA GAU AGU UAU UCA ACA AA-3', ISSN1, 5'-GAU UCA CUU UCA UAA UGC UGG-3', In7,11 5'-AUG CCA GCA UUU CCU GCA AAU GAG-3' and negative control RNAs; Scramble, 5'- Scramble 5'-CCU UCC CUG AAG GUU CCU CC-3'.. The modified oligos differ from the plasmid expressed bi-functional RNAs by the lack of a non-specific 6 nucleotide spacer sequence between the antisense domain and the SR recruitment domain, and furthermore do not have the U7-opt-sm sequence.

**Animal Injections**

All animals were housed and treated in accordance with ACUC guidelines. $SMN2^{+/+}$, $SMN\Delta7^{+/+}$, $Smn^{-/-}$ mice (149) were genotyped at day of birth, designated as day 1, and injected on day 2. Three intracerebralventricular (ICV) injections were performed on PND 2, 4, 6 neonates as previously described (150, 151, 162). Briefly, mice were immobilized via cryo-anesthesia and injected using μL calibrated sterilized glass micropipettes. The injection site was approximately 0.25 mm lateral to the sagittal suture and 0.50-0.75 mm rostral to the neonatal coronary suture. The needles were inserted perpendicular to the skull surface using a fiber-optic light (Boyce Scientific Inc.) to aid in illuminating pertinent anatomical structures. Needles were removed after 15 seconds of discontinuation of plunger movement to prevent backflow. Mice recovered for 5-10 minutes in a warmed container until movement was restored. Single injections of 6 μg of total 2'-O-methyl oligonucleotides were delivered via ICV described above for all mice.

**FIGURES**

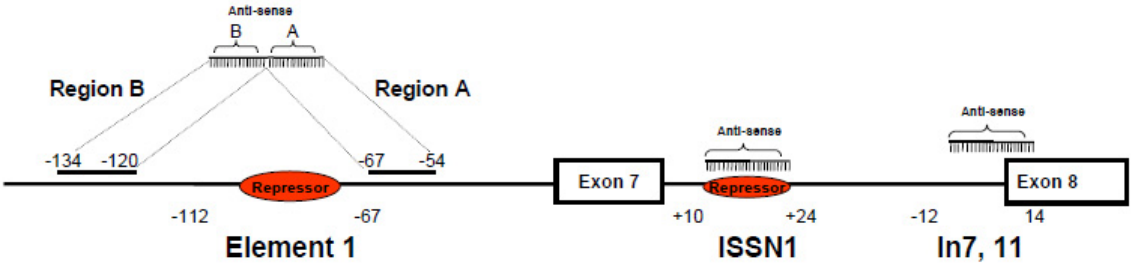


**Figure 1. Schematic of antisense RNAs delivered congruently in the 'Pool' approach.** The multi-antisense approach includes an antisense RNA against three separate regulatory elements within the SMN2 transcript. An antisense directed against a negatively acting region called Element1, a different inhibitory element down stream of exon 7 called ISSN1, and a short antisense moiety designed to competitively inhibit the 3' splice site of exon 8. All are designed to funnel all splice decisions to include exon 7 in the SMN2 transcript which is expected to increase full-length expression from this transcript.

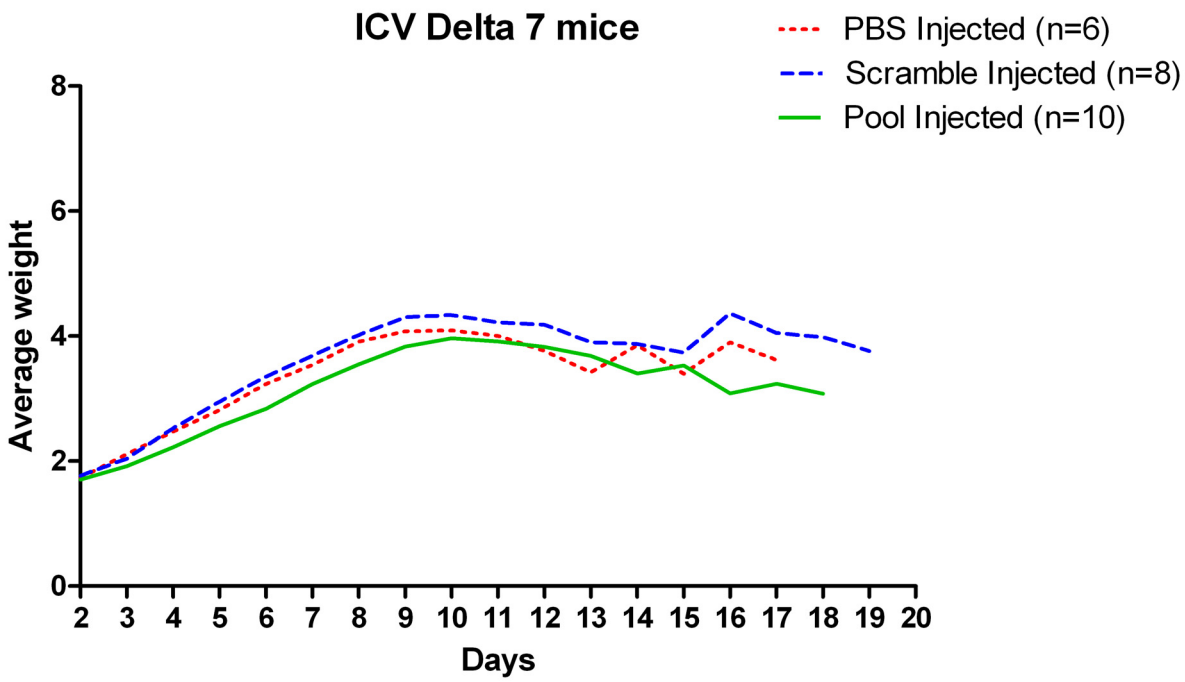


**Figure 2. ICV injection of multi-ASO cocktail does not change weight profile of Δ7 mice.** Mice were injected PND 2, 4 and 6 with 6 μg of RNA total each ICV injection. Mice were weighed every day until death and average weights by day are graphed.

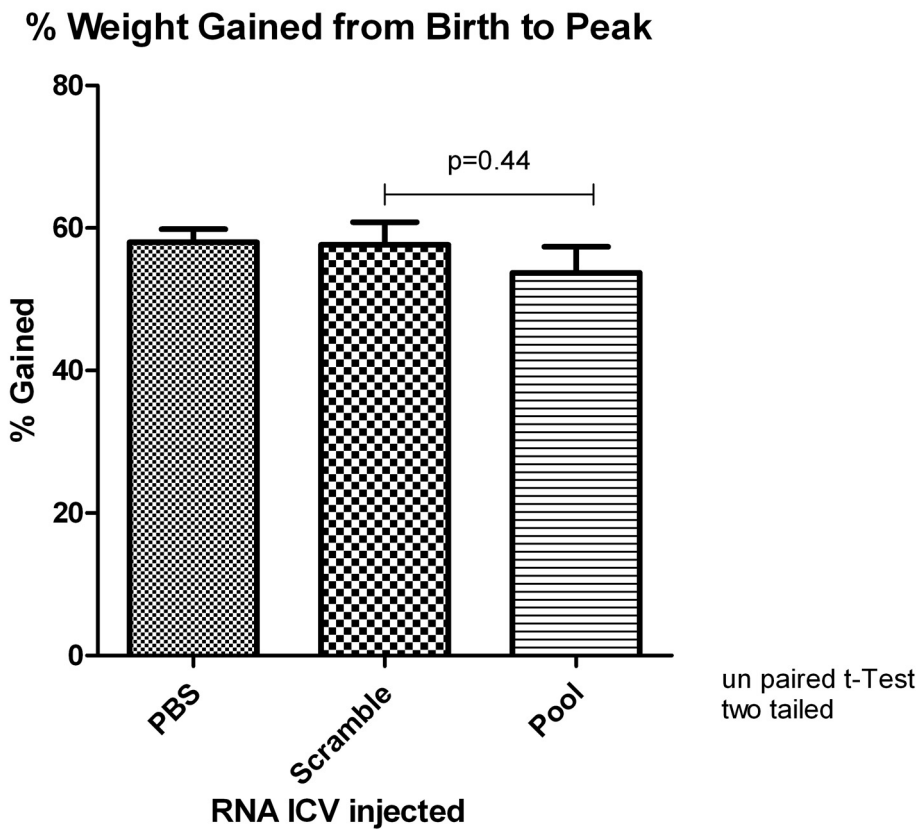


**Figure 3. ICV injected mice percent weight gained from birth to peak.** Mice were injected as previously described PND 2, 4 and 6 and percent weight gained graphed. There is no statistical significance in percent weight gained from birth to peak ( 1way ANOVA p=0.58) There is no statistical significance between 'pool' injected and scramble injected SMA mice (t-test p=0.44).

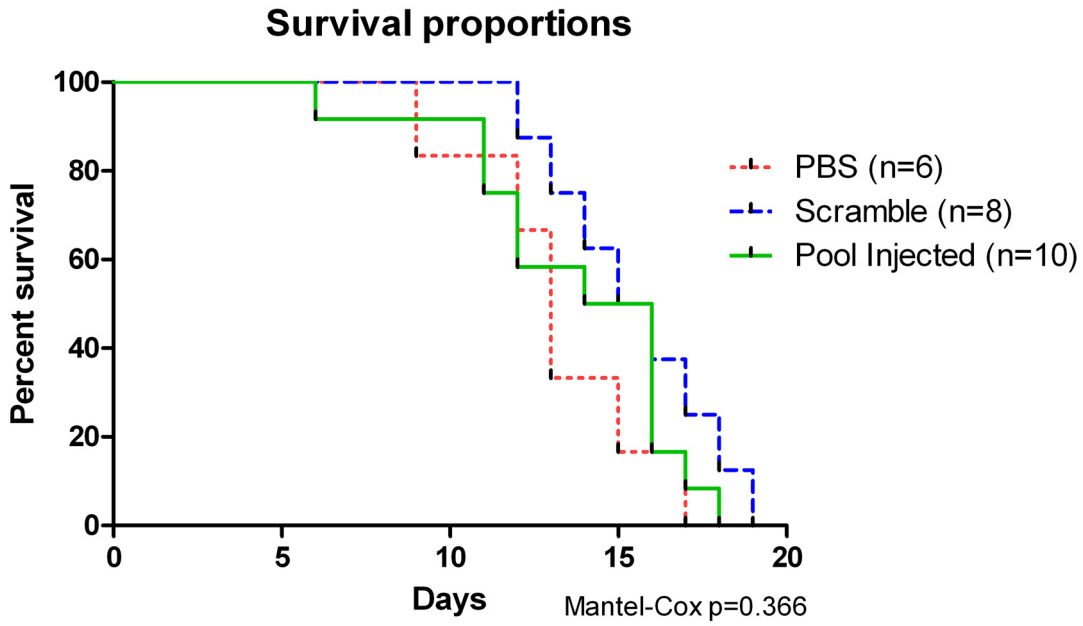


**Figure 4. Survival curve of ICV injected mice.** Kaplan-Meier survival curve of injected mice show no statistical difference between experimental groups (Mantel–Cox p=0.366).

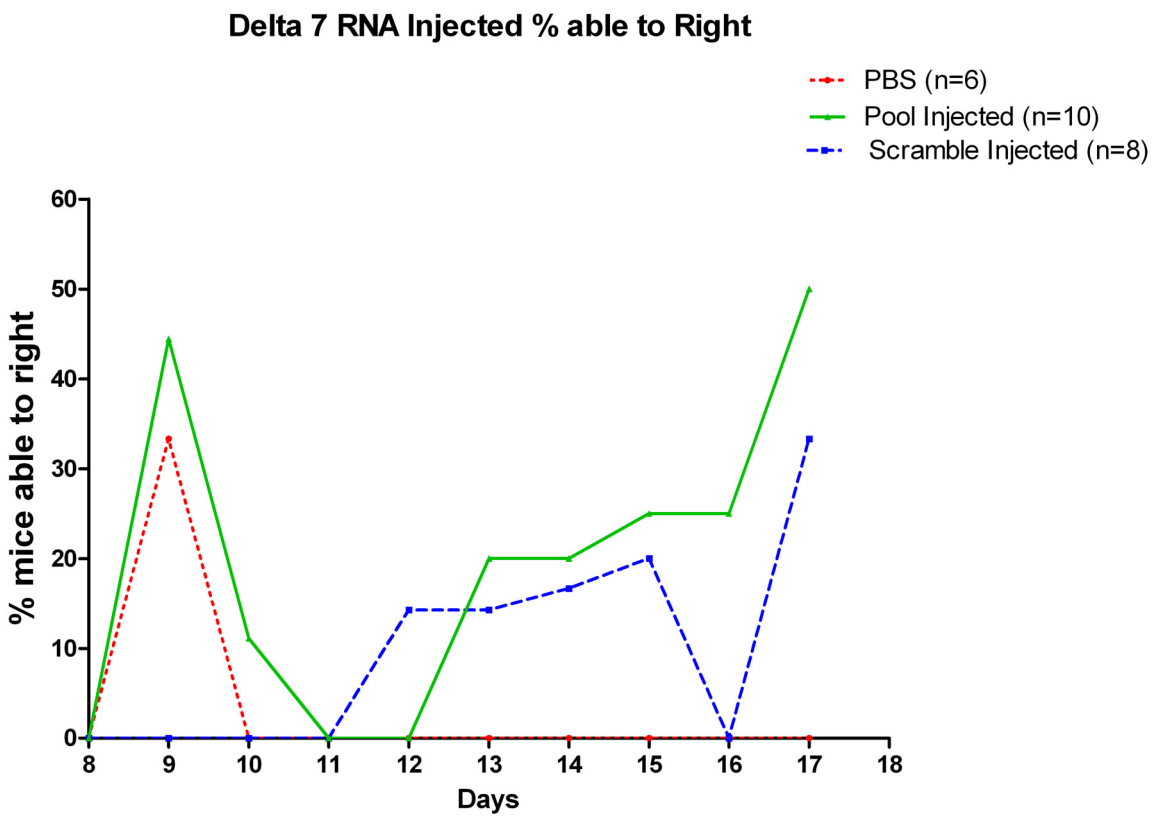


**Figure 5. Percent mice able to right themselves after ICV injection.** Gross motor function depicts significant difference in 'pool' injected mice. Mice were placed directly on their backs and allowed to freely move. A positive time to right score is registered as all four limbs correctly on the surface under a time of 60 seconds and this stance is maintained for at least 2 seconds (1way ANOVA, p=0.04). Scramble injected is not statistically significant above PBS injected (t-test p=0.206).

## Summary

SMA is the leading genetic cause of infantile death afflicting one in 6:000 live births. Phenotypically it is similar to the muscle atrophy family of diseases, but it is actually caused by the loss of motor neurons with degeneration seen primarily in the ventral horn area first. The neural degeneration and subsequent muscle atrophy is radially progressive with the eventual denervation of the intercostal and diaphragm muscles leading to death. The gene linked directly to SMA, the SMN1 gene, is positioned on chromosome 5q13 which is a highly unstable region of the genome. This instability created the mirror copy gene SMN2 which has been labeled as a disease modifier for SMA. SMN2 cannot compensate for the loss of SMN1 seen in nearly all SMA patients, because this gene primarily expresses a transcript that lacks a required exon for protein function and stability, exon 7. Though the SMN protein has not been linked to a single function that can explain the neuronal phenotype it is known that without exon 7 its cellular role is impeded.

## Current SMN Therapies

Since SMA is caused by the loss of SMN there are several strategies being investigated to increase SMN levels by, activating SMN2 gene expression, increasing exon 7 inclusion, and stabilizing SMN protein. There are also strategies focusing on non-SMN specific factors that could provide neural protection or muscle fitness.

Because the SMN2 transcript produces a fraction of full length mRNA there is active research in therapies that can increase overall transcription. The SMN2 gene is regulated by a promoter that is nearly identical to the SMN1 promoter (185). It was shown that the SMN promoter was associated with histone deacetylace (HDAC) 1 and 2 proteins that play a role in gene expression (99). This led to research aimed at identifying HDAC inhibitors as potential activators to increase full-length SMN2 expression. Studies have shown that the SMN2 promoter can be perturbed to achieve higher levels by these compounds which include phenylbutyrate, and valproic acid (84, 99, 100, 115, 116). Though HDAC inhibitors show promise there is the problem of global affects seen in off target up-regulation, as well the poor matriculation across the blood brain barrier. Newer HDAC inhibitors with better pharmacokenetics are being studied, along with their potential uses in other diseases.

Additional approaches to achieve the induction of full length expression from the SMN2 gene have been explored. One of those is the use of polyphenols. Curcumin, resveratrol and epigallocatechingalate (EGCG) are naturally occurring polyphenols that have been linked to alleviating neurodegenerative diseases (186). This and other data suggests that some botanicals can alleviate many different dystrophies and dementias. Along this hypothesis it was shown that EGCG, curcumin, and resveratrol could increase the SMN protein levels and nuclear gems in a primary fibroblast model of SMA (130). Though increasing SMN2 expression through botanicals is promising, complex natural products tend to have pleiotropic effects and a more specific therapy could have beneficial results with fewer potential off target effects.

Another potential avenue of therapy in SMA is to increase the stability of the primary product of SMN2. The normal translation termination codon is at the 3' end of exon 7. However, when exon 7 is skipped an alternative termination codon is used 4 amino acids into exon 8 (8). There is evidence to suggest that a heterologous sequence extended by a read-through event can substantially increase protein stability (103, 119). Aminoglycosides are compounds related to neomycin and function in suppression of stop codon recognition. These pharmacological agents disrupt the recognition of stop codons, and create a non-specific tail that presumably allows for an increase of stability of the SMN protein. This results in an increase in SMN protein levels and function (187). Though these compounds show promise they require further optimization to increase their ability to penetrate into the central nervous system. New generations of aminoglycosides are being derived to address this trait, and their potential for a proposed therapy will need to be studied.

Another important goal in SMA therapeutics is the development of neuroprotective agents that can alleviate the SMA phenotype through non-SMN specific pathways. Due to encouraging results for other neurodegenerative diseases like ALS (188-190), the neuroprotectant IGF-1 has become an attractive candidate in a potential SMA therapy. In addition there have been small SMA clinical trials involving two other neurotrophic factors, riluzole, and cardiotrophin-1 with encouraging results (121, 191).

**SMN Specific Therapies**

SMN2 presents a very unique therapeutic intervention opportunity due to three main points; 1) All patients lack SMN1 2) All patients have two or more copies of SMN2 3) SMN2 has the capacity to encode the identical protein as SMN1. In addition to these traits the finding that delivery of full length SMN1 has only minimal results (120), SMN2 is a very attractive target for potential therapies. Molecular manipulation of SMN2, with the emergence of antisense, and trans-splicing molecules is becoming a focal point in the SMA field. In this thesis we propose multiple different types of small molecule therapeutics designed to manipulate the regional splice signals found in the SMN2 transcript.

The first derivation of therapy was a bi-functional RNA targeting the 5' splice sight of SMN2 exon 7. This therapy showed increase in SMN protein in patient fibroblasts when delivered by a rAAV2 vector after 13 days of infection. This suggests that bi-functional RNAs have potential to be a SMA therapy. Recently published work shows that upon lentiviral integration; a transgenic construct producing bi-functional RNAs could increase life span of severe SMA mice to 100 days (192). This would suggest that molecular manipulation has the potential to be a very useful therapy.

**Therapeutic RNA for Spinal Muscular Atrophy**

There are some concerns with small molecule RNA therapies. In the case of our first bi-functional RNAs and the recently published RNAs one of the most obvious concerns is having an antisense domain that is targeting exonic sequences. It is known that there are many degenerate and often times difficult to predict binding sites (ESEs)

that are used by the extended family of auxiliary splicing factors that are required for competent splicing. Targeting an antisense to an exon has the possibility to disrupt additional positive signals that are required for splicing. Because the most understood, and studied splice signals are found in exons, it was known there are multiple ESEs found in SMN2 exon 7 that contribute to exonic inclusion. Our first bi-functional RNAs and recently published bi-functional RNAs (192) possessed antisense sequences against exon 7. Even though the data presented suggests a beneficial affect; this could lead to potential mis-regulation of additional auxiliary splice signals. This could place a therapy at a predetermined disadvantage from others that target intronic sequences, or negative sequences; as in the E1 and ISSN1 bi-functional RNAs.

To address this issue we characterized the Element 1 region upstream of exon 7. After the initial data suggested that this was a bona fide negative regulator development of antisense to target this region could be a feasible therapy. Identification of the negative regulator proteins PTB, and FUSEBP allowed us to propose a 2-fold mode of action for these bi-functional RNAs. This mode of action was corroborated by the fact that the ASO alone against the Element 1 region did not have an increased affect above the bi-functional RNAs. Bi-functional RNAs directed against the Element 1 region will presumably competitively deregulate the negative signals found there, and recruit positive splice signals to the region. Upon delivery of Element 1 targeted bifunctional RNAs to patient fibroblasts, and the CNS of severe SMA mice we observed an increase in SMN protein. In the SMA mouse model there was a significant change in percent weight gained, and a trend to increased life span.

Recently a new intronic negative regulator was identified down stream of exon 7 termed ISSN1. To verify if a 2-fold mechanism could potentially function around the 3' splice sight region we developed bi-functional RNAs targeting this area. These new bi-functional RNAs showed a marked improvement over the exon targeting bi-functional RNAs. In addition targeting the down-stream repressor region with a bifunctional RNA increased nuclear gems in patient fibroblasts, both by plasmid derived and 2'-O-methyl modified RNAs. In an in vivo proof of principle experiment, the ISSN1 bi-functional RNA designed to recruit hTra2β1 did not have a significant effect in the Δ7 SMA mouse model, however showed promise in the severe mouse model. An ICV injection of the ISSN1 bi-functional RNAs into the severe SMA mice is an area of research that will be perused in earnest.

One of the first concerns of RNA therapy is its efficiency. Here we present data suggesting the improvement of a *trans*-splicing molecule by use of a downstream antisense RNA, or ASO (antisense olgionucleotide). *Trans*-splicing in combination with an ASO was shown to increase the effect seen in the SMN2 transcript (133, 150). This was achieved by the use of a short ASO directed to the exon 8/intron 7 splice acceptor area, called $In7^{11}$. We show work done in collaboration with Tristan Coady, another graduate student in the lab, that suggests this effect was specific for this antisense because a library of ASOs surrounding this region did not increase trans-splicing. Further work in this area was not presented but in summary; upon use of a single vector (ASO/*trans*-splicing) it was shown that there is an increase of SMN protein, in a SMA mouse model. This is promising work and its applicability in vivo will be further examined in the future.

In addition to single ASO therapies we present in this work a multi-antisense approach for increased efficiency. Based upon encouraging results from work in Duchenne's muscular dystrophy, and anti-viral therapies we devised a multi-ASO 'pool' to target multiple processes simultaneously (154, 157, 193, 194). The use of three ASOs targeting Element 1, ISSN1, or the exon 8 spice acceptor site is novel for SMA, and we present data that suggest this is beneficial to the Δ7 mouse. Each ASO is affecting a different region and a different process with-in the SMN2 transcript maturation. Element 1 antisense presumably inhibits the negative signals found there (PTB, FUSEBP, and potentially others), ISSN1 antisense would function similarly however downstream of exon 7. The final ASO will competitively inhibit the ability of the splicesome to identify the exon 8 splice acceptor site. Irrespective of antisense identity all should function concurrently to force definition of exon 7 and increase its inclusion. Data shown here suggest a gain of functional response in Δ7 mice as there are a greater proportion of injected mice able to right themselves after 3 ICV injection of the 'Pool' therapy. Further studies are planned for the Δ7 mouse model, in addition to evaluating the 'Pool' applicability in the severe mouse model.

**Increasing Efficiency of Therapies**

Research using ASOs in the past few years has identified a number of ways to increase the efficiency of the RNAs. Thus, for improved efficiency in the bi-functional RNAs, we added sequences that can help with subcellular targeting of the RNA. RNA splicing occurs in the nucleus and since the bi-functional RNAs are designed to

manipulate a splice signal it would be beneficial to enrich the therapeutics in that subcellular compartment. In an attempt to accomplish this, a U7 stem loop was added to all Element 1 and ISSN1 target bifunctional RNAs. This sequence has been shown to increase RNA accumulation in the nucleus (145, 146, 195, 196).

**Viral Vectors**

Use of viral vectors in gene therapy has been gaining interest for nearly 15 years. The main requirements for a strong candidate viral vector is immunological avoidance, persistence, and appropriate tissue tropism. The main family of viruses used in gene therapies thus far has been the adeno-associated virus family because of ability and utility in addressing the aforementioned requirements. Additionally rAAV gene cassettes are transcribed without integration, and will readily persist for months to years in mitotically quiescent cells (197). From this, an increasing area of development in potential gene therapy is AAV vectorology which can engineer altered cell tropisms. There are some main viral centric avenues that can be taken to engineer a required tropism, 1) use newly isolated serotypes of AAV, 2) package a AAV2 genome into capsid protein expressed from different AAV serotypes 3) designer AAV vectors can be made that have non-AAV capsid proteins that can direct delivery to novel cell types with high specificity. In this report we showed the use of rAAV serotype 2 in elevating the SMN protein levels after 13 days of infection. Though this is just a first step analysis we can hypothesize various serotypes that could be beneficial for a proposed gene therapy in SMA. Currently in the SMA field there are conflicting results suggesting that SMN protein is needed in skeletal muscle tissue or neurons. Because of this uncertainty the use of a rAAV serotype that has

the capacity for high levels of transduction in both tissue types may be important. For instance, serotypes 7 or 8 have a high level of expression in skeletal muscle, where as serotypes 1, 2, 5, and 9 have been shown to work well in various areas of the CNS. Based from this we can speculate that a 9/7, or 9/8 psuedo-type rAAV could be beneficial in SMA. This is a very simplistic view of tissue tropism, because many of these serotypes have various levels of overlapping expression; however it is possible to engineer a rAAV capsid for SMA.

In addition to improving tissue tropisms further modifications to the delivered cassettes can be made to increase the specificity of therapeutics. This is required due to the fact that nearly all AAV serotypes show some level of "leaking". As previously stated AAV tissue tropism is not defined as tissue specific but rather a gradient of expression for various tissues. Other tactics are needed to patch the "leakyness" of rAAV tissue expression for a more refined viral profile in potential therapy arenas. One way to further delineate an expression profile is by engineering a specific promoter that reflects the requirements of the disease. For a neuronal specific expression use of the promoters, neuron-specfic enolase (NSE), platelet-derived growth factor β (PDGF-β), and myelin basic protein (MBP) have been shown to relate a more CNS specific expression. Furthermore they were better at long-term expression in the CNS than other non-specific high expressing promoters (198-201).

Using specific promoters is a leading tactic to turn on expression of viral delivered therapeutics, and confer greater tissue specificity. However there is a growing interest in potential pathways that could decrease expression in undesired tissues. This would effectively create an off switch for added refinement to tissue or even temporal

expression. One pathway that is in its infancy but appears to be very promising is the use of micro-RNA sensitive sequences as regulators of viral delivered cassettes (202). This commandeers the miRNA pathway and uses it to silence vector expression in a tissue and developmental manner. miRNAs are short, noncoding RNA molecules that function in downregulation of gene expression by instigating target mRNA degradation (203, 204). It can be theorized that miRNA binding sequences added to viral expression vectors can act as a refined knockdown for a more controlled expression.

**Non-Viral Vectors**

Though the main focus of potential gene therapy vectors is recombinant viruses, there is increasing use of non-viral gene therapies (131, 132, 150, 155, 156, 182, 183). In this thesis we use the modification of a 2'-O-methyl group on all of the nucleotides of our RNAs. The main concern for using modified ASOs in the brain and spinal cord is effective delivery to these tissues. We overcome this hurdle by direct delivery of the RNA into the CNS of the SMA mice. The fact that drug dosage by direct pumping into the CNS of human patients is routinely done allows us to propose this as a potential therapy (205). Though another concern of modified oligo therapies is impermanence this can actually be considered a benefit. This trait facilitates ease of termination of therapy if the AON is toxic, ease of variable dosage, switching of chemistries, change of target, and ease of spread throughout the CNS. In continuation with the advancement of technology the purity and large scale manufacturing ability of AONs allow this to be an even more attractive therapeutic approach.

**Future Directions**

Further work will continue to characterize the phenotype attained by introduction of the bi-functional RNAs and AONs into animal models. Proposed future work in the mouse model can include, counting motor neuron numbers, assessing the fitness of neuromuscular junctions, and measuring individual muscle mass. In addition an RT-PCR to measure splicing ratio of the hSMN2 in various tissues of injected mice would be beneficial.

Future work in vitro could include, verifying the deletion of intronic sequences similar to Element 1 upstream of exon 7 do not have an affect on splicing. (similar to -600-U7 AON), over expression or downregulation of FUSEBP/PTB in HeLa cells and verifying of splicing ratios of the SMN2 transcript by RT-PCR.

Work in this thesis support the hypothesis that using small therapeutic RNAs designed to manipulate the molecular landscape of the SMN2 RNA transcript is a tractable therapy for SMA. The use of both rAAV derived and 2'-O-methyl modified RNAs can have beneficial effects either in primary patient fibroblasts or SMA mouse models. The increased utility of AONs is evident in the data depicting increased trans-splicing by a downstream antisense which can open an entirely novel tract for AONs; increasing efficiency of previous therapies. Though these therapies show promise in SMA the scope of their potential reach much farther to include any disease state caused by an alternative splicing event.

## References


1. Pearn, J.H. and Wilson, J. (1973) Acute Werdnig-Hoffmann disease: acute infantile spinal muscular atrophy. *Arch Dis Child,* **48,** 425-30.
2. Pascalet-Guidon, M.J., Bois, E., Feingold, J., Mattei, J.F., Combes, J.C. and Hamon, C. (1984) Cluster of acute infantile spinal muscular atrophy (Werdnig-Hoffmann disease) in a limited area of Reunion Island. *Clin Genet,* **26,** 39-42.
3. Burlet, P., Burglen, L., Clermont, O., Lefebvre, S., Viollet, L., Munnich, A. and Melki, J. (1996) Large scale deletions of the 5q13 region are specific to Werdnig-Hoffmann disease. *J Med Genet,* **33,** 281-3.
4. Rodrigues, N.R., Owen, N., Talbot, K., Patel, S., Muntoni, F., Ignatius, J., Dubowitz, V. and Davies, K.E. (1996) Gene deletions in spinal muscular atrophy. *J Med Genet,* **33,** 93-6.
5. Zerres, K. and Rudnik-Schoneborn, S. (1995) Natural history in proximal spinal muscular atrophy. Clinical analysis of 445 patients and suggestions for a modification of existing classifications. *Arch Neurol,* **52,** 518-23.
6. Melki, J., Lefebvre, S., Burglen, L., Burlet, P., Clermont, O., Millasseau, P., Reboullet, S., Benichou, B., Zeviani, M., Le Paslier, D. *et al.* (1994) De novo and inherited deletions of the 5q13 region in spinal muscular atrophies. *Science,* **264,** 1474-7.
7. Brahe, C., Clermont, O., Zappata, S., Tiziano, F., Melki, J. and Neri, G. (1996) Frameshift mutation in the survival motor neuron gene in a severe case of SMA type I. *Hum Mol Genet,* **5,** 1971-6.
8. Lefebvre, S., Burglen, L., Reboullet, S., Clermont, O., Burlet, P., Viollet, L., Benichou, B., Cruaud, C., Millasseau, P., Zeviani, M. *et al.* (1995) Identification and characterization of a spinal muscular atrophy-determining gene. *Cell,* **80,** 155-65.
9. MacKenzie, A.E., Jacob, P., Surh, L. and Besner, A. (1994) Genetic heterogeneity in spinal muscular atrophy: a linkage analysis-based assessment. *Neurology,* **44,** 919-24.

10. MacKenzie, A., Roy, N., Besner, A., Mettler, G., Jacob, P., Korneluk, R. and Surh, L. (1993) Genetic linkage analysis of Canadian spinal muscular atrophy kindreds using flanking microsatellite 5q13 polymorphisms. *Hum Genet,* **90,** 501-4.
11. Burglen, L., Lefebvre, S., Clermont, O., Burlet, P., Viollet, L., Cruaud, C., Munnich, A. and Melki, J. (1996) Structure and organization of the human survival motor neurone (SMN) gene. *Genomics,* **32,** 479-82.
12. Lorson, C.L., Strasswimmer, J., Yao, J.M., Baleja, J.D., Hahnen, E., Wirth, B., Le, T., Burghes, A.H. and Androphy, E.J. (1998) SMN oligomerization defect correlates with spinal muscular atrophy severity. *Nat Genet,* **19,** 63-6.
13. Battaglia, G., Princivalle, A., Forti, F., Lizier, C. and Zeviani, M. (1997) Expression of the SMN gene, the spinal muscular atrophy determining gene, in the mammalian central nervous system. *Hum Mol Genet,* **6,** 1961-71.
14. Lefebvre, S., Burlet, P., Liu, Q., Bertrandy, S., Clermont, O., Munnich, A., Dreyfuss, G. and Melki, J. (1997) Correlation between severity and SMN protein level in spinal muscular atrophy. *Nat Genet,* **16,** 265-9.
15. van der Steege, G., Grootscholten, P.M., Cobben, J.M., Zappata, S., Scheffer, H., den Dunnen, J.T., van Ommen, G.J., Brahe, C. and Buys, C.H. (1996) Apparent gene conversions involving the SMN gene in the region of the spinal muscular atrophy locus on chromosome 5. *Am J Hum Genet,* **59,** 834-8.
16. Parsons, D.W., McAndrew, P.E., Iannaccone, S.T., Mendell, J.R., Burghes, A.H. and Prior, T.W. (1998) Intragenic telSMN mutations: frequency, distribution, evidence of a founder effect, and modification of the spinal muscular atrophy phenotype by cenSMN copy number. *Am J Hum Genet,* **63,** 1712-23.
17. Monani, U.R., Sendtner, M., Coovert, D.D., Parsons, D.W., Andreassi, C., Le, T.T., Jablonka, S., Schrank, B., Rossoll, W., Prior, T.W. *et al.* (2000) The human centromeric survival motor neuron gene (SMN2) rescues embryonic lethality in Smn(-/-) mice and results in a mouse with spinal muscular atrophy. *Hum Mol Genet,* **9,** 333-9.
18. McAndrew, P.E., Parsons, D.W., Simard, L.R., Rochette, C., Ray, P.N., Mendell, J.R., Prior, T.W. and Burghes, A.H. (1997) Identification of proximal spinal muscular atrophy carriers and patients by analysis of SMNT and SMNC gene copy number. *Am J Hum Genet,* **60,** 1411-22.
19. Parsons, D.W., McAndrew, P.E., Allinson, P.S., Parker, W.D., Jr., Burghes, A.H. and Prior, T.W. (1998) Diagnosis of spinal muscular atrophy in an SMN non-deletion patient using a quantitative PCR screen and mutation analysis. *J Med Genet,* **35,** 674-6.
20. Hahnen, E., Forkert, R., Marke, C., Rudnik-Schoneborn, S., Schonling, J., Zerres, K. and Wirth, B. (1995) Molecular analysis of candidate genes on chromosome 5q13 in autosomal recessive spinal muscular atrophy: evidence of homozygous deletions of the SMN gene in unaffected individuals. *Hum Mol Genet,* **4,** 1927-33.
21. Hahnen, E., Schonling, J., Rudnik-Schoneborn, S., Zerres, K. and Wirth, B. (1996) Hybrid survival motor neuron genes in patients with autosomal recessive spinal muscular atrophy: new insights into molecular mechanisms responsible for the disease. *Am J Hum Genet,* **59,** 1057-65.

22. Lorson, C.L., Hahnen, E., Androphy, E.J. and Wirth, B. (1999) A single nucleotide in the SMN gene regulates splicing and is responsible for spinal muscular atrophy. *Proc Natl Acad Sci U S A,* **96,** 6307-11.
23. Monani, U.R., Lorson, C.L., Parsons, D.W., Prior, T.W., Androphy, E.J., Burghes, A.H. and McPherson, J.D. (1999) A single nucleotide difference that alters splicing patterns distinguishes the SMA gene SMN1 from the copy gene SMN2. *Hum Mol Genet,* **8,** 1177-83.
24. Lorson, C.L. and Androphy, E.J. (2000) An exonic enhancer is required for inclusion of an essential exon in the SMA-determining gene SMN. *Hum Mol Genet,* **9,** 259-65.
25. Sakharkar, M.K., Chow, V.T. and Kangueane, P. (2004) Distributions of exons and introns in the human genome. *In Silico Biol,* **4,** 387-93.
26. Lander, E.S. and Linton, L.M. and Birren, B. and Nusbaum, C. and Zody, M.C. and Baldwin, J. and Devon, K. and Dewar, K. and Doyle, M. and FitzHugh, W. *et al.* (2001) Initial sequencing and analysis of the human genome. *Nature,* **409,** 860-921.
27. Soller, M. (2006) Pre-messenger RNA processing and its regulation: a genomic perspective. *Cell Mol Life Sci,* **63,** 796-819.
28. Jurica, M.S. and Moore, M.J. (2003) Pre-mRNA splicing: awash in a sea of proteins. *Mol Cell,* **12,** 5-14.
29. Burset, M., Seledtsov, I.A. and Solovyev, V.V. (2000) Analysis of canonical and non-canonical splice sites in mammalian genomes. *Nucleic Acids Res,* **28,** 4364-75.
30. Venter, J.C. and Adams, M.D. and Myers, E.W. and Li, P.W. and Mural, R.J. and Sutton, G.G. and Smith, H.O. and Yandell, M. and Evans, C.A. and Holt, R.A. *et al.* (2001) The sequence of the human genome. *Science,* **291,** 1304-51.
31. Cartegni, L., Chew, S.L. and Krainer, A.R. (2002) Listening to silence and understanding nonsense: exonic mutations that affect splicing. *Nat Rev Genet,* **3,** 285-98.
32. Faustino, N.A. and Cooper, T.A. (2003) Pre-mRNA splicing and human disease. *Genes Dev,* **17,** 419-37.
33. Graveley, B.R. (2000) Sorting out the complexity of SR protein functions. *RNA,* **6,** 1197-211.
34. Blencowe, B.J. (2000) Exonic splicing enhancers: mechanism of action, diversity and role in human genetic diseases. *Trends Biochem Sci,* **25,** 106-10.
35. Shen, H., Kan, J.L. and Green, M.R. (2004) Arginine-serine-rich domains bound at splicing enhancers contact the branchpoint to promote prespliceosome assembly. *Mol Cell,* **13,** 367-76.
36. Fairbrother, W.G., Yeh, R.F., Sharp, P.A. and Burge, C.B. (2002) Predictive identification of exonic splicing enhancers in human genes. *Science,* **297,** 1007-13.
37. Tacke, R. and Manley, J.L. (1999) Determinants of SR protein specificity. *Curr Opin Cell Biol,* **11,** 358-62.
38. Liu, H.X., Zhang, M. and Krainer, A.R. (1998) Identification of functional exonic splicing enhancer motifs recognized by individual SR proteins. *Genes Dev,* **12,** 1998-2012.

39. Liu, H.X., Chew, S.L., Cartegni, L., Zhang, M.Q. and Krainer, A.R. (2000) Exonic splicing enhancer motif recognized by human SC35 under splicing conditions. *Mol Cell Biol,* **20,** 1063-71.
40. Schaal, T.D. and Maniatis, T. (1999) Selection and characterization of pre-mRNA splicing enhancers: identification of novel SR protein-specific enhancer sequences. *Mol Cell Biol,* **19,** 1705-19.
41. Schaal, T.D. and Maniatis, T. (1999) Multiple distinct splicing enhancers in the protein-coding sequences of a constitutively spliced pre-mRNA. *Mol Cell Biol,* **19,** 261-73.
42. Coulter, L.R., Landree, M.A. and Cooper, T.A. (1997) Identification of a new class of exonic splicing enhancers by in vivo selection. *Mol Cell Biol,* **17,** 2143-50.
43. Tian, H. and Kole, R. (1995) Selection of novel exon recognition elements from a pool of random sequences. *Mol Cell Biol,* **15,** 6291-8.
44. Pozzoli, U. and Sironi, M. (2005) Silencers regulate both constitutive and alternative splicing events in mammals. *Cell Mol Life Sci,* **62,** 1579-604.
45. Fairbrother, W.G. and Chasin, L.A. (2000) Human genomic sequences that inhibit splicing. *Mol Cell Biol,* **20,** 6816-25.
46. Singh, N.K., Singh, N.N., Androphy, E.J. and Singh, R.N. (2006) Splicing of a critical exon of human Survival Motor Neuron is regulated by a unique silencer element located in the last intron. *Mol Cell Biol,* **26,** 1333-46.
47. Zheng, Z.M., Huynen, M. and Baker, C.C. (1998) A pyrimidine-rich exonic splicing suppressor binds multiple RNA splicing factors and inhibits spliceosome assembly. *Proc Natl Acad Sci U S A,* **95,** 14088-93.
48. Miyajima, H., Miyaso, H., Okumura, M., Kurisu, J. and Imaizumi, K. (2002) Identification of a cis-acting element for the regulation of SMN exon 7 splicing. *J Biol Chem,* **277,** 23271-7.
49. Del Gatto-Konczak, F., Olive, M., Gesnel, M.C. and Breathnach, R. (1999) hnRNP A1 recruited to an exon in vivo can function as an exon splicing silencer. *Mol Cell Biol,* **19,** 251-60.
50. Datar, K.V., Dreyfuss, G. and Swanson, M.S. (1993) The human hnRNP M proteins: identification of a methionine/arginine-rich repeat motif in ribonucleoproteins. *Nucleic Acids Res,* **21,** 439-46.
51. Dreyfuss, G., Matunis, M.J., Pinol-Roma, S. and Burd, C.G. (1993) hnRNP proteins and the biogenesis of mRNA. *Annu Rev Biochem,* **62,** 289-321.
52. Carstens, R.P., Wagner, E.J. and Garcia-Blanco, M.A. (2000) An intronic splicing silencer causes skipping of the IIIb exon of fibroblast growth factor receptor 2 through involvement of polypyrimidine tract binding protein. *Mol Cell Biol,* **20,** 7388-400.
53. Chan, R.C. and Black, D.L. (1997) The polypyrimidine tract binding protein binds upstream of neural cell-specific c-src exon N1 to repress the splicing of the intron downstream. *Mol Cell Biol,* **17,** 4667-76.
54. Wagner, E.J. and Garcia-Blanco, M.A. (2001) Polypyrimidine tract binding protein antagonizes exon definition. *Mol Cell Biol,* **21,** 3281-8.
55. Krecic, A.M. and Swanson, M.S. (1999) hnRNP complexes: composition, structure, and function. *Curr Opin Cell Biol,* **11,** 363-71.

56. Cartegni, L. and Krainer, A.R. (2002) Disruption of an SF2/ASF-dependent exonic splicing enhancer in SMN2 causes spinal muscular atrophy in the absence of SMN1. *Nat Genet,* **30,** 377-84.
57. Kashima, T. and Manley, J.L. (2003) A negative element in SMN2 exon 7 inhibits splicing in spinal muscular atrophy. *Nat Genet,* **34,** 460-3.
58. Hofmann, Y., Lorson, C.L., Stamm, S., Androphy, E.J. and Wirth, B. (2000) Htra2-beta 1 stimulates an exonic splicing enhancer and can restore full-length SMN expression to survival motor neuron 2 (SMN2). *Proc Natl Acad Sci U S A,* **97,** 9618-23.
59. Young, P.J., DiDonato, C.J., Hu, D., Kothary, R., Androphy, E.J. and Lorson, C.L. (2002) SRp30c-dependent stimulation of survival motor neuron (SMN) exon 7 inclusion is facilitated by a direct interaction with hTra2 beta 1. *Hum Mol Genet,* **11,** 577-87.
60. Novelli, G., Calza, L., Amicucci, P., Giardino, L., Pozza, M., Silani, V., Pizzuti, A., Gennarelli, M., Piombo, G., Capon, F. *et al.* (1997) Expression study of survival motor neuron gene in human fetal tissues. *Biochem Mol Med,* **61,** 102-6.
61. Tizzano, E.F., Cabot, C. and Baiget, M. (1998) Cell-specific survival motor neuron gene expression during human development of the central nervous system: implications for the pathogenesis of spinal muscular atrophy. *Am J Pathol,* **153,** 355-61.
62. Soler-Botija, C., Ferrer, I., Gich, I., Baiget, M. and Tizzano, E.F. (2002) Neuronal death is enhanced and begins during foetal development in type I spinal muscular atrophy spinal cord. *Brain,* **125,** 1624-34.
63. Liu, Q. and Dreyfuss, G. (1996) A novel nuclear structure containing the survival of motor neurons protein. *EMBO J,* **15,** 3555-65.
64. Fischer, U., Liu, Q. and Dreyfuss, G. (1997) The SMN-SIP1 complex has an essential role in spliceosomal snRNP biogenesis. *Cell,* **90,** 1023-9.
65. Charroux, B., Pellizzoni, L., Perkinson, R.A., Shevchenko, A., Mann, M. and Dreyfuss, G. (1999) Gemin3: A novel DEAD box protein that interacts with SMN, the spinal muscular atrophy gene product, and is a component of gems. *J Cell Biol,* **147,** 1181-94.
66. Charroux, B., Pellizzoni, L., Perkinson, R.A., Yong, J., Shevchenko, A., Mann, M. and Dreyfuss, G. (2000) Gemin4. A novel component of the SMN complex that is found in both gems and nucleoli. *J Cell Biol,* **148,** 1177-86.
67. Pellizzoni, L., Baccon, J., Rappsilber, J., Mann, M. and Dreyfuss, G. (2002) Purification of native survival of motor neurons complexes and identification of Gemin6 as a novel component. *J Biol Chem,* **277,** 7540-5.
68. Gubitz, A.K., Feng, W. and Dreyfuss, G. (2004) The SMN complex. *Exp Cell Res,* **296,** 51-6.
69. Pellizzoni, L., Charroux, B. and Dreyfuss, G. (1999) SMN mutants of spinal muscular atrophy patients are defective in binding to snRNP proteins. *Proc Natl Acad Sci U S A,* **96,** 11167-72.
70. Raker, V.A., Hartmuth, K., Kastner, B. and Luhrmann, R. (1999) Spliceosomal U snRNP core assembly: Sm proteins assemble onto an Sm site RNA nonanucleotide in a specific and thermodynamically stable manner. *Mol Cell Biol,* **19,** 6554-65.

71. Buhler, D., Raker, V., Luhrmann, R. and Fischer, U. (1999) Essential role for the tudor domain of SMN in spliceosomal U snRNP assembly: implications for spinal muscular atrophy. *Hum Mol Genet,* **8,** 2351-7.
72. Selenko, P., Sprangers, R., Stier, G., Buhler, D., Fischer, U. and Sattler, M. (2001) SMN tudor domain structure and its interaction with the Sm proteins. *Nat Struct Biol,* **8,** 27-31.
73. Sprangers, R., Selenko, P., Sattler, M., Sinning, I. and Groves, M.R. (2003) Definition of domain boundaries and crystallization of the SMN Tudor domain. *Acta Crystallogr D Biol Crystallogr,* **59,** 366-8.
74. Winkler, C., Eggert, C., Gradl, D., Meister, G., Giegerich, M., Wedlich, D., Laggerbauer, B. and Fischer, U. (2005) Reduced U snRNP assembly causes motor axon degeneration in an animal model for spinal muscular atrophy. *Genes Dev,* **19,** 2320-30.
75. Rossoll, W., Kroning, A.K., Ohndorf, U.M., Steegborn, C., Jablonka, S. and Sendtner, M. (2002) Specific interaction of Smn, the spinal muscular atrophy determining gene product, with hnRNP-R and gry-rbp/hnRNP-Q: a role for Smn in RNA processing in motor axons? *Hum Mol Genet,* **11,** 93-105.
76. Rossoll, W., Jablonka, S., Andreassi, C., Kroning, A.K., Karle, K., Monani, U.R. and Sendtner, M. (2003) Smn, the spinal muscular atrophy-determining gene product, modulates axon growth and localization of beta-actin mRNA in growth cones of motoneurons. *J Cell Biol,* **163,** 801-12.
77. Zhang, H.L., Pan, F., Hong, D., Shenoy, S.M., Singer, R.H. and Bassell, G.J. (2003) Active transport of the survival motor neuron protein and the role of exon-7 in cytoplasmic localization. *J Neurosci,* **23,** 6627-37.
78. Luo, L. (2002) Actin cytoskeleton regulation in neuronal morphogenesis and structural plasticity. *Annu Rev Cell Dev Biol,* **18,** 601-35.
79. Crawford, T.O. and Pardo, C.A. (1996) The neurobiology of childhood spinal muscular atrophy. *Neurobiol Dis,* **3,** 97-110.
80. Munsat, T.L., Skerry, L., Korf, B., Pober, B., Schapira, Y., Gascon, G.G., al-Rajeh, S.M., Dubowitz, V., Davies, K., Brzustowicz, L.M. *et al.* (1990) Phenotypic heterogeneity of spinal muscular atrophy mapping to chromosome 5q11.2-13.3 (SMA 5q). *Neurology,* **40,** 1831-6.
81. Wehner, K.A., Ayala, L., Kim, Y., Young, P.J., Hosler, B.A., Lorson, C.L., Baserga, S.J. and Francis, J.W. (2002) Survival motor neuron protein in the nucleolus of mammalian neurons. *Brain Res,* **945,** 160-73.
82. Young, P.J., Le, T.T., Dunckley, M., Nguyen, T.M., Burghes, A.H. and Morris, G.E. (2001) Nuclear gems and Cajal (coiled) bodies in fetal tissues: nucleolar distribution of the spinal muscular atrophy protein, SMN. *Exp Cell Res,* **265,** 252-61.
83. Coovert, D.D., Le, T.T., McAndrew, P.E., Strasswimmer, J., Crawford, T.O., Mendell, J.R., Coulson, S.E., Androphy, E.J., Prior, T.W. and Burghes, A.H. (1997) The survival motor neuron protein in spinal muscular atrophy. *Hum Mol Genet,* **6,** 1205-14.
84. Andreassi, C., Jarecki, J., Zhou, J., Coovert, D.D., Monani, U.R., Chen, X., Whitney, M., Pollok, B., Zhang, M., Androphy, E. *et al.* (2001) Aclarubicin

treatment restores SMN levels to cells derived from type I spinal muscular atrophy patients. *Hum Mol Genet,* **10,** 2841-9.
85. Andreassi, C., Patrizi, A.L., Monani, U.R., Burghes, A.H., Brahe, C. and Eboli, M.L. (2002) Expression of the survival of motor neuron (SMN) gene in primary neurons and increase in SMN levels by activation of the N-methyl-D-aspartate glutamate receptor. *Neurogenetics,* **4,** 29-36.
86. Liu, Q., Fischer, U., Wang, F. and Dreyfuss, G. (1997) The spinal muscular atrophy disease gene product, SMN, and its associated protein SIP1 are in a complex with spliceosomal snRNP proteins. *Cell,* **90,** 1013-21.
87. Pellizzoni, L., Kataoka, N., Charroux, B. and Dreyfuss, G. (1998) A novel function for SMN, the spinal muscular atrophy disease gene product, in pre-mRNA splicing. *Cell,* **95,** 615-24.
88. Williams, B.Y., Hamilton, S.L. and Sarkar, H.K. (2000) The survival motor neuron protein interacts with the transactivator FUSE binding protein from human fetal brain. *FEBS Lett,* **470,** 207-10.
89. Strasswimmer, J., Lorson, C.L., Breiding, D.E., Chen, J.J., Le, T., Burghes, A.H. and Androphy, E.J. (1999) Identification of survival motor neuron as a transcriptional activator-binding protein. *Hum Mol Genet,* **8,** 1219-26.
90. Kerr, D.A., Nery, J.P., Traystman, R.J., Chau, B.N. and Hardwick, J.M. (2000) Survival motor neuron protein modulates neuron-specific apoptosis. *Proc Natl Acad Sci U S A,* **97,** 13312-7.
91. Young, P.J., Day, P.M., Zhou, J., Androphy, E.J., Morris, G.E. and Lorson, C.L. (2002) A direct interaction between the survival motor neuron protein and p53 and its relationship to spinal muscular atrophy. *J Biol Chem,* **277,** 2852-9.
92. Vyas, S., Bechade, C., Riveau, B., Downward, J. and Triller, A. (2002) Involvement of survival motor neuron (SMN) protein in cell death. *Hum Mol Genet,* **11,** 2751-64.
93. Lefebvre, S., Burlet, P., Viollet, L., Bertrandy, S., Huber, C., Belser, C. and Munnich, A. (2002) A novel association of the SMN protein with two major non-ribosomal nucleolar proteins and its implication in spinal muscular atrophy. *Hum Mol Genet,* **11,** 1017-27.
94. Hofmann, Y. and Wirth, B. (2002) hnRNP-G promotes exon 7 inclusion of survival motor neuron (SMN) via direct interaction with Htra2-beta1. *Hum Mol Genet,* **11,** 2037-49.
95. Singh, N.N., Androphy, E.J. and Singh, R.N. (2004) The regulation and regulatory activities of alternative splicing of the SMN gene. *Crit Rev Eukaryot Gene Expr,* **14,** 271-85.
96. Singh, N.N., Androphy, E.J. and Singh, R.N. (2004) In vivo selection reveals combinatorial controls that define a critical exon in the spinal muscular atrophy genes. *RNA,* **10,** 1291-305.
97. Singh, N.N., Androphy, E.J. and Singh, R.N. (2004) An extended inhibitory context causes skipping of exon 7 of SMN2 in spinal muscular atrophy. *Biochem Biophys Res Commun,* **315,** 381-8.
98. Miyaso, H., Okumura, M., Kondo, S., Higashide, S., Miyajima, H. and Imaizumi, K. (2003) An Intronic Splicing Enhancer Element in Survival Motor Neuron (SMN) Pre-mRNA. *J Biol Chem,* **278,** 15825-31.

99. Kernochan, L.E., Russo, M.L., Woodling, N.S., Huynh, T.N., Avila, A.M., Fischbeck, K.H. and Sumner, C.J. (2005) The role of histone acetylation in SMN gene expression. *Hum Mol Genet,* **14,** 1171-82.
100. Sumner, C.J., Huynh, T.N., Markowitz, J.A., Perhac, J.S., Hill, B., Coovert, D.D., Schussler, K., Chen, X., Jarecki, J., Burghes, A.H. *et al.* (2003) Valproic acid increases SMN levels in spinal muscular atrophy patient cells. *Ann Neurol,* **54,** 647-54.
101. Brahe, C., Vitali, T., Tiziano, F.D., Angelozzi, C., Pinto, A.M., Borgo, F., Moscato, U., Bertini, E., Mercuri, E. and Neri, G. (2005) Phenylbutyrate increases SMN gene expression in spinal muscular atrophy patients. *Eur J Hum Genet,* **13,** 256-9.
102. Chang, J.G., Hsieh-Li, H.M., Jong, Y.J., Wang, N.M., Tsai, C.H. and Li, H. (2001) Treatment of spinal muscular atrophy by sodium butyrate. *Proc Natl Acad Sci U S A,* **98,** 9808-13.
103. Mattis, V.B., Rai, R., Wang, J., Chang, C.W., Coady, T. and Lorson, C.L. (2006) Novel aminoglycosides increase SMN levels in spinal muscular atrophy fibroblasts. *Hum Genet,* **120,** 589-601.
104. Madocsai, C., Lim, S.R., Geib, T., Lam, B.J. and Hertel, K.J. (2005) Correction of SMN2 Pre-mRNA splicing by antisense U7 small nuclear RNAs. *Mol Ther,* **12,** 1013-22.
105. Lim, S.R. and Hertel, K.J. (2001) Modulation of survival motor neuron pre-mRNA splicing by inhibition of alternative 3' splice site pairing. *J Biol Chem,* **276,** 45476-83.
106. Sangiuolo, F., Filareto, A., Spitalieri, P., Scaldaferri, M.L., Mango, R., Bruscia, E., Citro, G., Brunetti, E., De Felici, M. and Novelli, G. (2005) In vitro restoration of functional SMN protein in human trophoblast cells affected by spinal muscular atrophy by small fragment homologous replacement. *Hum Gene Ther,* **16,** 869-80.
107. Skordis, L.A., Dunckley, M.G., Yue, B., Eperon, I.C. and Muntoni, F. (2003) Bifunctional antisense oligonucleotides provide a trans-acting splicing enhancer that stimulates SMN2 gene expression in patient fibroblasts. *Proc Natl Acad Sci U S A,* **100,** 4114-9.
108. Cartegni, L. and Krainer, A.R. (2003) Correction of disease-associated exon skipping by synthetic exon-specific activators. *Nat Struct Biol,* **10,** 120-5.
109. Cartegni, L., Wang, J., Zhu, Z., Zhang, M.Q. and Krainer, A.R. (2003) ESEfinder: A web resource to identify exonic splicing enhancers. *Nucleic Acids Res,* **31,** 3568-71.
110. Vacek, M., Sazani, P. and Kole, R. (2003) Antisense-mediated redirection of mRNA splicing. *Cell Mol Life Sci,* **60,** 825-33.
111. Lacerra, G., Sierakowska, H., Carestia, C., Fucharoen, S., Summerton, J., Weller, D. and Kole, R. (2000) Restoration of hemoglobin A synthesis in erythroid cells from peripheral blood of thalassemic patients. *Proc Natl Acad Sci U S A,* **97,** 9591-6.
112. Mansfield, S.G., Kole, J., Puttaraju, M., Yang, C.C., Garcia-Blanco, M.A., Cohn, J.A. and Mitchell, L.G. (2000) Repair of CFTR mRNA by spliceosome-mediated RNA trans-splicing. *Gene Ther,* **7,** 1885-95.

113. Puttaraju, M., Jamison, S.F., Mansfield, S.G., Garcia-Blanco, M.A. and Mitchell, L.G. (1999) Spliceosome-mediated RNA trans-splicing as a tool for gene therapy. *Nat Biotechnol,* **17,** 246-52.
114. Dallinger, G., Puttaraju, M., Mitchell, L.G., Yancey, K.B., Yee, C., Klausegger, A., Hintner, H. and Bauer, J.W. (2003) Development of spliceosome-mediated RNA trans-splicing (SMaRT) for the correction of inherited skin diseases. *Exp Dermatol,* **12,** 37-46.
115. Brichta, L., Hofmann, Y., Hahnen, E., Siebzehnrubl, F.A., Raschke, H., Blumcke, I., Eyupoglu, I.Y. and Wirth, B. (2003) Valproic acid increases the SMN2 protein level: a well-known drug as a potential therapy for spinal muscular atrophy. *Hum Mol Genet,* **12,** 2481-9.
116. Andreassi, C., Angelozzi, C., Tiziano, F.D., Vitali, T., De Vincenzi, E., Boninsegna, A., Villanova, M., Bertini, E., Pini, A., Neri, G. *et al.* (2004) Phenylbutyrate increases SMN expression in vitro: relevance for treatment of spinal muscular atrophy. *Eur J Hum Genet,* **12,** 59-65.
117. Grzeschik, S.M., Ganta, M., Prior, T.W., Heavlin, W.D. and Wang, C.H. (2005) Hydroxyurea enhances SMN2 gene expression in spinal muscular atrophy cells. *Ann Neurol,* **58,** 194-202.
118. Lunn, M.R., Root, D.E., Martino, A.M., Flaherty, S.P., Kelley, B.P., Coovert, D.D., Burghes, A.H., Man, N.T., Morris, G.E., Zhou, J. *et al.* (2004) Indoprofen upregulates the survival motor neuron protein through a cyclooxygenase-independent mechanism. *Chem Biol,* **11,** 1489-93.
119. Wolstencroft, E.C., Mattis, V., Bajer, A.A., Young, P.J. and Lorson, C.L. (2005) A non-sequence-specific requirement for SMN protein activity: the role of aminoglycosides in inducing elevated SMN protein levels. *Hum Mol Genet,* **14,** 1199-210.
120. Azzouz, M., Le, T., Ralph, G.S., Walmsley, L., Monani, U.R., Lee, D.C., Wilkes, F., Mitrophanous, K.A., Kingsman, S.M., Burghes, A.H. *et al.* (2004) Lentivector-mediated SMN replacement in a mouse model of spinal muscular atrophy. *J Clin Invest,* **114,** 1726-31.
121. Haddad, H., Cifuentes-Diaz, C., Miroglio, A., Roblot, N., Joshi, V. and Melki, J. (2003) Riluzole attenuates spinal muscular atrophy disease progression in a mouse model. *Muscle Nerve,* **28,** 432-7.
122. Garcia-Blanco, M.A., Baraniak, A.P. and Lasda, E.L. (2004) Alternative splicing in disease and therapy. *Nat Biotechnol,* **22,** 535-46.
123. Matsushita, T., Elliger, S., Elliger, C., Podsakoff, G., Villarreal, L., Kurtzman, G.J., Iwaki, Y. and Colosi, P. (1998) Adeno-associated virus vectors can be efficiently produced without helper virus. *Gene Ther,* **5,** 938-45.
124. Xiao, X., Li, J. and Samulski, R.J. (1998) Production of high-titer recombinant adeno-associated virus vectors in the absence of helper adenovirus. *J Virol,* **72,** 2224-32.
125. Zhang, M.L., Lorson, C.L., Androphy, E.J. and Zhou, J. (2001) An in vivo reporter system for measuring increased inclusion of exon 7 in SMN2 mRNA: potential therapy of SMA. *Gene Ther,* **8,** 1532-8.
126. Wirth, B., Herz, M., Wetter, A., Moskau, S., Hahnen, E., Rudnik-Schoneborn, S., Wienker, T. and Zerres, K. (1999) Quantitative analysis of survival motor neuron

copies: identification of subtle SMN1 mutations in patients with spinal muscular atrophy, genotype-phenotype correlation, and implications for genetic counseling. *Am J Hum Genet,* **64,** 1340-56.
127. Meister, G., Eggert, C. and Fischer, U. (2002) SMN-mediated assembly of RNPs: a complex story. *Trends Cell Biol,* **12,** 472-8.
128. Singh, N.N., Singh, R.N. and Androphy, E.J. (2007) Modulating role of RNA structure in alternative splicing of a critical exon in the spinal muscular atrophy genes. *Nucleic Acids Res,* **35,** 371-89.
129. Riessland, M., Brichta, L., Hahnen, E. and Wirth, B. (2006) The benzamide M344, a novel histone deacetylase inhibitor, significantly increases SMN2 RNA/protein levels in spinal muscular atrophy cells. *Hum Genet,* **120,** 101-10.
130. Sakla, M.S. and Lorson, C.L. (2008) Induction of full-length survival motor neuron by polyphenol botanical compounds. *Hum Genet,* **122,** 635-43.
131. Hua, Y., Vickers, T.A., Baker, B.F., Bennett, C.F. and Krainer, A.R. (2007) Enhancement of SMN2 exon 7 inclusion by antisense oligonucleotides targeting the exon. *PLoS Biol,* **5,** e73.
132. Hua, Y., Vickers, T.A., Okunola, H.L., Bennett, C.F. and Krainer, A.R. (2008) Antisense masking of an hnRNP A1/A2 intronic splicing silencer corrects SMN2 splicing in transgenic mice. *Am J Hum Genet,* **82,** 834-48.
133. Coady, T.H., Shababi, M., Tullis, G.E. and Lorson, C.L. (2007) Restoration of SMN function: delivery of a trans-splicing RNA re-directs SMN2 pre-mRNA splicing. *Mol Ther,* **15,** 1471-8.
134. Marquis, J., Meyer, K., Angehrn, L., Kampfer, S.S., Rothen-Rutishauser, B. and Schumperli, D. (2007) Spinal muscular atrophy: SMN2 pre-mRNA splicing corrected by a U7 snRNA derivative carrying a splicing enhancer sequence. *Mol Ther,* **15,** 1479-86.
135. Baughan, T., Shababi, M., Coady, T.H., Dickson, A.M., Tullis, G.E. and Lorson, C.L. (2006) Stimulating full-length SMN2 expression by delivering bifunctional RNAs via a viral vector. *Mol Ther,* **14,** 54-62.
136. Jiang, M., Arzumanov, A.A., Gait, M.J. and Milner, J. (2005) A bi-functional siRNA construct induces RNA interference and also primes PCR amplification for its own quantification. *Nucleic Acids Res,* **33,** e151.
137. Ashiya, M. and Grabowski, P.J. (1997) A neuron-specific splicing switch mediated by an array of pre-mRNA repressor sites: evidence of a regulatory role for the polypyrimidine tract binding protein and a brain-specific PTB counterpart. *RNA,* **3,** 996-1015.
138. Irwin, N., Baekelandt, V., Goritchenko, L. and Benowitz, L.I. (1997) Identification of two proteins that bind to a pyrimidine-rich sequence in the 3'-untranslated region of GAP-43 mRNA. *Nucleic Acids Res,* **25,** 1281-8.
139. Grossman, J.S., Meyer, M.I., Wang, Y.C., Mulligan, G.J., Kobayashi, R. and Helfman, D.M. (1998) The use of antibodies to the polypyrimidine tract binding protein (PTB) to analyze the protein components that assemble on alternatively spliced pre-mRNAs that use distant branch points. *RNA,* **4,** 613-25.
140. Zhang, L., Liu, W. and Grabowski, P.J. (1999) Coordinate repression of a trio of neuron-specific splicing events by the splicing regulator PTB. *RNA,* **5,** 117-30.

141. Liu, J., Kouzine, F., Nie, Z., Chung, H.J., Elisha-Feil, Z., Weber, A., Zhao, K. and Levens, D. (2006) The FUSE/FBP/FIR/TFIIH system is a molecular machine programming a pulse of c-myc expression. *EMBO J,* **25,** 2119-30.
142. Liu, J., He, L., Collins, I., Ge, H., Libutti, D., Li, J., Egly, J.M. and Levens, D. (2000) The FBP interacting repressor targets TFIIH to inhibit activated transcription. *Mol Cell,* **5,** 331-41.
143. He, L., Liu, J., Collins, I., Sanford, S., O'Connell, B., Benham, C.J. and Levens, D. (2000) Loss of FBP function arrests cellular proliferation and extinguishes c-myc expression. *EMBO J,* **19,** 1034-44.
144. Goyenvalle, A., Vulin, A., Fougerousse, F., Leturcq, F., Kaplan, J.C., Garcia, L. and Danos, O. (2004) Rescue of dystrophic muscle through U7 snRNA-mediated exon skipping. *Science,* **306,** 1796-9.
145. Suter, D., Tomasini, R., Reber, U., Gorman, L., Kole, R. and Schumperli, D. (1999) Double-target antisense U7 snRNAs promote efficient skipping of an aberrant exon in three human beta-thalassemic mutations. *Hum Mol Genet,* **8,** 2415-23.
146. Gorman, L., Suter, D., Emerick, V., Schumperli, D. and Kole, R. (1998) Stable alteration of pre-mRNA splicing patterns by modified U7 small nuclear RNAs. *Proc Natl Acad Sci U S A,* **95,** 4929-34.
147. Alter, J., Lou, F., Rabinowitz, A., Yin, H., Rosenfeld, J., Wilton, S.D., Partridge, T.A. and Lu, Q.L. (2006) Systemic delivery of morpholino oligonucleotide restores dystrophin expression bodywide and improves dystrophic pathology. *Nat Med,* **12,** 175-7.
148. Smith, R.A., Miller, T.M., Yamanaka, K., Monia, B.P., Condon, T.P., Hung, G., Lobsiger, C.S., Ward, C.M., McAlonis-Downes, M., Wei, H. *et al.* (2006) Antisense oligonucleotide therapy for neurodegenerative disease. *J Clin Invest,* **116,** 2290-6.
149. Le, T.T., Pham, L.T., Butchbach, M.E., Zhang, H.L., Monani, U.R., Coovert, D.D., Gavrilina, T.O., Xing, L., Bassell, G.J. and Burghes, A.H. (2005) SMNDelta7, the major product of the centromeric survival motor neuron (SMN2) gene, extends survival in mice with spinal muscular atrophy and associates with full-length SMN. *Hum Mol Genet,* **14,** 845-57.
150. Coady, T.H., Baughan, T.D., Shababi, M., Passini, M.A. and Lorson, C.L. (2008) Development of a Single Vector System that Enhances Trans-Splicing of SMN2 Transcripts. *PLoS ONE,* **3,** e3468.
151. Dickson, A., Osman, E. and Lorson, C. (2008) A Negatively-Acting Bifunctional RNA Increases Survival Motor Neuron in vitro and in vivo. *Hum Gene Ther*.
152. Singh, R., Valcarcel, J. and Green, M.R. (1995) Distinct binding specificities and functions of higher eukaryotic polypyrimidine tract-binding proteins. *Science,* **268,** 1173-6.
153. Matsushita, K., Tomonaga, T., Shimada, H., Shioya, A., Higashi, M., Matsubara, H., Harigaya, K., Nomura, F., Libutti, D., Levens, D. *et al.* (2006) An essential role of alternative splicing of c-myc suppressor FUSE-binding protein-interacting repressor in carcinogenesis. *Cancer Res,* **66,** 1409-17.
154. Aartsma-Rus, A., Bremmer-Bout, M., Janson, A.A., den Dunnen, J.T., van Ommen, G.J. and van Deutekom, J.C. (2002) Targeted exon skipping as a

potential gene correction therapy for Duchenne muscular dystrophy. *Neuromuscul Disord,* **12 Suppl 1,** S71-7.
155. van Deutekom, J.C., Bremmer-Bout, M., Janson, A.A., Ginjaar, I.B., Baas, F., den Dunnen, J.T. and van Ommen, G.J. (2001) Antisense-induced exon skipping restores dystrophin expression in DMD patient derived muscle cells. *Hum Mol Genet,* **10,** 1547-54.
156. Mann, C.J., Honeyman, K., Cheng, A.J., Ly, T., Lloyd, F., Fletcher, S., Morgan, J.E., Partridge, T.A. and Wilton, S.D. (2001) Antisense-induced exon skipping and synthesis of dystrophin in the mdx mouse. *Proc Natl Acad Sci U S A,* **98,** 42-7.
157. Aartsma-Rus, A., Janson, A.A., Kaman, W.E., Bremmer-Bout, M., van Ommen, G.J., den Dunnen, J.T. and van Deutekom, J.C. (2004) Antisense-induced multiexon skipping for Duchenne muscular dystrophy makes more sense. *Am J Hum Genet,* **74,** 83-92.
158. Williams, J.H., Sirsi, S.R., Latta, D.R. and Lutz, G.J. (2006) Induction of dystrophin expression by exon skipping in mdx mice following intramuscular injection of antisense oligonucleotides complexed with PEG-PEI copolymers. *Mol Ther,* **14,** 88-96.
159. van Deutekom, J.C., Janson, A.A., Ginjaar, I.B., Frankhuizen, W.S., Aartsma-Rus, A., Bremmer-Bout, M., den Dunnen, J.T., Koop, K., van der Kooi, A.J., Goemans, N.M. *et al.* (2007) Local dystrophin restoration with antisense oligonucleotide PRO051. *N Engl J Med,* **357,** 2677-86.
160. Passini, M.A., Macauley, S.L., Huff, M.R., Taksir, T.V., Bu, J., Wu, I.H., Piepenhagen, P.A., Dodge, J.C., Shihabuddin, L.S., O'Riordan, C.R. *et al.* (2005) AAV vector-mediated correction of brain pathology in a mouse model of Niemann-Pick A disease. *Mol Ther,* **11,** 754-62.
161. Passini, M.A., Bu, J., Fidler, J.A., Ziegler, R.J., Foley, J.W., Dodge, J.C., Yang, W.W., Clarke, J., Taksir, T.V., Griffiths, D.A. *et al.* (2007) Combination brain and systemic injections of AAV provide maximal functional and survival benefits in the Niemann-Pick mouse. *Proc Natl Acad Sci U S A,* **104,** 9505-10.
162. Passini, M.A., Watson, D.J., Vite, C.H., Landsburg, D.J., Feigenbaum, A.L. and Wolfe, J.H. (2003) Intraventricular brain injection of adeno-associated virus type 1 (AAV1) in neonatal mice results in complementary patterns of neuronal transduction to AAV2 and total long-term correction of storage lesions in the brains of beta-glucuronidase-deficient mice. *J Virol,* **77,** 7034-40.
163. Briese, M., Esmaeili, B., Fraboulet, S., Burt, E.C., Christodoulou, S., Towers, P.R., Davies, K.E. and Sattelle, D.B. (2008) Deletion of smn-1, the Caenorhabditis elegans orthologue of the spinal muscular atrophy gene, results in locomotor dysfunction and reduced lifespan. *Hum Mol Genet*.
164. Rajendra, T.K., Gonsalvez, G.B., Walker, M.P., Shpargel, K.B., Salz, H.K. and Matera, A.G. (2007) A Drosophila melanogaster model of spinal muscular atrophy reveals a function for SMN in striated muscle. *J Cell Biol,* **176,** 831-41.
165. Pearn, J.H. (1973) The gene frequency of acute Werdnig-Hoffmann disease (SMA type 1). A total population survey in North-East England. *J Oral Surg,* **10,** 260-5.

166. van der Steege, G., Draaijers, T.G., Grootscholten, P.M., Osinga, J., Anzevino, R., Velona, I., Den Dunnen, J.T., Scheffer, H., Brahe, C., van Ommen, G.J. *et al.* (1995) A provisional transcript map of the spinal muscular atrophy (SMA) critical region. *Eur J Hum Genet,* **3,** 87-95.
167. Sorek, R. and Ast, G. (2003) Intronic sequences flanking alternatively spliced exons are conserved between human and mouse. *Genome Res,* **13,** 1631-7.
168. Sanford, J.R., Coutinho, P., Hackett, J.A., Wang, X., Ranahan, W. and Caceres, J.F. (2008) Identification of nuclear and cytoplasmic mRNA targets for the shuttling protein SF2/ASF. *PLoS ONE,* **3,** e3369.
169. Hengge, U.R. (2008) SMaRT technology enables gene expression repair in skin gene therapy. *J Invest Dermatol,* **128,** 499-500.
170. Garcia-Blanco, M.A. (2003) Messenger RNA reprogramming by spliceosome-mediated RNA trans-splicing. *J Clin Invest,* **112,** 474-80.
171. Rodriguez-Martin, T., Garcia-Blanco, M.A., Mansfield, S.G., Grover, A.C., Hutton, M., Yu, Q., Zhou, J., Anderton, B.H. and Gallo, J.M. (2005) Reprogramming of tau alternative splicing by spliceosome-mediated RNA trans-splicing: implications for tauopathies. *Proc Natl Acad Sci U S A,* **102,** 15659-64.
172. Zayed, H., Xia, L., Yerich, A., Yant, S.R., Kay, M.A., Puttaraju, M., McGarrity, G.J., Wiest, D.L., McIvor, R.S., Tolar, J. *et al.* (2007) Correction of DNA protein kinase deficiency by spliceosome-mediated RNA trans-splicing and sleeping beauty transposon delivery. *Mol Ther,* **15,** 1273-9.
173. Wood, M., Yin, H. and McClorey, G. (2007) Modulating the expression of disease genes with RNA-based therapy. *PLoS Genet,* **3,** e109.
174. Oskoui, M., Levy, G., Garland, C.J., Gray, J.M., O'Hagen, J., De Vivo, D.C. and Kaufmann, P. (2007) The changing natural history of spinal muscular atrophy type 1. *Neurology,* **69,** 1931-6.
175. Sumner, C.J., Kolb, S.J., Harmison, G.G., Jeffries, N.O., Schadt, K., Finkel, R.S., Dreyfuss, G. and Fischbeck, K.H. (2006) SMN mRNA and protein levels in peripheral blood: biomarkers for SMA clinical trials. *Neurology,* **66,** 1067-73.
176. DiMatteo, D., Callahan, S. and Kmiec, E.B. (2008) Genetic conversion of an SMN2 gene to SMN1: a novel approach to the treatment of spinal muscular atrophy. *Exp Cell Res,* **314,** 878-86.
177. de la Mata, M., Alonso, C.R., Kadener, S., Fededa, J.P., Blaustein, M., Pelisch, F., Cramer, P., Bentley, D. and Kornblihtt, A.R. (2003) A slow RNA polymerase II affects alternative splicing in vivo. *Mol Cell,* **12,** 525-32.
178. Stephenson, M.L. and Zamecnik, P.C. (1978) Inhibition of Rous sarcoma viral RNA translation by a specific oligodeoxyribonucleotide. *Proc Natl Acad Sci U S A,* **75,** 285-8.
179. Friedman, K.J., Kole, J., Cohn, J.A., Knowles, M.R., Silverman, L.M. and Kole, R. (1999) Correction of aberrant splicing of the cystic fibrosis transmembrane conductance regulator (CFTR) gene by antisense oligonucleotides. *J Biol Chem,* **274,** 36193-9.
180. Scaffidi, P. and Misteli, T. (2005) Reversal of the cellular phenotype in the premature aging disease Hutchinson-Gilford progeria syndrome. *Nat Med,* **11,** 440-5.

181. Renshaw, J., Orr, R.M., Walton, M.I., Te Poele, R., Williams, R.D., Wancewicz, E.V., Monia, B.P., Workman, P. and Pritchard-Jones, K. (2004) Disruption of WT1 gene expression and exon 5 splicing following cytotoxic drug treatment: antisense down-regulation of exon 5 alters target gene expression and inhibits cell survival. *Mol Cancer Ther,* **3,** 1467-84.
182. Aartsma-Rus, A., Janson, A.A., Kaman, W.E., Bremmer-Bout, M., den Dunnen, J.T., Baas, F., van Ommen, G.J. and van Deutekom, J.C. (2003) Therapeutic antisense-induced exon skipping in cultured muscle cells from six different DMD patients. *Hum Mol Genet,* **12,** 907-14.
183. Lu, Q.L., Mann, C.J., Lou, F., Bou-Gharios, G., Morris, G.E., Xue, S.A., Fletcher, S., Partridge, T.A. and Wilton, S.D. (2003) Functional amounts of dystrophin produced by skipping the mutated exon in the mdx dystrophic mouse. *Nat Med,* **9,** 1009-14.
184. Muntoni, F., Bushby, K. and van Ommen, G. (2005) 128th ENMC International Workshop on 'Preclinical optimization and Phase I/II Clinical Trials Using Antisense Oligonucleotides in Duchenne Muscular Dystrophy' 22-24 October 2004, Naarden, The Netherlands. *Neuromuscul Disord,* **15,** 450-7.
185. Echaniz-Laguna, A., Miniou, P., Bartholdi, D. and Melki, J. (1999) The promoters of the survival motor neuron gene (SMN) and its copy (SMNc) share common regulatory elements. *Am J Hum Genet,* **64,** 1365-70.
186. Ramassamy, C. (2006) Emerging role of polyphenolic compounds in the treatment of neurodegenerative diseases: a review of their intracellular targets. *Eur J Pharmacol,* **545,** 51-64.
187. Mattis, V.B., Bowerman, M., Kothary, R. and Lorson, C.L. (2008) A SMNDelta7 read-through product confers functionality to the SMNDelta7 protein. *Neurosci Lett,* **442,** 54-8.
188. Dodge, J.C., Haidet, A.M., Yang, W., Passini, M.A., Hester, M., Clarke, J., Roskelley, E.M., Treleaven, C.M., Rizo, L., Martin, H. *et al.* (2008) Delivery of AAV-IGF-1 to the CNS extends survival in ALS mice through modification of aberrant glial cell activity. *Mol Ther,* **16,** 1056-64.
189. Kaspar, B.K., Llado, J., Sherkat, N., Rothstein, J.D. and Gage, F.H. (2003) Retrograde viral delivery of IGF-1 prolongs survival in a mouse ALS model. *Science,* **301,** 839-42.
190. Nagano, I., Shiote, M., Murakami, T., Kamada, H., Hamakawa, Y., Matsubara, E., Yokoyama, M., Moritaz, K., Shoji, M. and Abe, K. (2005) Beneficial effects of intrathecal IGF-1 administration in patients with amyotrophic lateral sclerosis. *Neurol Res,* **27,** 768-72.
191. Lesbordes, J.C., Cifuentes-Diaz, C., Miroglio, A., Joshi, V., Bordet, T., Kahn, A. and Melki, J. (2003) Therapeutic benefits of cardiotrophin-1 gene transfer in a mouse model of spinal muscular atrophy. *Hum Mol Genet,* **12,** 1233-9.
192. Meyer, K., Marquis, J., Trub, J., Nlend Nlend, R., Verp, S., Ruepp, M.D., Imboden, H., Barde, I., Trono, D. and Schumperli, D. (2008) Rescue of a severe mouse model for Spinal Muscular Atrophy by U7 snRNA-mediated splicing modulation. *Hum Mol Genet*.
193. Beroud, C., Tuffery-Giraud, S., Matsuo, M., Hamroun, D., Humbertclaude, V., Monnier, N., Moizard, M.P., Voelckel, M.A., Calemard, L.M., Boisseau, P. *et al.*

(2007) Multiexon skipping leading to an artificial DMD protein lacking amino acids from exons 45 through 55 could rescue up to 63% of patients with Duchenne muscular dystrophy. *Hum Mutat,* **28,** 196-202.
194. Scherer, L., Rossi, J.J. and Weinberg, M.S. (2007) Progress and prospects: RNA-based therapies for treatment of HIV infection. *Gene Ther,* **14,** 1057-64.
195. Grimm, C., Stefanovic, B. and Schumperli, D. (1993) The low abundance of U7 snRNA is partly determined by its Sm binding site. *EMBO J,* **12,** 1229-38.
196. Stefanovic, B., Hackl, W., Luhrmann, R. and Schumperli, D. (1995) Assembly, nuclear import and function of U7 snRNPs studied by microinjection of synthetic U7 RNA into Xenopus oocytes. *Nucleic Acids Res,* **23,** 3141-51.
197. Gao, G., Vandenberghe, L.H. and Wilson, J.M. (2005) New recombinant serotypes of AAV vectors. *Curr Gene Ther,* **5,** 285-97.
198. Paterna, J.C., Moccetti, T., Mura, A., Feldon, J. and Bueler, H. (2000) Influence of promoter and WHV post-transcriptional regulatory element on AAV-mediated transgene expression in the rat brain. *Gene Ther,* **7,** 1304-11.
199. Chen, H., McCarty, D.M., Bruce, A.T. and Suzuki, K. (1999) Oligodendrocyte-specific gene expression in mouse brain: use of a myelin-forming cell type-specific promoter in an adeno-associated virus. *J Neurosci Res,* **55,** 504-13.
200. Klein, R.L., Meyer, E.M., Peel, A.L., Zolotukhin, S., Meyers, C., Muzyczka, N. and King, M.A. (1998) Neuron-specific transduction in the rat septohippocampal or nigrostriatal pathway by recombinant adeno-associated virus vectors. *Exp Neurol,* **150,** 183-94.
201. Fu, H., Samulski, R.J., McCown, T.J., Picornell, Y.J., Fletcher, D. and Muenzer, J. (2002) Neurological correction of lysosomal storage in a mucopolysaccharidosis IIIB mouse model by adeno-associated virus-mediated gene delivery. *Mol Ther,* **5,** 42-9.
202. Barnes, D., Kunitomi, M., Vignuzzi, M., Saksela, K. and Andino, R. (2008) Harnessing endogenous miRNAs to control virus tissue tropism as a strategy for developing attenuated virus vaccines. *Cell Host Microbe,* **4,** 239-48.
203. Bartel, D.P. (2004) MicroRNAs: genomics, biogenesis, mechanism, and function. *Cell,* **116,** 281-97.
204. Bartel, D.P. and Chen, C.Z. (2004) Micromanagers of gene expression: the potentially widespread influence of metazoan microRNAs. *Nat Rev Genet,* **5,** 396-400.
205. Dash, A.K. and Cudworth, G.C., 2nd (1998) Therapeutic applications of implantable drug delivery systems. *J Pharmacol Toxicol Methods,* **40,** 1-12.

## VITA

Travis Baughan was born in Grand Rapids Michigan to Mark and Maureen Baughan on April 4th 1980. The family spent most of his pre-teen years in Orlando Florida, where he and his little brother Derick cultivated a great fondness of the ocean and any kind of fishing. After relocating to Washington State he dove into outdoor activities that would include, hiking, fishing, hunting, and whitewater rafting. Finding talent in track and field Travis, with the support of his family, attained All-American status in the 400m Intermediate Hurdles by the age of 16. Travis graduated High School in 1998 the same year he was state champion in the 110m High Hurdles. After injury stopped his ability to hurdle, he focused on microbiology. Undergraduate work was done at Montana State University, and culminated in a bachelor's degree in microbiology in 2002 with honors. After working in an immunology lab for three years he was fourth author in a publication for his contributions. After starting graduate school at the University of Missouri in 2003, he moved away from immunology and started work in Dr. Chris Lorsons' lab in January of 2004. In 2005 Travis met his future wife Keli whom has always been a great

supportive person throughout this stage of life. Without her understanding and always steady foresight this graduate process would not have been feasible. During graduate school Travis was able to present his work multiple times and had many people examine his projects with great questions.